SUMMARY FINAL REPORT
THE COMPUTERIZED ANATOMICAL MAN (CAM) MODEL

SEPTEMBER 1973

By: M. P. BILLINGS and W. R. YUCKER

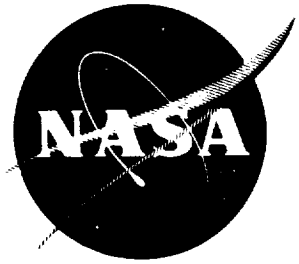

Prepared For
NATIONAL AERONAUTICS AND SPACE ADMINISTRATION
Johnson Space Center
Houston, Texas
Contract NAS9-13228

ABSTRACT

A computerized anatomical man (CAM) model, representing the most detailed and anatomically correct geometrical model of the human body yet prepared, has been developed for use in analyzing radiation dose distribution in man. This model of a 50-percentile standing USAF man, which has been substantially refined from the original version prepared by Kase of Martin-Marietta, comprises some 1100 unique geometric surfaces and some 2450 solid regions. Internal body geometry such as organs, voids, bones, and bone marrow are explicitly modeled. A computer program called CAMERA has also been developed for performing analyses with the model. Such analyses include tracing rays through the CAM geometry, placing results on magnetic tape in various forms, collapsing areal density data from ray tracing information to areal density distributions, preparing cross section views, etc. Numerous computer drawn cross sections through the CAM model are presented to illustrate the complexity and accuracy of the anatomical representations. A sample problem illustrating the capabilities of the CAMERA program is also included.

PREFACE

This document is the Summary Final Report describing work conducted by the McDonnell Douglas Astronautics Company (MDAC) under NASA Contract NAS 9-13228, "Development of the Computerized Anatomical Man Model". The work was performed for the NASA Johnson Space Center, Houston, Texas, and was monitored by Mr. J. V. Bailey, Mail Code DD-63, Health Services Division, Johnson Space Center, Houston, Texas 70058.

The contributions of several MDAC personnel are gratefully acknowledged, particularly Mr. R. W. Langley for guiding and reviewing the work, Mr. B. R. Heckman for assisting with the anatomical modeling, and Dr. H. B. Kelly for critiquing the anatomical representations.

CONTENTS

	LIST OF FIGURES		ix
	LIST OF TABLES		xvii
Section 1	INTRODUCTION AND SUMMARY		1
Section 2	CAM MODEL DEVELOPMENT		5
	2.1	ORIGINAL VERSION	5
		2.1.1 MEVDP Geometry System	5
		2.1.2 MEVDP Version of CAM Model	7
	2.2	CONVERSION TO IMPROVED GEOMETRY SYSTEM	8
		2.2.1 QUAD Geometry System	10
		2.2.2 Computer Aided Data Conversion	13
	2.3	EVALUATION AND VERIFICATION	14
		2.3.1 Error Tests	15
		2.3.2 Evaluation of Anatomical Representations	15
	2.4	REVISION AND IMPROVEMENT	16
		2.4.1 Bone Marrow Modeling	18
		2.4.2 Body Joint Modeling	18

	2.5	FINAL VERIFICATION	19
	2.6	DOSE POINT SELECTION	20
		2.6.1 Dose Points in Skin	20
		2.6.2 Dose Points in Bone Marrow	21
		2.6.3 Dose Points in Gastrointestinal Tract	21
Section 3	CAM MODEL DESCRIPTION		23
	3.1	GEOMETRICAL DESCRIPTION	23
		3.1.1 Subsections and Joints	23
		3.1.2 Identifiers	24
		3.1.3 Materials	25
		3.1.4 Cross Section Views	31
	3.2	MATERIALS AND MASSES	91
	3.3	DOSE POINT LOCATIONS	97
Section 4	CAMERA PROGRAM DESCRIPTION		107
	4.1	CAPABILITIES	107
	4.2	INPUT PREPARATION	108
Section 5	RESULTS AND RECOMMENDATIONS		111
	5.1	RECOMMENDATIONS FOR EXTENDING PRESENT CAPABILITY	112
	5.2	RECOMMENDATIONS FOR APPLYING PRESENT CAPABILITY	112
	APPENDIX – CAMERA PROGRAM UTILIZATION		115
	REFERENCES		145

FIGURES

1	Cross Section Through the CAM Model	2
2	Body Sections and Joint Locations	24
3	Cross Sections Through Right Shoulder	25
4	Vertical Cross Section Through the Head at x = 0	32
5	Vertical Cross Section Through the Head at x = 3	32
6	Vertical Cross Section Through the Head at y = 0	33
7	Vertical Cross Section Through the Head at y = 1.245	33
8	Horizontal Cross Section Through the Head at z = 1	34
9	Horizontal Cross Section Through the Head at z = 2	34
10	Horizontal Cross Section Through the Head at z = 3	35
11	Horizontal Cross Section Through the Head at z = 4	35
12	Horizontal Cross Section Through the Head at z = 5	36
13	Horizontal Cross Section Through the Head at z = 5.99	36
14	Horizontal Cross Section Through the Head at z = 7	37
15	Horizontal Cross Section Through the Head at z = 8	37
16	Vertical Cross Section Through the Neck at x = 0	38

17	Vertical Cross Section Through the Neck at y = 0	38
18	Horizontal Cross Section Through the Neck at z = 9.01	39
19	Horizontal Cross Section Through the Neck at z = 10	39
20	Horizontal Cross Section Through the Neck at z = 11	40
21	Horizontal Cross Section Through the Neck at z = 11.99	40
22	Vertical Cross Section Through the Upper Torso at x = 0	41
23	Vertical Cross Section Through the Upper Torso at y = 0	41
24	Horizontal Cross Section Through the Upper Torso at z = 12.01	42
25	Horizontal Cross Section Through the Upper Torso at z = 12.99	42
26	Horizontal Cross Section Through the Upper Torso at z = 13.01	43
27	Horizontal Cross Section Through the Upper Torso at z = 14	43
28	Horizontal Cross Section Through the Upper Torso at z = 15.01	44
29	Vertical Cross Section Through the Mid Torso at x = 0	44
30	Vertical Cross Section Through the Mid Torso at y = 0	45
31	Horizontal Cross Section Through the Mid Torso at z = 16	45
32	Horizontal Cross Section Through the Mid Torso at z = 17	46
33	Horizontal Cross Section Through the Mid Torso at z = 18	46

34	Horizontal Cross Section Through the Mid Torso at z = 19.01	47
35	Horizontal Cross Section Through the Mid Torso at z = 20	47
36	Horizontal Cross Section Through the Mid Torso at z = 21	48
37	Horizontal Cross Section Through the Mid Torso at z = 22.01	48
38	Horizontal Cross Section Through the Mid Torso at z = 23.01	49
39	Horizontal Cross Section Through the Mid Torso at z = 24	49
40	Horizontal Cross Section Through the Mid Torso at z = 25.01	50
41	Horizontal Cross Section Through the Mid Torso at z = 26.01	50
42	Horizontal Cross Section Through the Mid Torso at z = 27	51
43	Horizontal Cross Section Through the Mid Torso at z = 28.01	51
44	Horizontal Cross Section Through the Mid Torso at z = 28.99	52
45	Vertical Cross Section Through the Lower Torso at x = 0	52
46	Vertical Cross Section Through the Lower Torso at y = 0	53
47	Horizontal Cross Section Through the Lower Torso at z = 30.1	53
48	Horizontal Cross Section Through the Lower Torso at z = 31	54
49	Horizontal Cross Section Through the Lower Torso at z = 32	54
50	Horizontal Cross Section Through the Lower Torso at z = 32.9	55

51	Horizontal Cross Section Through the Lower Torso at z = 34	55
52	Horizontal Cross Section Through the Lower Torso at z = 35	56
53	Horizontal Cross Section Through the Lower Torso at z = 36	56
54	Horizontal Cross Section Through the Lower Torso at z = 37	57
55	Vertical Cross Section Through the Upper Arm at x = 0	57
56	Vertical Cross Section Through the Upper Arm at y = 7.5	58
57	Horizontal Cross Section Through the Upper Arm at z = 14	58
58	Horizontal Cross Section Through the Upper Arm at z = 16	59
59	Horizontal Cross Section Through the Upper Arm at z = 18	59
60	Horizontal Cross Section Through the Upper Arm at z = 20	60
61	Horizontal Cross Section Through the Upper Arm at z = 22	60
62	Horizontal Cross Section Through the Upper Arm at z = 24	61
63	Horizontal Cross Section Through the Upper Arm at z = 25.9	61
64	Vertical Cross Section Through the Forearm at x = -0.5	62
65	Vertical Cross Section Through the Forearm at y = 7	62
66	Vertical Cross Section Through the Forearm at y = 8	62
67	Horizontal Cross Section Through the Forearm at z = 26	63
68	Horizontal Cross Section Through the Forearm at z = 28.1	64

69	Horizontal Cross Section Through the Forearm at z = 30	64
70	Horizontal Cross Section Through the Forearm at z = 32	65
71	Horizontal Cross Section Through the Forearm at z = 34	65
72	Horizontal Cross Section Through the Forearm at z = 36	66
73	Vertical Cross Section Through the Hand at x = 0.5	66
74	Horizontal Cross Section Through the Hand at z = 36.3	67
75	Horizontal Cross Section Through the Hand at z = 38	67
76	Horizontal Cross Section Through the Hand at z = 40	68
77	Horizontal Cross Section Through the Hand at z = 42	69
78	Vertical Cross Section Through the Upper Leg at x = 1.0	69
79	Vertical Cross Section Through the Upper Leg at y = 4	69
80	Horizontal Cross Section Through the Upper Leg at z = 34	70
81	Horizontal Cross Section Through the Upper Leg at z = 35	70
82	Horizontal Cross Section Through the Upper Leg at z = 36	71
83	Horizontal Cross Section Through the Upper Leg at z = 37	71
84	Horizontal Cross Section Through the Upper Leg at z = 38	72
85	Horizontal Cross Section Through the Upper Leg at z = 39	72
86	Horizontal Cross Section Through the Upper Leg at z = 40.1	73

87	Horizontal Cross Section Through the Upper Leg at z = 41	73
88	Horizontal Cross Section Through the Upper Leg at z = 42	74
89	Horizontal Cross Section Through the Upper Leg at z = 43	74
90	Horizontal Cross Section Through the Upper Leg at z = 44	75
91	Horizontal Cross Section Through the Upper Leg at z = 45	75
92	Horizontal Cross Section Through the Upper Leg at z = 46	76
93	Horizontal Cross Section Through the Upper Leg at z = 47.1	76
94	Horizontal Cross Section Through the Upper Leg at z = 48	77
95	Horizontal Cross Section Through the Upper Leg at z = 49	77
96	Horizontal Cross Section Through the Upper Leg at z = 50	78
97	Horizontal Cross Section Through the Upper Leg at z = 50.9	78
98	Vertical Cross Section Through the Lower Leg at x = 0.6	79
99	Vertical Cross Section Through the Lower Leg at y = 2	79
100	Horizontal Cross Section Through the Lower Leg at z = 51.1	80
101	Horizontal Cross Section Through the Lower Leg at z = 52	80
102	Horizontal Cross Section Through the Lower Leg at z = 53.1	81
103	Horizontal Cross Section Through the Lower Leg at z = 54	81
104	Horizontal Cross Section Through the Lower Leg at z = 55	82

105	Horizontal Cross Section Through the Lower Leg at z = 56	82
106	Horizontal Cross Section Through the Lower Leg at z = 57	83
107	Horizontal Cross Section Through the Lower Leg at z = 58	83
108	Horizontal Cross Section Through the Lower Leg at z = 59	84
109	Horizontal Cross Section Through the Lower Leg at z = 60	84
110	Horizontal Cross Section Through the Lower Leg at z = 61.1	85
111	Horizontal Cross Section Through the Lower Leg at z = 62	85
112	Horizontal Cross Section Through the Lower Leg at z = 63.1	86
113	Horizontal Cross Section Through the Lower Leg at z = 64	86
114	Horizontal Cross Section Through the Lower Leg at z = 65	87
115	Horizontal Cross Section Through the Lower Leg at z = 66	87
116	Horizontal Cross Section Through the Lower Leg at z = 67	88
117	Horizontal Cross Section Through the Lower Leg at z = 68	88
118	Horizontal Cross Section Through the Lower Leg at z = 69	89
A-1	Listing of Input Cards for Sample Problem	124
A-2	Printed Output from RGEOM Task	126
A-3	Printed Output from Plotting Tasks	128
A-4	Plotted Output from PLOTB* Task	129
A-5	Plotted Output from PLOTB Task	129

A-6	Plotted Output from PLOTM* Task	130
A-7	Plotted Output from PLOTM Task	130
A-8	Printed Output from TRACES Task	132
A-9	Printed Output from TRACAS Task	133
A-10	Printed Output from TRACER Task	134
A-11	Printed Output from TRACAR Task	135
A-12	Printed Output from DUMPRT Task	137
A-13	Printed Output from EDITM and EDITS Tasks	138
A-14	Listing of Data Written on Tape-3 by EDITM Task	139
A-15	Listing of Data Written on Tape-3 by EDITS Task	140
A-16	Listing of Data Written on Tape-3 by EDITS Task	141
A-17	Printed Output from UPDATE Task	143

TABLES

1	Summary of Recommended Improvements	17
2	Region Identifiers	26
3	Materials Code	30
4	Material Compositions	92
5	Volume, Mass, and Skin Area of Body Sections	94
6	Mass Distribution by Material and Body Section	95
7	Comparison of Marrow Distribution in CAM with Experimental Data	96
8	Dose Point Locations for Various Organs	98
9	Dose Point Locations for Bone Marrow	99
10	Dose Point Locations for Gastrointestinal Tract	101
11	Dose Point Locations for Skin	103
12	Dose Point Weights	104
13	Geometrical Quantities for Body Sections	109
A-1	CAMERA Task List	116
A-2	Special Surface Forms	121

Section 1
INTRODUCTION AND SUMMARY

An extremely detailed geometrical model of the human anatomy, the most detailed yet prepared, has been developed for use in investigations dealing with exposure of astronauts to the natural space radiation environment. The model is equally applicable to investigations dealing with exposure of humans to radiation associated with nuclear weapon and nuclear power system environments and with medical applications, i.e., radiotherapy and radiography. Computer-drawn cross sections through this model are shown in Figure 1.

With this model, called the Computerized Anatomical Man (CAM) model, data on the amount and type of materials traversed by radiations penetrating the body can be provided in a form compatible with radiation transport computations. Usually these delineate the lengths and material compositions of each path element associated with tracing a ray through the geometrical system comprising the model. In this context the "ray" represents some portion of the track of a nuclear particle within the body. The actual radiation transport analyses are independent of the CAM model, the function of the model being only to provide problem definition data in the form of input geometric information for the radiation transport analyses. This generality stems from the revised geometry framework, which is compatible with Monte Carlo tracking as well as with point kernel ray tracking. Thus, there is no real restriction on the type of transport code with which the CAM model can be used. The CAM model data format is compatible with a number of existing Monte Carlo and point kernel codes for nuclear and space radiation transport.

The CAM model was originally developed in 1969 by Kase, et al., of the Martin-Marietta Corporation under contract to the Air Force Weapons Laboratory (AFWL), and with funds provided by the NASA Manned Spacecraft

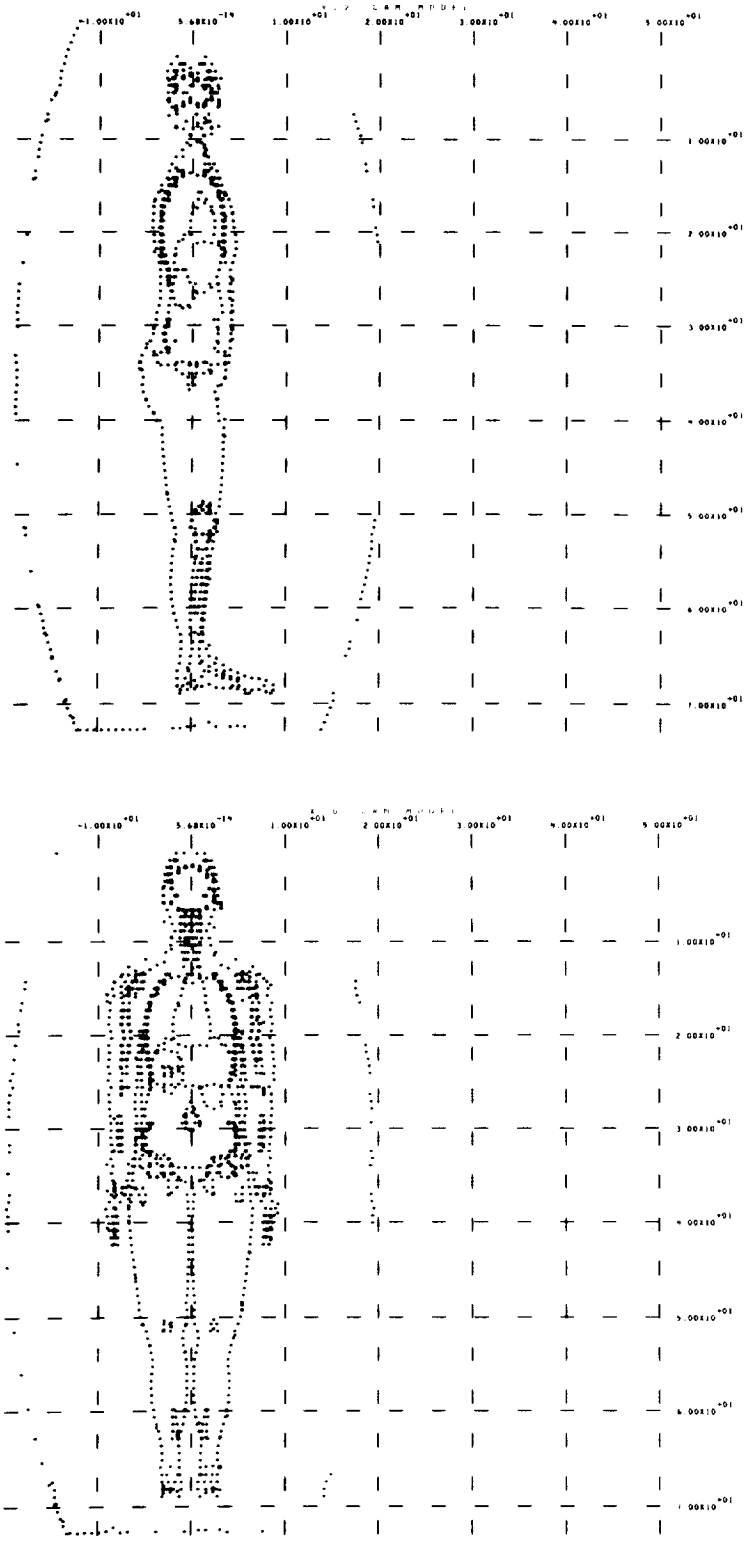

F igure 1. Cross Section Through the CAM Model

Center (Reference 1). The CAM geometrical data were extensively reviewed and modified by personnel at the AFWL in the 1970-71 period. The version of the model existing in January 1971 was acquired by McDonnell Douglas Astronautics Company (MDAC) and applied in Company-funded studies of space radiation problems in the 1971-72 period. In parallel with research based on application of the original model, MDAC converted the geometrical data comprising the model from the geometry framework in which it was prepared to one more effective for routine use in shielding analyses. This converted form of the CAM model has been further refined in the study reported here, the major refinements being to evaluate and improve the initial representations of anatomy, especially of bone geometry, and to explicitly model bone marrow sites, which were not incorporated in the original version.

Another item that was prepared is a computer program, called CAMERA, specifically designed to perform geometrical operations with the data of the CAM model. This program performs ray tracing computations, the results of which can be used in point kernel shielding analyses. It also outputs the ray tracing results in various forms, and it plots cross section views through the model. The CAMERA program has been designed to facilitate future addition of a capability to scale the CAM data to represent body postures and physiques other than the standing 50-percentile USAF man on which it was based. In anticipation of this extension, the model has been subdivided into 15 body sections, and interfaces between them have been modified to resemble body joints.

This report describes the activities conducted to develop the present version of the CAM model from the original version; this effort is described in Section 2. A description of the revised model, including numerous computer-drawn cross-section views through the model, is presented in Section 3. The CAMERA program is described in Section 4, and recommendations for application and extension of the CAM/CAMERA capability are presented in Section 5.

Section 2
CAM MODEL DEVELOPMENT

A number of activities were conducted to complete the development of the computerized anatomical man model, working forward from the data base prepared by Kase, et al., of the Martin-Marietta Corporation and augmented by personnel at the Air Force Weapons Laboratory. These activities included (1) familiarization with, and use of, the model in its original form, (2) conversion of the model from data requirements of the MEVDP geometry system to those of the QUAD geometry system, (3) debugging the converted model, (4) evaluation of the anatomical correctness of the model, (5) improving on anatomical representations, and (6) verifying the refined and extended model. The rationale for executing this work, and the techniques employed, are presented in the following sections.

2.1 ORIGINAL VERSION

The original CAM model was designed to operate with the MEVDP program developed by North American for modeling complex spacecraft configurations (Reference 2). The MEVDP program optionally uses a built-in man model, which is much simpler than the CAM model, in conjunction with a spacecraft geometric system defined by input. This geometric data is used to determine the mass distribution of the vehicle and the body and hence to calculate the extent to which radiation-sensitive body organs are protected against space radiations. In view of the complexity of the CAM model, the portion of the MEVDP program usually used to describe the spacecraft geometry was also used to describe the astronaut geometry.

2.1.1 MEVDP Geometry System

The MEVDP geometry description uses simple shapes called "elemental shield volumes" (EV) as the basic unit of geometry. Several of these EVs may be specified to be contained in a more complex unit, called a "composite shield volume" (CV). The CV concept is necessary to allow void EVs to

overlap a non-void or material EV, which has the effect of cancelling the material inside the overlapping region. The CVs are considered to be independent, disconnected building blocks without identification of contiguous volumes. Hence, ray tracing calculations cannot be performed by progressing continuously along a ray through successive regions. Instead, each CV must be tested to determine whether it is traversed by a given ray.

In order to reduce the number of CVs that must be tested, MEVDP defines for each CV the octant of space that it occupies. This introduces the need to translate the geometry data from the input absolute coordinate system (ABCS) to a coordinate system centered at the origin of the ray (DSCS). Then the direction cosines of the ray can be examined to determine which CVs lie in the same octant. However, the octant concept is not always effective since a shield may occupy more than one octant, depending on the detector location. All such CVs are grouped into the "ninth octant", and hence must all be inspected for each ray. For example, in the sample case obtained with the CAM data, the octant test failed to reduce the testing in this way for about 90 percent of the CVs. Also, since all rays must pass through the origin, this treatment is extremely inefficient if used for following particle tracks in a Monte Carlo calculation or for handling calculations for a detector that is not fixed with respect to the geometry.

The ray tracing involves simultaneous solution of the equation of the ray and that of each surface bounding each EV in a CV. This task is reduced somewhat by using simplified tests to determine if the EV is not traversed by the ray. Since the surface equations are simplified by expressing them in special coordinate systems (RDCS), (e.g., the principal axes of an ellipsoid) a rotation matrix is generated for each EV, transforming from the DSCS. The first step in tracing each ray is thus to transform the equation of the ray to the RDCS for the EV. The simultaneous equations are then solved for all points of intersection of the ray with all bounding surfaces of the EV. Further tests are required to eliminate spurious solutions and identify the true entrance and exit points. Because the volume of geometrical data is too large to store in core, it is used from a disk file. As each CV is read in, all rays are traced in that volume.

The results of this ray tracing procedure are presented in two ways. First, the path lengths for equivalent thicknesses of a standard material are accumulated over all volumes for each ray. These total areal density values are then sorted and used to construct the cumulative distribution function (CDF) of areal density for use in proton and heavy particle dose calculations. For electron transport calculations, MEVDP saves the data on path increment, material, and distance from the detector on magnetic tape for each volume and each ray. This data is sorted first by ray number and secondly by position along the ray, giving for each ray the order and thickness of each material. This sorting operation, which turns out to be rather costly, is made necessary by the lack of spatial continuity in the geometry description.

2.1.2 MEVDP Version of CAM Model

The original version of the CAM model, as prepared for use with the MEVDP program, was designed to the exterior conformation and dimensions corresponding to the 50th percentile Air Force man. Two configurations were prepared, standing and seated, comprised of some 11,000 data cards each.

In the MEVDP geometrical system, the standing CAM model was described by approximately 2500 elemental volumes constituting some 560 composite shields. This number of elemental volumes involves many duplicated shapes because of the absence of continuity in the geometrical description. That is, contiguous solid shapes required specifications of the common surface of each solid. The number of unduplicated shapes was more nearly 1200.

The chemical composition of this model was expressed by assigning each region a material index corresponding to one of five standard material compositions: lung, organ, intestine, muscle, and skeleton.

Two modes of operation of the model with MEVDP were possible. One mode involved tracing rays from an internal point to the model exterior, writing the details of the ray tracing results on magnetic tape in a form in which the ray origin and angular orientation were preserved; such data could later be

combined with similar results for locations within a spacecraft model to provide data on the combined shielding effect of vehicle and body. Experience with this mode of operation on the MDAC CDC 6500 computer indicated computer times to be of the order of 1100 seconds per point for 512 rays, of which approximately 100 seconds were for initialization (i.e., octant sorting of CVs) and the remainder for ray tracing through the CVs and sorting path length data for each ray into the order in which they would be traversed.

The second mode, introduced by MDAC to help reduce computer time, was to construct only the areal density distributions, which did not require ordering the path data. This change reduced computer time to approximately 700 seconds per point for 512 rays.

The MEVDP version of the CAM model was partially corrected and modified and used by MDAC in a number of studies of space radiation dose to body organs as reported in References 3-6. These studies used the second mode of operation of the CAM/MEVDP combination, constructing CDF data on the body mass distribution about several points in the spatially distributed BFO and GIT as well as a point in the testes. In these computations 100 rays per point were traced, requiring approximately 200 seconds each.

2.2 CONVERSION TO IMPROVED GEOMETRY SYSTEM

The studies that were conducted with the CAM model, using the MEVDP program, indicated a number of further potentially fruitful applications of the model to assessment of radiobiological dose quantities and procedures. However, it appeared that the computer-time requirements for such production applications would be substantial, and that some effort to further reduce computer time without sacrificing results was desirable. It also appeared that some work on the data of the model was also required prior to large scale production use, to eliminate "bugs" and to rework some portions of the anatomical representations.

The most attractive prospect was to convert the model to another geometry system, one that was substantially more efficient in ray-tracing computations

as well as one that would facilitate detecting and correcting errors in the model to an extent not feasible within the MEVDP geometry framework. Consequently, a comparison was made between MEVDP and the geometry analysis techniques used in several computer programs, including the MDAC SIGMA code (Reference 7), the MAGI SAM-C code (Reference 8), and the ORNL MORSE program (Reference 9). Three significant conclusions were reached:

A. The geometrical techniques incorporated in the MEVDP program were inefficient in ray tracing computations, relative to other geometrical techniques which were developed and available. Experience with these other techniques had been gained with considerably less complex geometrical models, but nonetheless indicated that a factor of 40 or so improvement in ray tracing efficiency was possible.

B. Whatever geometry system was chosen, the conversion effort would be an appreciable task because of the quantity of data (11,000 data cards), the absence of information in the MEVDP geometry approach on spatial continuity of the geometry, and errors in the model data. (The latter are probably due to the absence of information on spatial continuity, since overlapping regions and undefined regions are not detected by MEVDP, as they are by the other codes.) Automation of the conversion effort would necessarily be limited because any alternative geometry system required data on spatial continuity that were not available in the MEVDP system and would have to be provided manually.

C. Working with the model, once it had been converted, to remove geometrical "bugs" and to remodel portions of the anatomy, would be considerably easier because automatic plotting of cross sections through the model would be feasible. With the MEVDP scheme such cross section plots were extremely time-consuming and prohibitive.

The geometry system finally selected for the conversion process was the MDAC QUAD system (Reference 10). The reasons for its selection were (1) an intimate knowledge of its capabilities, (2) experience with use of the

system in performing error tests on complex geometric models, and (3) the fact that numerous operational codes used the system. For example, QUAD is used by the SIGMA code, the MDAC PATCH neutron and gamma ray point kernel code (Reference 11), the MDAC SWORD space radiation dose analysis and shield optimization code (Reference 12) and the FASTER/BETA (References 13-15) series of neutron/gamma/electron/x-ray Monte Carlo transport codes. Hence selection of the QUAD system meant that a variety of potentially interesting radiation transport calculations and dose analyses involving the model would be feasible.

2.2.1 QUAD Geometry System

In the QUAD system, a geometric system is assumed to be described by a series of homogeneous material regions. Each region is defined by specifying the surface which form its boundaries, where each surface is defined by a general quadratic equation:

$$G(x, y, z) = A_0 + A_1x + A_2y + A_3z + A_4x^2 + A_5y^2 + A_6z^2 + A_7xy, + A_8yz + A_9zx = 0$$

A list of all the surfaces needed to subdivide the system is provided to the code by specifying for each surface the values of each of the 10 possible cartesian quadratic surface coefficients. These coefficients can be calculated by the code from simplified inputs for several simple shapes which are commonly used, as identified in Table A-2 of the Appendix.

A region is defined by providing data on the material contained, a list of the surfaces which bound the region, and the coordinates of any point inside the region. These coordinates are used by the code to calculate "ambiguity indices" for each bounding surface, which indicate on which side of the surface the region is found. The code evaluates the surface quadratic expression at the specified point, the sign of the result giving the ambiguity index. This feature relieves the user of the task of providing the ambiguity index for every boundary, which is required by other codes which use quadratic surfaces, e.g., MORSE and COHORT-II (Reference 16).

Ray tracing proceeds continuously from one region into the adjacent region, providing three pieces of information about each path segment: identification of region, path length in the region, and identification of the boundary crossed in leaving the region. This series of calculations is repeated for the neighboring regions along the ray until either the maximum distance of interest to the user is reached, or until the exterior of the system is encountered.

The ambiguity indices are used in identifying the region in which a point is located. For use in ray tracing, the point used is either the origin of the ray, or the point where the ray exits the previous region. The coordinates of the point are used to evaluate the equations of all boundaries of a candidate region. The region is successfully identified if the ambiguity indices for all boundaries with respect to the point in question are identical to those generated by the code from the region description. A cross reference list of all regions which are bounded by a given surface is used to reduce significantly the number of candidate regions to be tested as the ray crosses that surface from an adjacent region. The testing is further reduced by the knowledge that the indices associated with the surface must be of opposite sign (±) for regions on opposite sides. This technique can be extremely effective in reducing ray tracing computer time, as evidenced by the fact that in the converted CAM model, the number of regions that had to be tested averaged 8 out of the 2450 candidates.

The calculation of the path length across a region involves solving simultaneously the equations of the ray with those of each bounding surface, except the entry surface. A list of possible lengths is assembled containing up to two roots of a quadratic equation for each surface. The actual path length is taken to be the minimum of the positive roots. This selection identifies the exit surface for the region and completes the calculation for the current path length segment. Since the same intermediate quantities, dependent on bounding surface, ray origin and ray direction, are used for calculating ambiguity indices for a surface and path lengths to the surface, they are computed and saved for only those surfaces needed.

Since the ray tracing technique operates on continuously defined regions, the normal sequence of operations cannot be followed if geometry definition errors are present. The major geometry errors are usually undefined volumes (or holes) and multiply-defined volumes (or overlaps). Two tests are provided in the geometry routines to aid the user in locating these errors. The first test involves calculations of ambiguity indices for each point in the region definition data with respect to all other regions. A diagnostic message is printed if any point satisfies the conditions to be located in more than one region. This simple test partially locates overlapping regions.

The second test, which is more complicated, locates all errors. It is performed optionally while tracing rays. In order to use this capability, additional regions must be defined to fill the space from the outer boundaries of the system to a single ellipsoidal surface which entirely encloses the system. Any ray which ends on a surface other than this outer surface has detected an error. An error message is printed which includes information about each region traversed by the ray up to the point of the error.

The printed error messages from this second test enable the user to correct these errors in geometry description following the run. However, it is also possible to continue the run, producing data without gross distortions as might be introduced by the errors encountered, by means of an error recovery procedure. In this procedure, the program automatically extrapolates the ray to the outer surface and traces a ray in the opposite direction, back to the end of the first ray. If a hole is detected before the reversed ray reaches this point, the undefined space is assumed to contain the same material as the last region crossed by the reversed ray. The data from both rays is then combined to produce a set of ray trace data, approximating the data that would have been obtained if no error had been encountered.

The features described above make the QUAD geometry analysis routines particularily well suited for application to the CAM model. The possible shapes are restricted only by the limitations of quadratic surfaces. Programs which use only pre-defined shapes, such as MEVDP and SAM-C are

much more restricted. The QUAD input data is simplified for the user, and redundant data is neither required nor in fact allowed. The MEVDP data, on the other hand, requires input of identical EV data many times. While MEVDP is performing rotations for each CV on every ray and solving surface equations for each of the repeated references to a surface, the QUAD subprogram performs only the minimum number of operations required. The great complexity of the CAM model makes these comparisons very significant. Finally, unlike MEVDP which ignores any errors in geometry description, the QUAD error tests detect and describe all errors present in the data.

2.2.2 Computer-Aided Data Conversion

The GETRAN (GEometry TRansformation ANalysis) (Reference 17) program was developed by MDAC to perform automatically, to the extent possible, the conversion and checking of CAM data. This activity had been completed prior to initiation of the present contractual effort. However many of the capabilities originally incorporated in the GETRAN code have been included in the CAMERA code prepared under the contract.

After the original data tape was scanned for format errors, and corrections were made to ensure that all EVs defined for a CV were being read in the proper group, the conversion process was begun. The GETRAN code evolved as the conversion proceeded and the requirements for computer aids to conversion were identified. An important part of these aids were several optional plotting techniques which were added to the basic GETRAN code. Later, as the emphasis shifted from conversion to evaluation, automatic error-seeking features were added to GETRAN; these error-detection techniques are identified in the discussions of the evaluation phase, during which they were employed.

GETRAN read the original MEVDP data cards for a CV and provided a printed description of each of the EVs. Quadratic surface coefficients were calculated for every surface defined. By their nature, the EVs defined for a CV can and do overlap on each other, making the automatic definition of regions a difficult task. The simplifying assumption was made that each EV formed one region, bounded by the surfaces defined for that EV. The

surface equations were scanned for duplicated surfaces, which were then discarded. The surface and region data were punched on cards, and plots were produced of the intersection of all surfaces with several planes perpendicular to the coordinate axes.

This output from GETRAN was then inspected, with many superfluous surfaces being discarded and with the region data being corrected to conform to the restrictions imposed by the QUAD ray tracing routines. The corrected CV was then checked using GETRAN to produce additional plots of surface intersections at more appropriate planes and to punch a final geometric subsystem deck. In the event that the plots did not make obvious the corrections required, corresponding plots of the CV were made using a GETRAN plotting feature in which MEVDP transformation and ray tracing routines were used to prepare the plotting data. Comparison of these two types of plots greatly simplified the correction of the region data, but because of the inefficiency of the MEVDP ray tracing technique (by a factor of 40 relative to QUAD), these plots were used for only the most difficult CVs.

The next step in the conversion procedure was the automatic assembly by the code of all the CVs contained in a body section (e.g., the head) into a single geometry system. The surface and region data were assigned new identification numbers sequentially in the new section model. The surface data were examined and all repeated surfaces (i.e., boundaries common to two or more CVs) were discarded. When a surface was discarded, the list of boundaries in the region definitions was scanned to allow replacement of the discarded surface and to decrement by one the number of all larger surface numbers. The surface data were then collapsed to delete the repeated data. Finally the condensed body section data were punched on cards by GETRAN to facilitate their use in subsequent operations.

2.3 EVALUATION AND VERIFICATION

Following the conversion from MEVDP to QUAD geometry systems, the model was intensively reviewed and tested to determine its validity. A number of tests were performed to enhance detection of "bugs" in the geometrical data, with the bugs that were recognized being corrected. Also,

the model was reviewed by a physiologist, both to assess the accuracy with which anatomy had been modeled and to suggest desirable improvements.

2.3.1 Error Tests

The GETRAN program was used to perform a number of tests designed to detect inconsistencies and errors in the model. The error tests were performed separately for each geometric subsystem assembled from the CV data and were applied in three steps. The first test, called the point-in-region test, was applied to detect gross overlaps between regions. The other test, the outer boundary test, was optionally applied while tracing rays through the system. The three steps in which the error tests were performed are as follows:

1. The first step of the checkout process consisted of tracing rays in planes perpendicular to the coordinate axes, to produce plane section plots of the system. The plotting planes were moved through the system at approximately one inch intervals. These plots were examined, along with the printed description of any errors which were identified, and with the CV plots generated during the conversion. The errors were corrected and the plots regenerated until no more errors were located by this procedure.
2. In the second step of the evaluation, rays were traced in random directions from each of several points in each of the body sections. The mass of each body section was computed during this step. The degree of convergence of the mass was used as an indication of how well the system had been examined by the error testing procedure.
3. The third step was similar to the second, except that the origin of the rays was systematically moved from region to region of the body section, until all regions had been explicitly tested.

2.3.2 Evaluation of Anatomical Representations

The process of evaluating the degree to which the converted and debugged CAM model actually represented human anatomy had several facets. Some of the recommended changes were of sufficient magnitude that their incorporation was not feasible under the present contract. Others were deferred

until the extensive remodeling associated with representation of bone marrow was implemented, as discussed in Section 2.4. Other relatively minor changes were incorporated as the need was identified.

The process of critiquing the shapes of the current anatomical representations relied heavily on cross section plots. Plots were prepared for all planes for which anatomical drawings identifying the intended model were given in Reference 1. Additional plots were prepared for many cross sections presented in standard cross section anatomy texts (References 18 and 19). These cross section plots were reviewed, compared, etc., by a physiologist, and a list of suggested changes were prepared. These changes are summarized in Table 1 and were incorporated with the six exceptions noted.

One obvious improvement was to expand on the identification of the regions presently modeled. Initially the boundaries of organs could not be plotted because there was no organ-related identification of regions. It was evident that such plots would be extremely useful, and hence the material index associated with each region was modified to also denote an organ label. The expanded capability to use this index to distinguish among other variations, such as red versus yellow marrow, was also provided. A list of the revised material indices is given in Section 3.

Another modification to the region data was also implemented. The ID field used in the original data to denote shield composite number was deleted, and a coded identification of body part and anatomical name was added. For example the regions defining the humerus in the right upper arm are now labeled RUAHUMO1, RUAHUMO2, etc.

2.4 REVISION AND IMPROVEMENT

Substantial modifications to the model were effected, both to improve the accuracy of the anatomical representation and to provide capabilities not previously available. The anatomical improvements included incorporation of the changes noted in Table 1 and addition of explicit models of the spatially distributed bone marrow, which previously was homogenized with bone and called "skeleton". The primary additional capability was division

Table 1

SUMMARY OF RECOMMENDED IMPROVEMENTS

Range Affected*	Modification
4.3 - 5.	Add missing skull bone
5.7 - 7.	Revise tissue boundaries in face
7.	Widen back teeth
13. - 23.	Modify rib curvature at juncture with vertebrae **
19.	Extend ribs at sides Move sternum forward in chest
23.	Extend lower boundary of rib cage **
29.	Remove bone connecting pelvis to 5th lumbar vertebra **
31. - 32.	Remove boundary causing region behind pelvis to be labeled as intestine
36. - 47.	Round femur cross sections and slant inward to knee
45.5 - 50.	Reduce thigh cross section
50.	Add patella **
53. - 63.	Modify bone cross-section shape. Reduce calf.
63. - 67.	Round ankle and foot cross sections **
67	Add bone region to foot **
16 - 25	Round humerus cross section
20 - 25	Reduce bicep
25	Round elbow joint and move toward rear
29 - 34	Round ulna and radius
33	Move ulna to be within arm
36	Enlarge wrist bones
—	Add bone marrow regions

*Vertical range (Z-coordinate) over which the change extends (inches).

**Suggested modification, not scheduled for implementation.

of the body into a number of subsections and providing models of "joints" so that these body subsections could be moved relative to one another. This provision was made in anticipation of adding a posture scaling technique in a future effort.

2.4.1 Bone Marrow Modeling

The general procedure for modeling bone and bone marrow was to shape the bone external contour to resemble the contour depicted in anatomy texts, then to represent the marrow location by approximately the same shape, but in reduced size. This approach simplified specification of the boundaries of the marrow regions and minimized introduction of geometrical bugs. In some locations this approach was not feasible because of the particular and differing cross section shapes of bone and marrow, and special provisions had to be made. The distinction between red and yellow marrow was made by distinguishing between marrow in the torso, head and neck, and marrow in the extremities, using the material index for the regions. Similarly a distinction was made between marrow in trabecular bone regions and in larger bone cavities.

This activity was a time-consuming process in that it involved: (1) scanning numerous cross section plots and computer printouts to identify all material indices, ID labels, surfaces, regions, and point-in-region data to be changed to conform to the improvements discussed previously; then (2) reworking the region specifications because of the changes associated with rounding of bones and introduction of marrow modeling.

2.4.2 Body Joint Modeling

As initially modeled, the geometry at the locations of major body joints (elbows, shoulders, knees, hip, neck, waist) could not easily be manipulated to accommodate body postures other than standing. Because the scheme for manipulating joints to attain other postures would necessarily influence geometrical representations of these joints, it was appropriate to identify the general technique at this time, when the geometry of bones, etc., was being modified. Once the technique for posture scaling was determined, joints were introduced into the model in a manner compatible with its future implementation.

The approach selected was based on subdivision of the body into 15 sections (head, neck, upper torso, mid torso, lower torso, upper arms, lower arms, hands, upper legs, lower legs). At each interface an ellipsoidal surface was defined for one of the body sections, about which the other section rotates. For ball and socket type joints, the spheroidal surface corresponds approximately to the ball, and hence is slightly larger than the bone; for "waist", "neck" or wrist joints joints the ellipsoidal surface spans the full dimensions of the interface. With this scheme the necessary corrections to mass distribution at the joint, to obviate section overlap or creation of a gap, can be made within the ray tracking package, and thus the flexed geometry need not be modeled explicitly. An example of the modification of the interface geometry, as required to accommodate the procedure for approximating posture changes, is presented in Section 3.1.

2.5 FINAL VERIFICATION

The revised and improved CAM model was subjected to a number of tests in an effort to remove any errors introduced in the re-modeling and re-shaping process, similar tests having been run on the converted model prior to its refinement, as described in Section 2.3. An intensive review of computer-drawn cross section plots was also conducted as a means of reaffirming the anatomical correctness of the revised model. In this latter activity, the standard by which the cross section views were measured was the cross section anatomy figures in the medical texts.

The error tests were again conducted separately for each of the 15 body sections into which the model was divided in making provision for the posture change capability. These tests included the "point-in-region" test which was repeated until no error messages were printed and the two types of ray-tracing tests summarized in Section 2.3.1. The first ray-tracing test was to trace numerous rays from one or more points within the body section to the exterior surface, printing error messages for any errors encountered by the ray. In this test the body section mass and surface area were estimated, the values being updated with each additional ray traced, until these quantities converged to specified values with zero errors having been detected. This technique of determining a shutoff value for the number

of rays traced, in lieu of tracing a specified number, ensures that errors that remain undetected are no larger than a given size. For the convergence criteria that were imposed, 5% mass convergence for extended sections such as arms and legs and 2% mass convergence for more uniform sections such as the neck, some 1000-1500 rays were usually traced.

The second ray-tracing test was similar to the first, but involved each point-in-region as the origin. Substantially fewer rays were traced for each such point, but far more points included. In this test, the region masses were computed and output on punched cards for subsequent operations.

2.6 DOSE POINT SELECTION

Techniques were developed for automatic determination of dose point locations in spatially-distributed body organs such as the BFO or bone marrow, gastro-intestinal tract, and the skin. A number of randomly selected locations in each organ were identified and are presented in Section 3.3. These dose point locations were selected randomly because the Monte Carlo technique is an accepted and preferred method for numerical integration over complex distributions with relatively few evaluations of the integrand, and because unbiased selection of dose points for these organs in a systematic fashion would be a formidable task.

2.6.1 Dose Points in Skin

The technique for selecting randomly-located skin dose points was effectively one for sampling randomly from skin area. The procedure consisted of directing rays at the model from points randomly located on an external spherical surface surrounding the model. These rays were random in origin and inward direction and produced a uniform isotropic density within the sphere. Hence their probability of penetrating the CAM geometry at any point was proportional to skin area. Once a penetration was recognized, the surface normal was computed and the coordinates of a point 0.1 mm inward along the normal was determined. Some skin locations are appreciably shadowed by other parts of the body (i.e., the extremeties). Such locations are represented in the list of skin dose points by including

points based on all penetrations (i.e., entry, exit, re-entry, etc.) along each ray intersecting the model. This provision is a requirement to obtain uniformly distributed skin points.

2.6.2 Dose Points in Bone Marrow

The technique for selecting the locations of dose points in the bone marrow or blood-forming organs (BFO) is one of selecting uniformly from BFO mass (volume) as modeled in CAM. These same dose point locations could be used in conjunction with a BFO mass distribution other than the one modeled by adjusting the dose point weights which are provided in Table 12. For example, the listed weights would be scaled by the ratio of BFO region-wise mass values specified by input to the values built into the random selection, different ratios thus being determined for each BFO dose point.

The dose point random-selection procedure is a rejection technique and consists of selecting the three coordinates of a point randomly and testing whether it is located in a BFO region, either trabecular bone or marrow. Hence the frequency with which a BFO region is selected is proportional to its volume relative to the total volume within which points are randomly selected. This frequency was enhanced by working with individual sections of the model and by restricting x, y, and z values to a rectangular box enclosing the section. With this procedure BFO dose points were selected at an approximate rate of one every 10 seconds on the CDC 6500 computer.

2.6.3 Dose Points in Gastrointestinal Tract

The technique for selecting dose points within the gastrointestinal tract was identical to that used for the BFO.

Section 3
CAM MODEL DESCRIPTION

3.1 GEOMETRICAL DESCRIPTION

The CAM model is defined by some 1100 unique, unduplicated surfaces which form the boundaries of some 2450 regions. Each surface is identified by specification of the numerical values of the coefficients of the generalized quadratic equation used to describe surfaces. Each region is identified by the specification of the indices of the surfaces that bound it, by the coordinates of a point internal to the region, by the index of the material composition of which the region is comprised and by the region density. The geometry is a continuous system in which there are no intended overlapping regions or undefined regions within the ellipsoidal surface forming the closed outer boundary of the total geometric system (some relatively insignificant overlaps and/or holes undoubtedly do remain in a system this complex, despite the extensive error tests that have been conducted to detect them). On the average each surface bounds 15 regions and, conversely, each region is bounded by an average of 7 surfaces. The total model requires some 6000 data cards (whereas 11,000 cards were required for the original standing version).

3.1.1 Subsections and Joints

The geometric data has been divided into 15 subgeometries for some applications, these subgeometries corresponding to major body sections connected by "joints," such as would be required to introduce a change in posture from the standing man currently modeled. (Such a posture change capability would be provided via routines in the CAMERA program, but is not presently available.) This division is illustrated in Figure 2, as is the coordinate system used to define the geometrical data.

The geometry at body joint locations has been modeled so that relative motion of the adjacent sections will not create either a separation

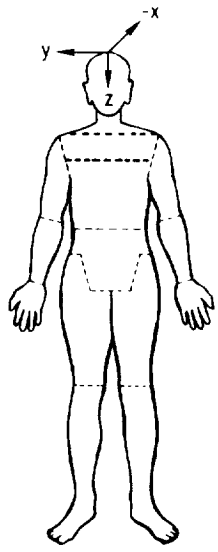

Figure 2. Body Sections and Joint Locations

(discontinuity) or overlapping of the sections. Corrections for overlapping are made by the geometry routine in the CAMERA code. The separation or void problem has been treated in a somewhat different manner for different types of joints, but is generally as shown for a "ball and socket" type joint illustrated in Figure 3. The "ball" which is the head of the humerus protrudes across the plane surface interfaces between body sections. Arm rotation would require rotation on this spheriodal surface. Separation, as the arm is raised away from the body, is prevented by providing a second spheroidal region which also rotates with the arm section within the torso and which grows as the arm is raised and fills the space between the two interface planes. Figure 3 also shows the humerus after marrow regions were added; the apparent taper to the humerus is the result of the cross section plane cutting diagonally across the bone.

3.1.2 Identifiers

In addition to the numerical data that define surfaces and regions, the model description also contains alphameric data for each region in which a coded identifier is provided. Such descriptors indicate the body section to which

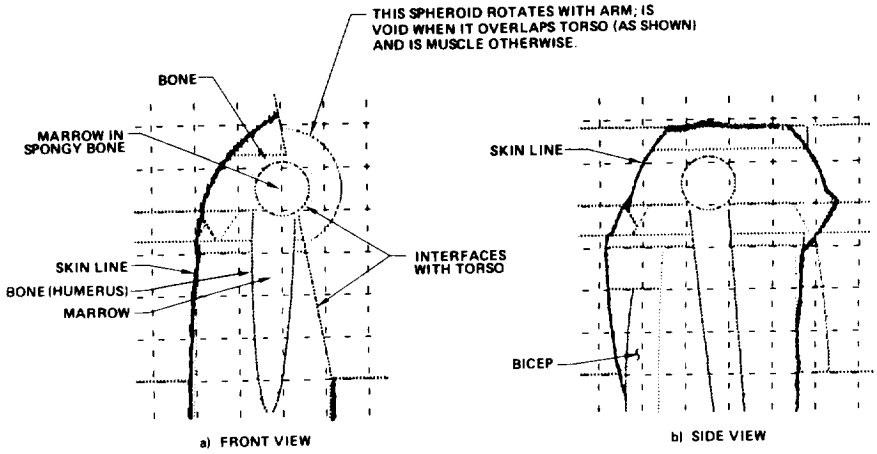

Figure 3. Cross Sections Through Right Shoulder

the specific region belongs and the anatomical name of the piece. For example, the pieces of the geometry comprising the humerus in the right upper arm are labeled RUAHUM01, .02, ...etc. At the present time these identifiers are used only to collate data cards, but their eventual use in preparing specialized plots of specific body parts is contemplated; this would require some modifications to CAMERA. Identifiers are listed in Table 2.

3.1.3 Materials

Each solid region is assigned a material index that defines its chemical composition. There are nine different compositions in the revised CAM model, replacing the five used in the original version. The material indices serve the additional function of distinguishing among different organs which have the same assigned composition, or distinguishing among various locations of a distributed organ, as the BFO. The materials code is given in Table 3, in which all entries with the identical last digit have the same composition. This expanded materials code capability makes it possible to prepare cross section plots that indicate the boundaries between different organs (different materials) without showing all boundaries of all regions.

Table 2 (Page 1 of 4)

ALPHAMERIC REGION IDENTIFIERS

HEAD

HDMUSC	Muscle regions 1-99
MUS1	Muscle regions 100-199
MUS2	Muscle regions 200-299
MUS3	Muscle regions 300-399
REAR	Right ear
LEAR	Left ear
NOSE	Nose
TONG	Tongue
BRAI	Brain
REYE	Right eye
LEYE	Left eye
CVER	Cervical vertebrae
SCOR	Spinal Cord
SBFO	Spinal BFO (in CVER)
SKUL	Skull
SKBF	Skull BFO
MAND	Mandible
MBFO	Mandible BFO
TEET	Teeth
SINU	Sinuses
PHAR	Pharynx
NASV	Nasal void
ORAV	Oral void
EXVO	External void
bLDV	Lower disconnect void (at neck)

NECK

NKMUSC	Muscle regions 1-99
MUS1	Muscle regions 100-199
CVER	Cervical vertebrae
SBFO	Spinal BFO (in CVER)
SCOR	Spinal cord
ESOP	Esophagus
TRAC	Trachea
THYR	Thyroid
bEXV	External void
bUDV	Upper disconnect void (at head)
bLDV	Lower disconnect void (at upper torso)

Table 2 (Page 2 of 4)

ALPHAMERIC REGION IDENTIFIERS

UPPER TORSO

UTMUSC	Muscle
THYR	Thyroid
CLAV	Clavicle
bBFO	Clavicle or scapula BFO
SCAP	Scapula
RIBS	Ribs
RBFO	Rib BFO
TVER	Thoracic vertebrae
SBFO	Spinal BFO (in TVER)
SCOR	Spinal cord
LUNG	Lung
ESOP	Esophagus
TRAC	Trachea
bEXV	External void
RADV	Right arm disconnect void
LADV	Left arm disconnect void
bUDV	Upper disconnect void (at neck)
bLDV	Lower disconnect void (at mid torso)

MID TORSO

MTMUSC	Muscle
RIBS	Ribs
RBFO	Rib BFO
TVER	Thoracic vertebrae
LVER	Lumbar vertebrae
SCOR	Spinal cord
HEAR	Heart
LUNG	Lung
LIVR	Liver
STOM	Stomach
SPLE	Spleen
PANC	Pancreas
KIDN	Kidney
INTS	Intestine
bEXV	External void
RADV	Right arm disconnect void
LADV	Left arm disconnect void
bUDV	Upper disconnect void (at upper torso)
bLDV	Lower disconnect void (at lower torso)

Table 2 (Page 3 of 4)

ALPHAMERIC REGION IDENTIFIERS

LOWER TORSO

LTMUSC	Muscle regions 1-99
MUS1	Muscle regions 100-199
SCOR	Spinal Cord
LVER	Lumbar vertebrae
SBFO	Spinal BFO (in LVER)
PELV	Pelvis
PBFO	Pelvis BFO
BLAD	Bladder
INTS	Intestine
SCRO	Scrotum
bEXV	External void
bUDV	Upper disconnect void
RLDV	Right leg disconnect void
LLDV	Left leg disconnect void
RADV	Right arm disconnect void
LADV	Left arm disconnect void
bLDV	Lower disconnect void

RIGHT UPPER ARM (LEFT SIMILAR)

RUAMUS	Muscle
HUM	Humerus
BFO	Humerus BFO
EXV	External void
UDV	Upper disconnect void (at upper torso)
TDV	Torso disconnect void
LDV	Lower disconnect void (at forearm)

RIGHT FOREARM (LEFT SIMILAR)

RFAMUS	Muscle
RAD	Radius
ULN	Ulna
BNE	Bone
BFO	Radius and ulna BFO
EXV	External void
UDV	Upper disconnect void (at upper arm)
TDV	Torso disconnect void
LDV	Lower disconnect void (at hand)

Table 2 (Page 4 of 4)

ALPHAMERIC REGION IDENTIFIERS

RIGHT HAND (LEFT SIMILAR)

RHMUS	Muscle
BN1	Bone in fingers
BN2	Bone in fingers
BN3	Bone in fingers
BN4	Bone in fingers
BN5	Bone in fingers
BFO	BFO
BNE	Bone in hand and wrist
WRI	Wrist
EXV	External void
TDV	Torso disconnect void
LDV	Lower disconnect void
UDV	Upper disconnect void

RIGHT UPPER LEG (LEFT SIMILAR)

RULMUS	Muscle
BNE	Bone
HIP	Hip
BFO	BFO
FEM	Femur
KNE	Knee
EXV	External void
UDV	Upper disconnect void
IDV	Inner disconnect void
HDV	Hand disconnect void
LDV	Lower disconnect void

RIGHT LOWER LEG (LEFT SIMILAR)

RLLMUS	Muscle regions 1-99
MU1	Muscle regions 100-199
BNE	Bone
KNE	Knee
TIB	Tibia
FIB	Fibula
BFO	BFO
EXV	External void
TDV	Torso disconnect void
UDV	Upper disconnect void

Table 3 (Page 1 of 2)

MATERIALS CODE

Index	Material	Density (gm/cm^3)
1	Void (External)	0
11	Void (Internal)	0
21	Void (Disconnect)	0
2	Lung	0.257
4	Intestine	0.451
5	Muscle	1.06
6	Bone	1.75
7	Red Marrow (Torso)	0.918
17	Yellow Marrow (Limbs)	0.918
8	Skeleton* (Torso)	1.50
18	Skeleton* (Limbs)	1.50
9	Tissue	1.0
3	Brain	1.058
13	Spinal Cord	1.058
23	Eye	1.058
33	Thyroid	1.058
43	Heart	1.058
53	Stomach	1.058
63	Liver and Gall Bladder	1.058
73	Spleen	1.058
83	Kidneys	1.058

Table 3 (Page 2 of 2)
MATERIALS CODE

Index	Material	Density (gm/cm^3)
93	Bladder	1.058
103	Pancreas	1.058
113	Testes	1.058

*Bone/marrow homogenization to represent spongy bone.

Three types of void are identified in the materials code. "External void" denotes regions that are defined only to provide continuity in the geometric description from the body exterior to the outer surface. The distinction between external and "internal voids" allows recognition of "skin" in ray tracing calculations, as in selection of skin dose points, because skin is always bounded by external void. "Disconnect voids" are defined only for individual body sections and disappear when body sections are joined to form a whole model. They are dummy void regions which fill the volume occupied by an adjacent body section when the sections are assembled.

3.1.4 Cross Section Views

Computer-drawn cross sections through the CAM model are presented in Figures 4-118. The cross sections were prepared separately for each of the 10 unique body sections (the five left-limb sections are not illustrated) and used the CAMERA plotting option where only boundaries between regions of dissimilar material are shown. All views for each section have been drawn to the same scale to facilitate their review. The grid displayed in the figures is the CAM coordinate system. The general arrangement of cross section views is by body section, with vertical cross sections (x=constant or y=constant) being presented first. Horizontal cross sections (z=constant) are then shown, these views being at one inch intervals through head, torso and

Note: Text continued on Page 89.

CR145

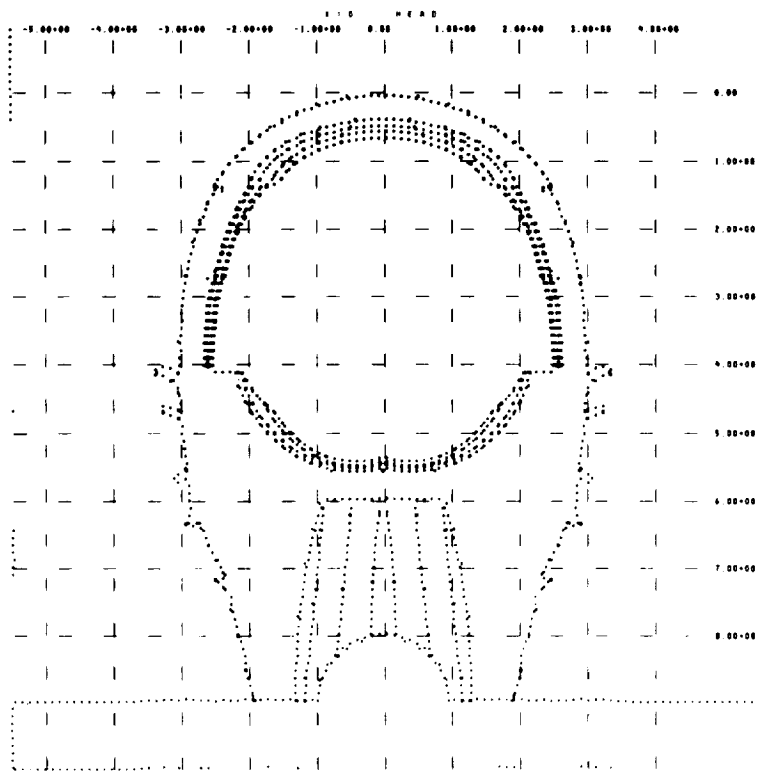

Figure 4. Vertical Cross Section Through the Head at x = 0

CR145

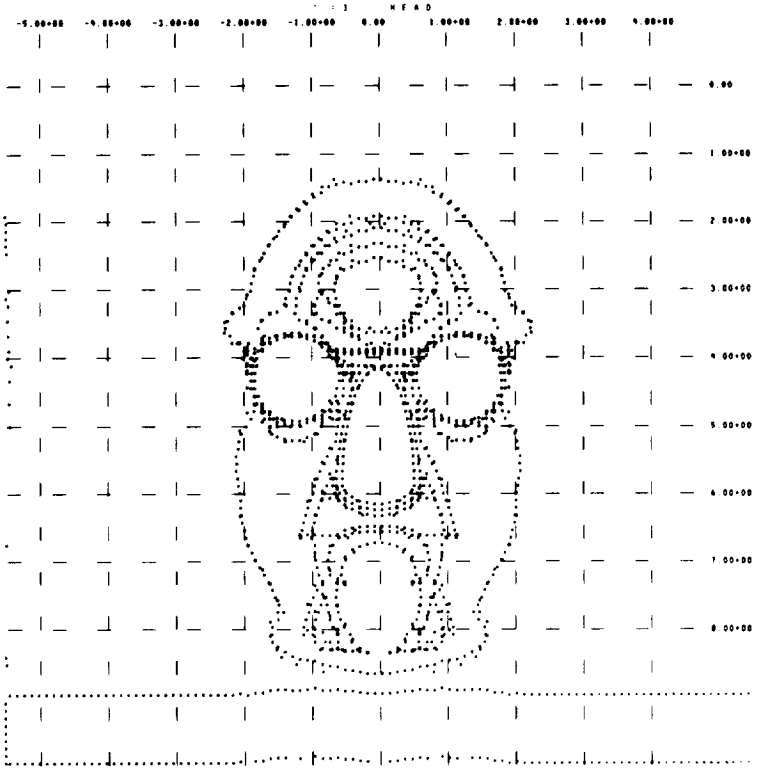

Figure 5. Vertical Cross Section Through the Head at x = 3

CR145

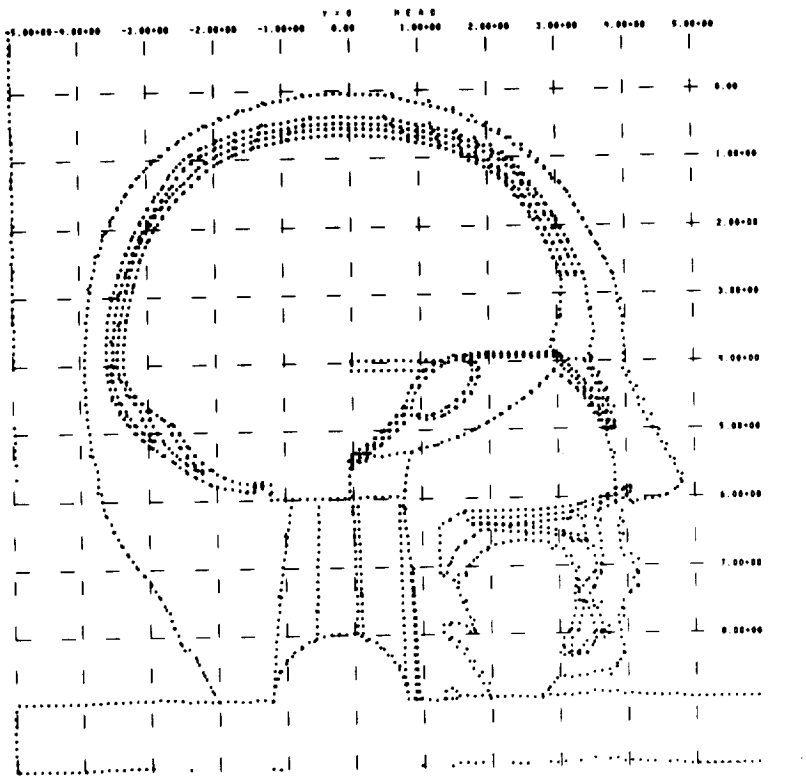

Figure 6. Vertical Cross Section Through the Head at y = 0

CR145

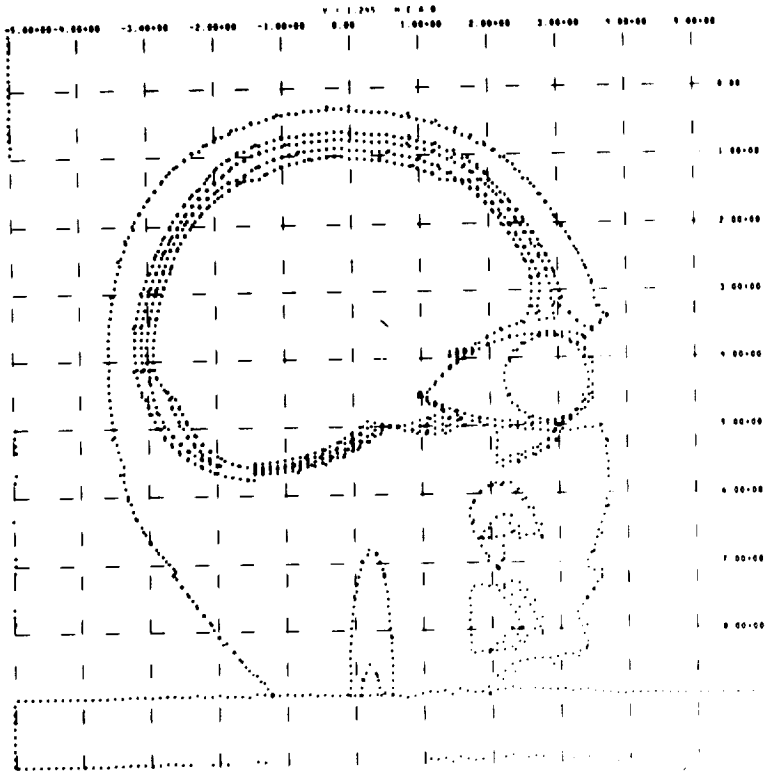

Figure 7. Vertical Cross Section Through the Head at y = 1.245

CR145

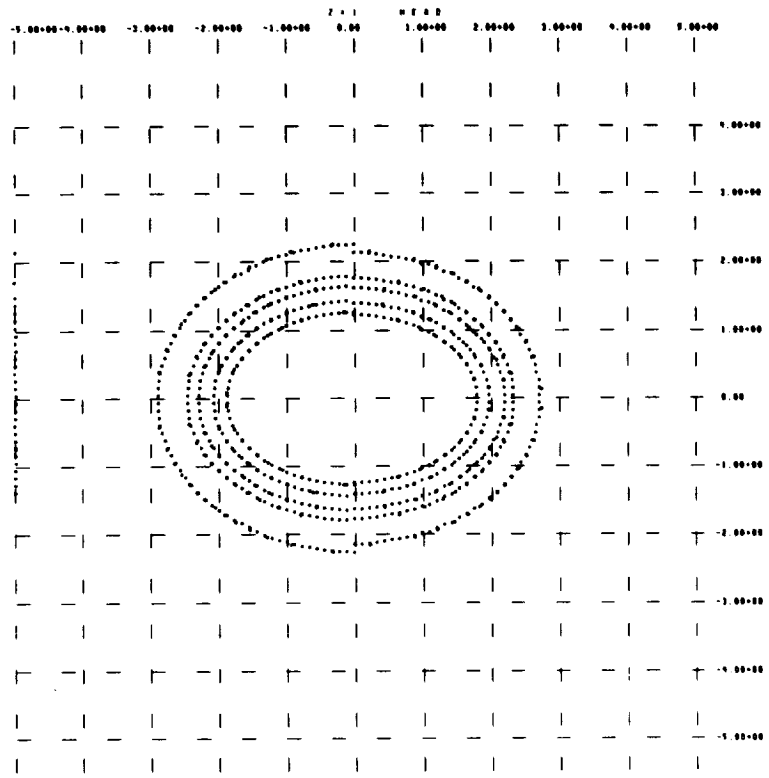

Figure 8. Horizontal Cross Section Through the Head at z = 1

CR145

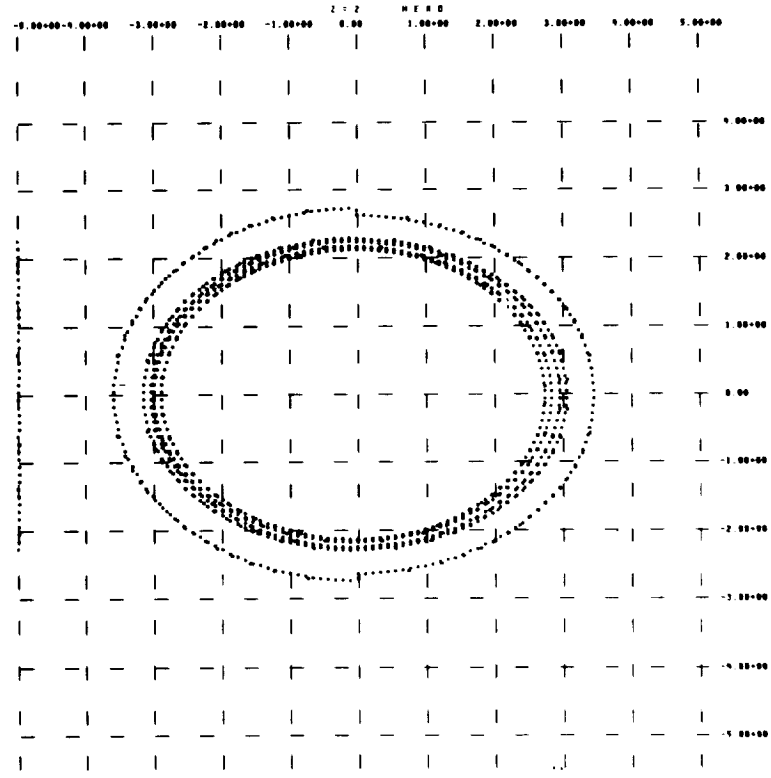

Figure 9. Horizontal Cross Section Through the Head at z = 2

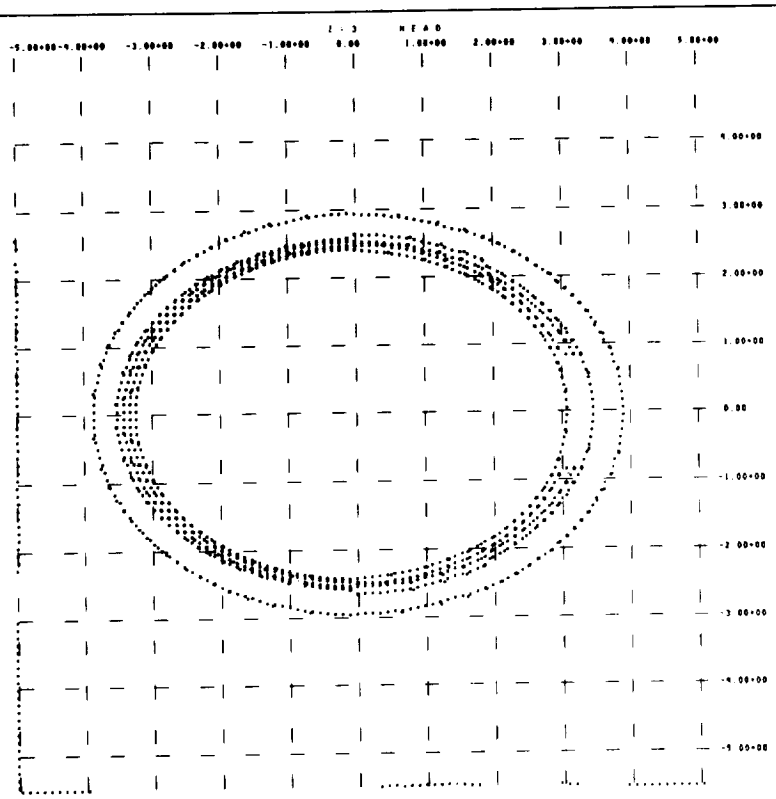

Figure 10. Horizontal Cross Section Through the Head at z = 3

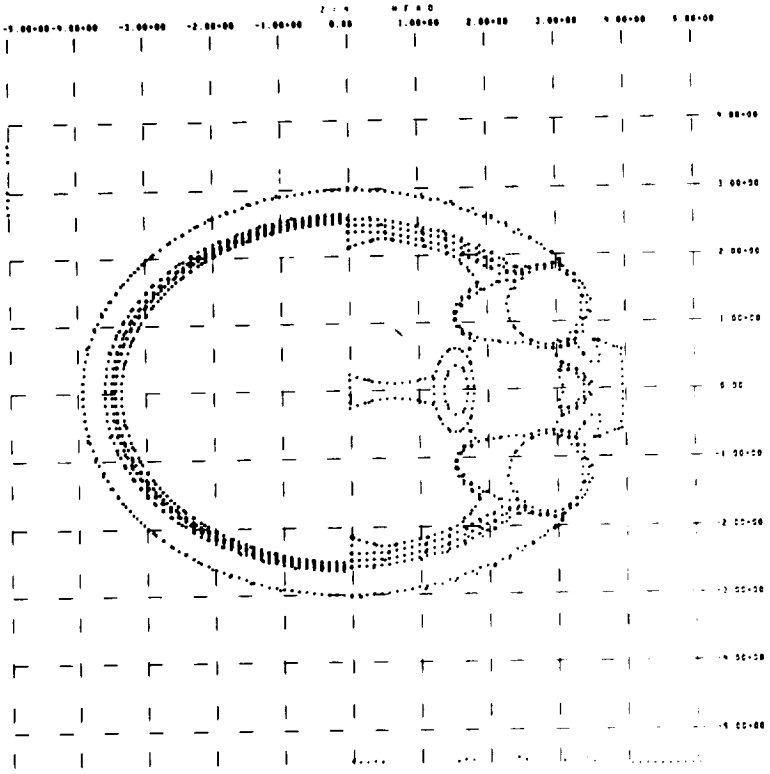

Figure 11. Horizontal Cross Section Through the Head at z = 4

CR145

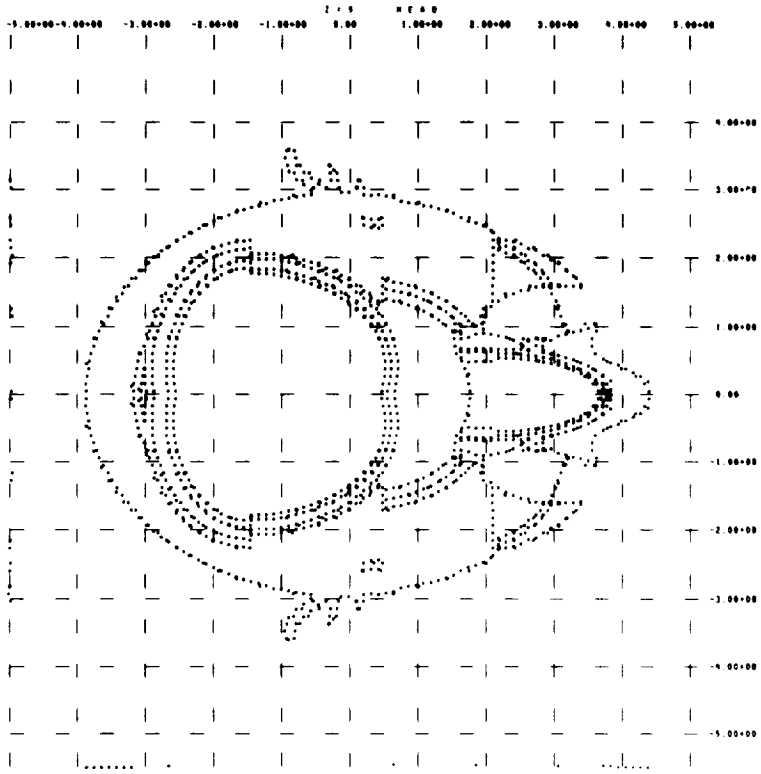

Figure 12. Horizontal Cross Section Through the Head at z = 5

CR145

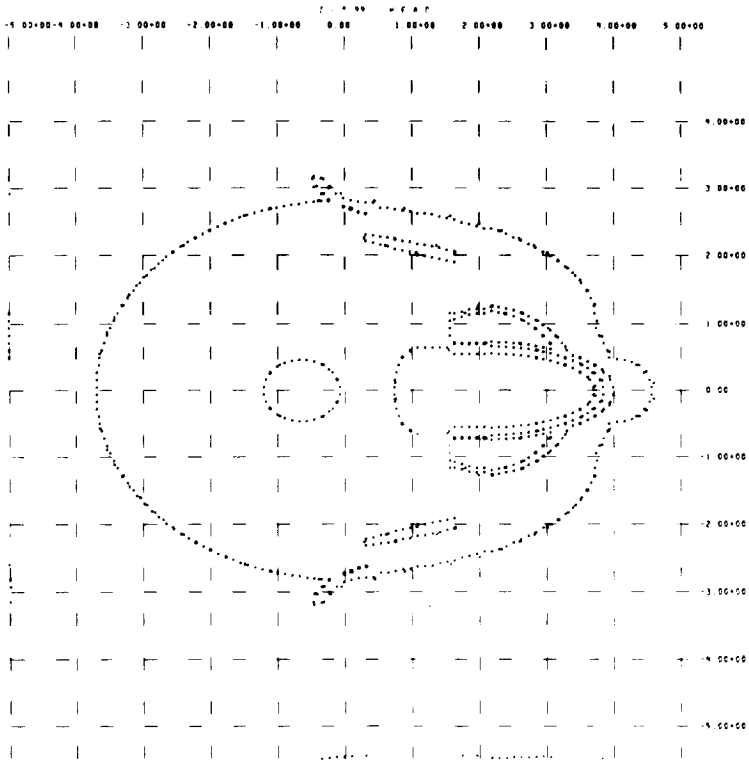

Figure 13. Horizontal Cross Section Through the Head at z = 5.99

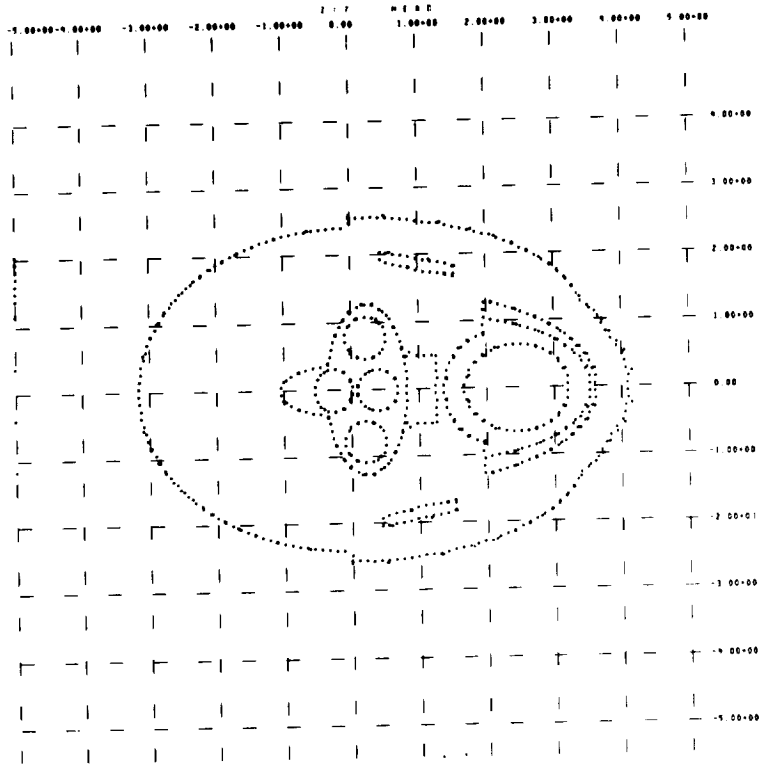

Figure 14. Horizontal Cross Section Through the Head at z = 7

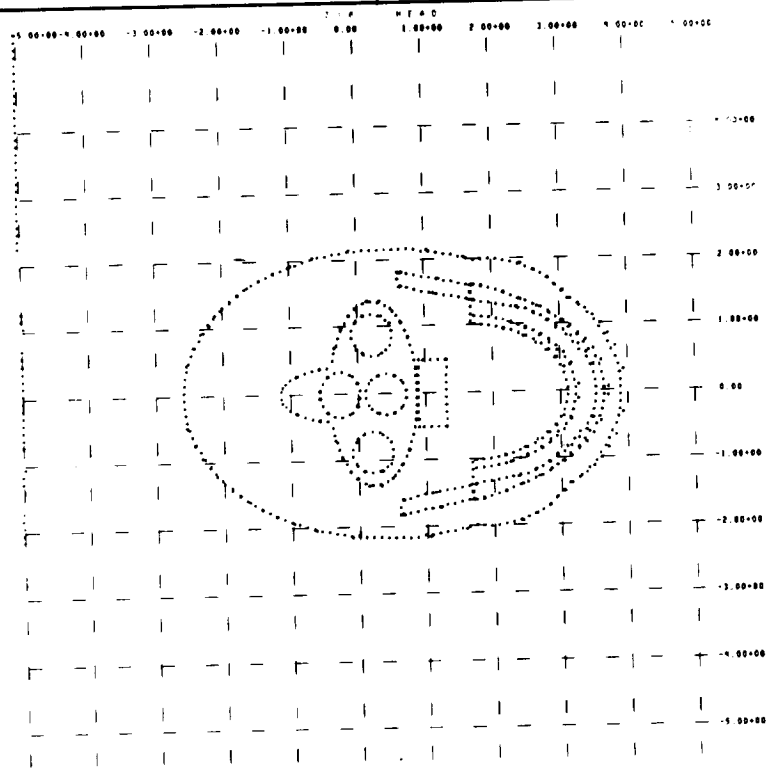

Figure 15. Horizontal Cross Section Through the Head at z = 8

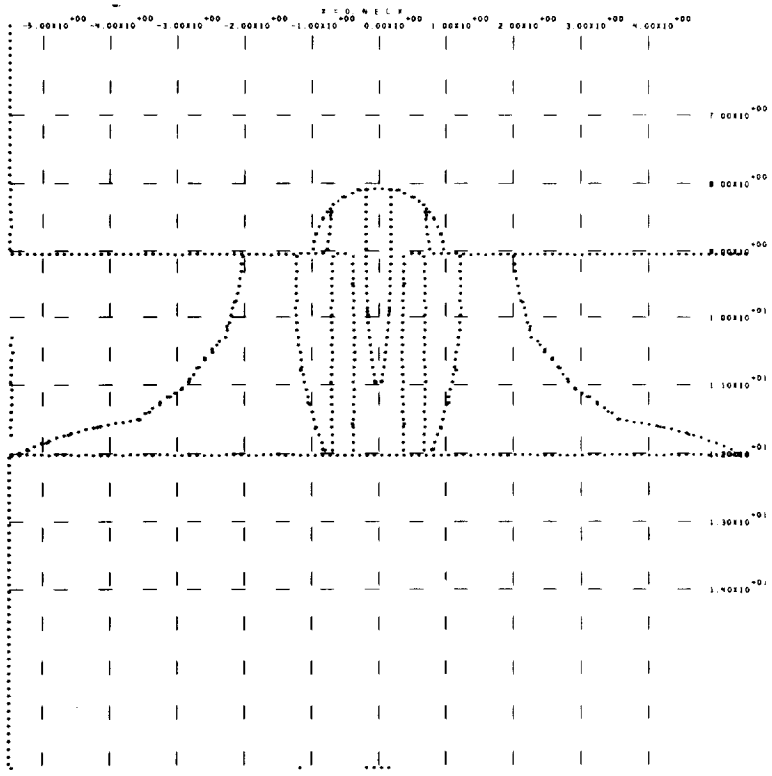

Figure 16. Vertical Cross Section Through the Neck at x = 0

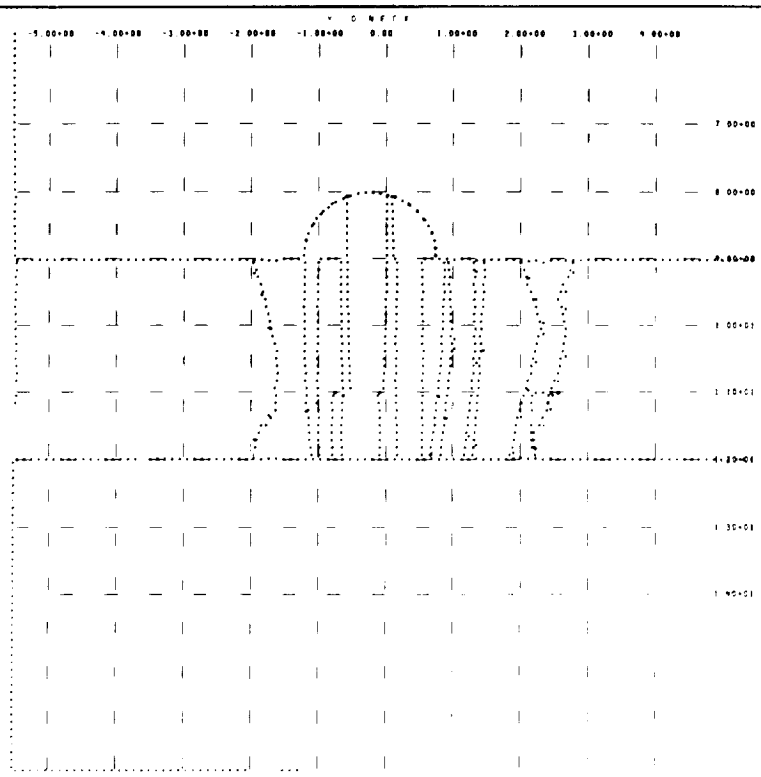

Figure 17. Vertical Cross Section Through the Neck at y = 0

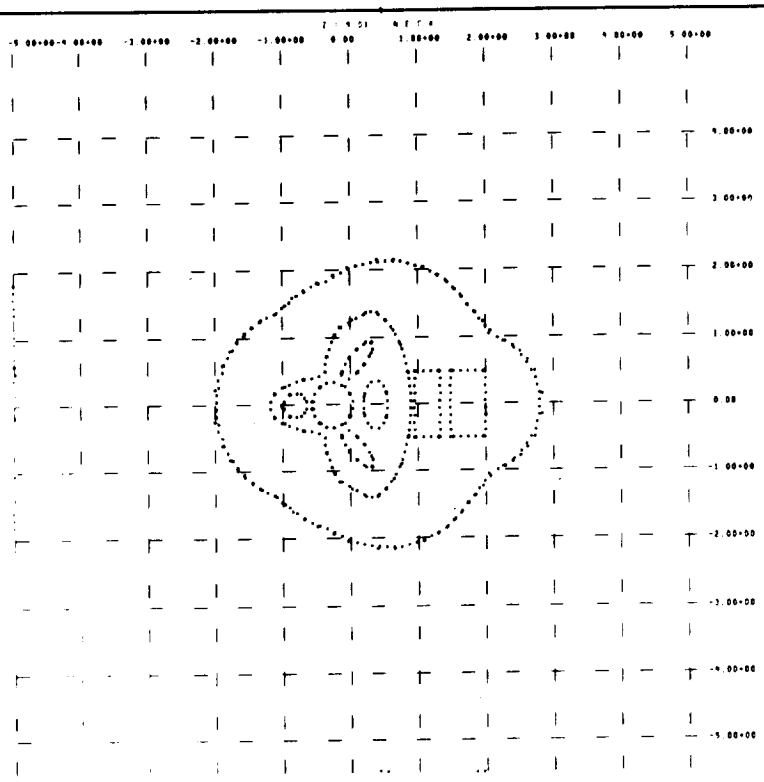

Figure 18. Horizontal Cross Section Through the Neck at z = 9.01

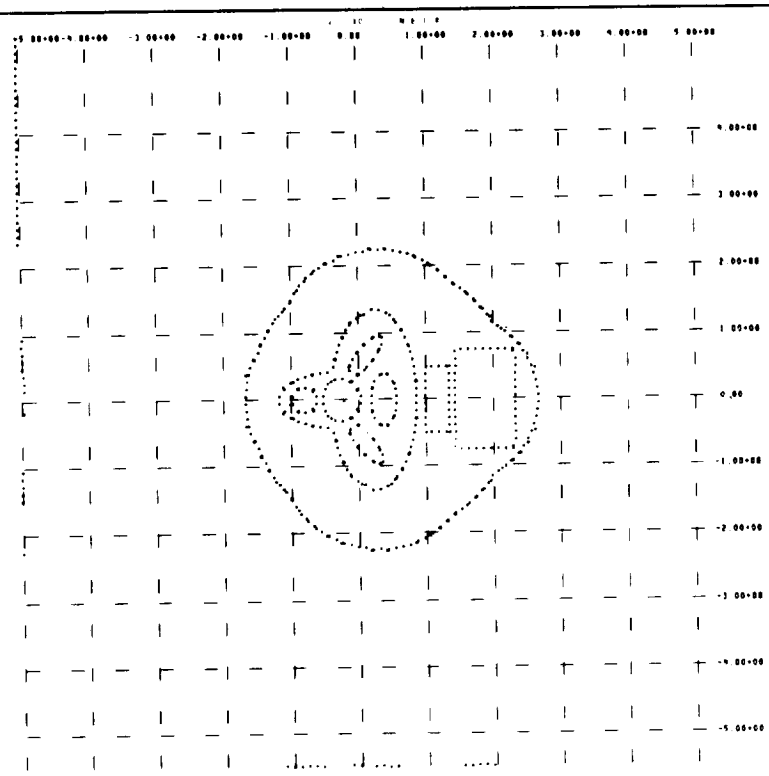

Figure 19. Horizontal Cross Section Through the Neck at z = 10

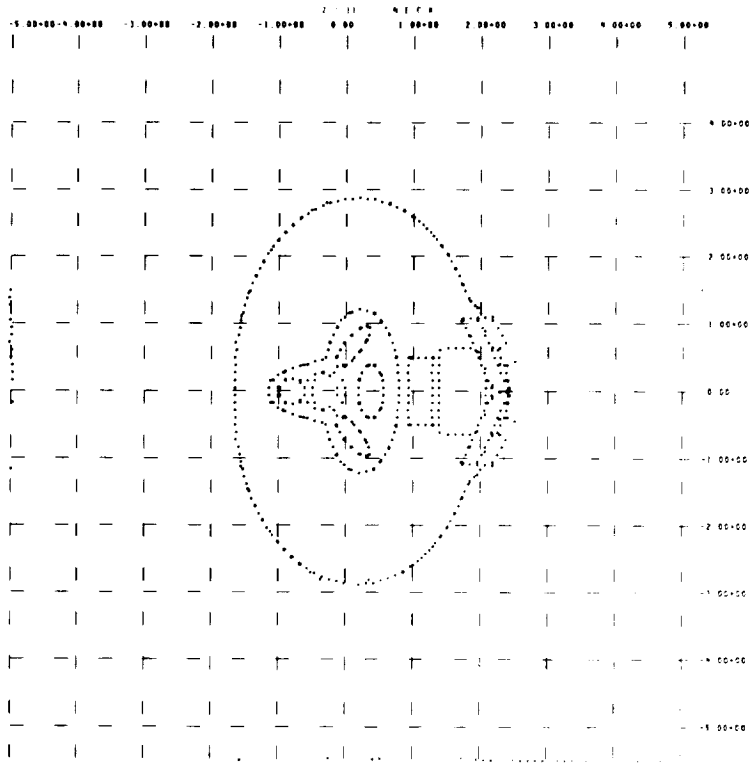

Figure 20. Horizontal Cross Section Through the Neck at z = 11

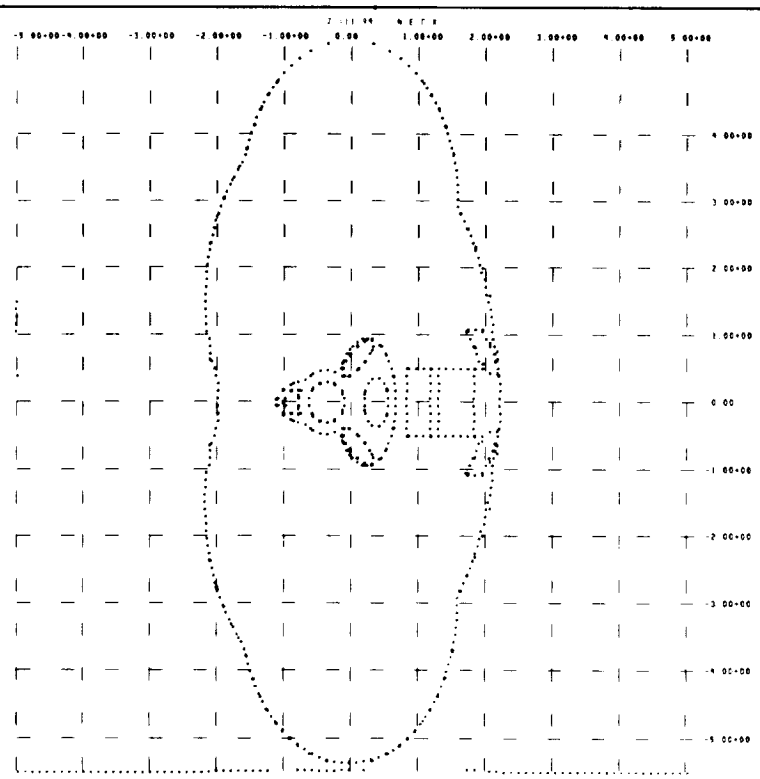

Figure 21. Horizontal Cross Section Through the Neck at z =11.99

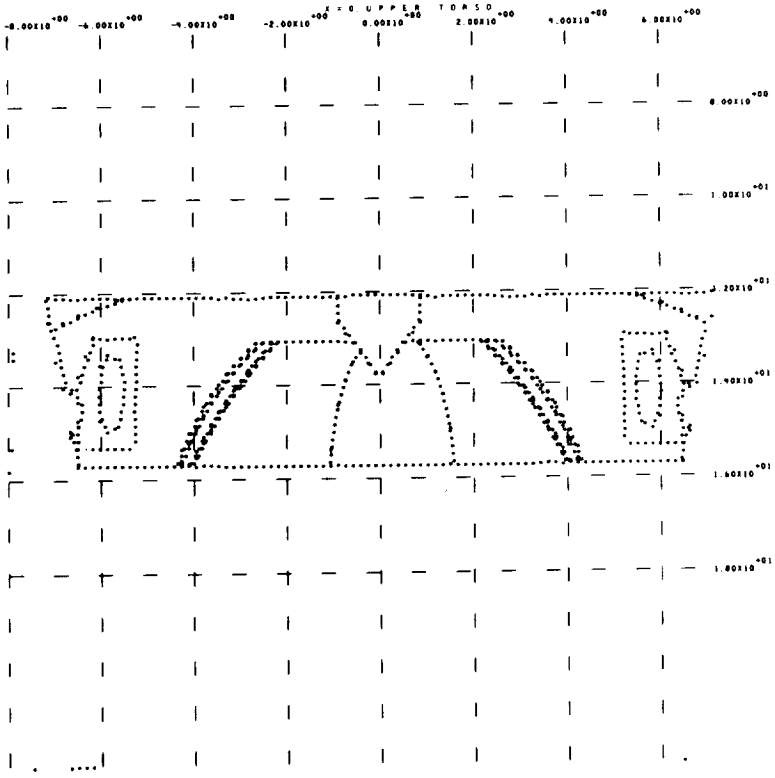

Figure 22. Vertical Cross Section Through the Upper Torso at x = 0

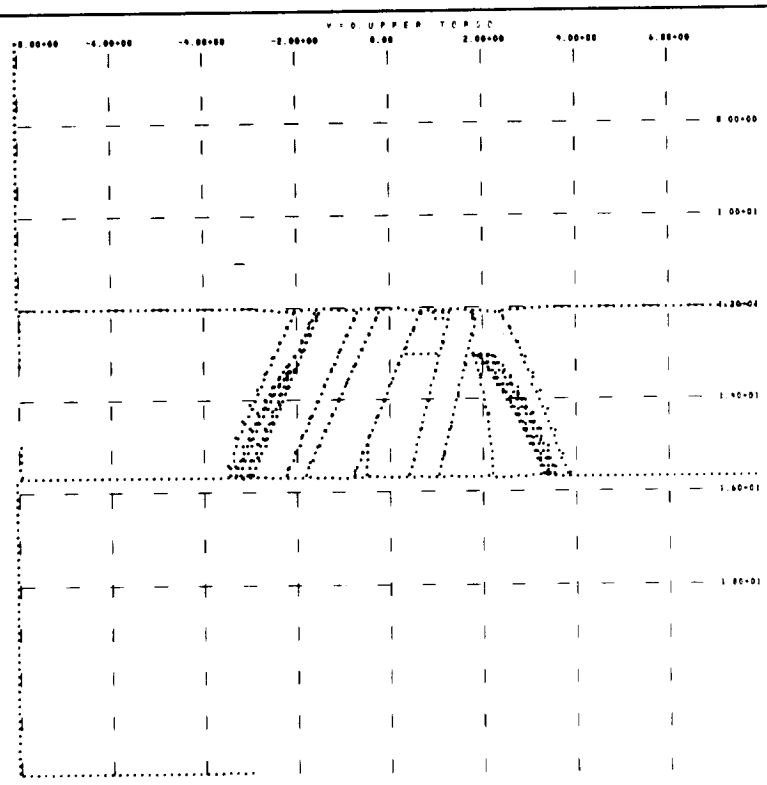

Figure 23. Vertical Cross Section Through the Upper Torso at y = 0

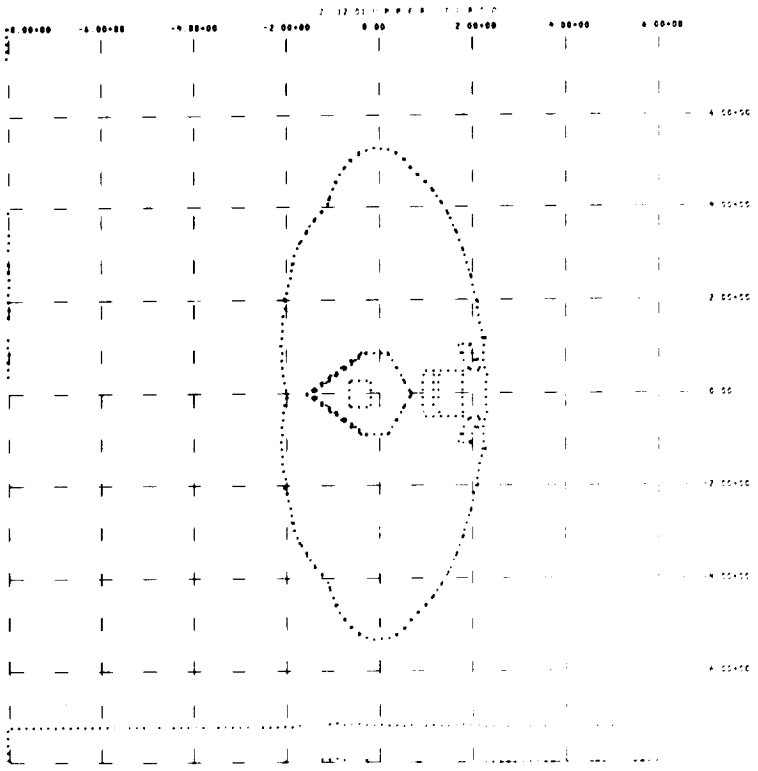

Figure 24. Horizontal Cross Section Through the Upper Torso at z = 12.01

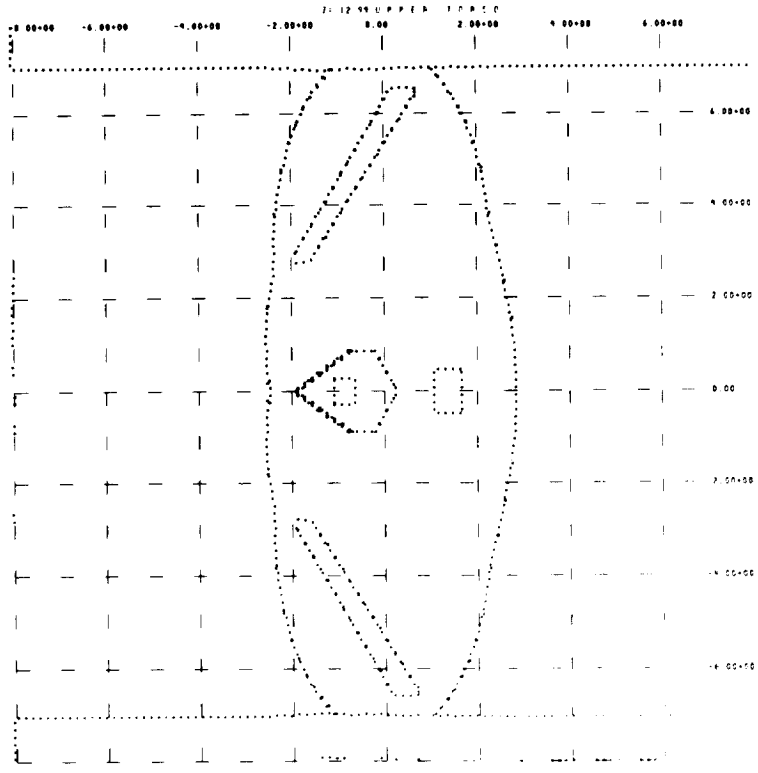

Figure 25. Horizontal Cross Section Through the Upper Torso at z = 12.99

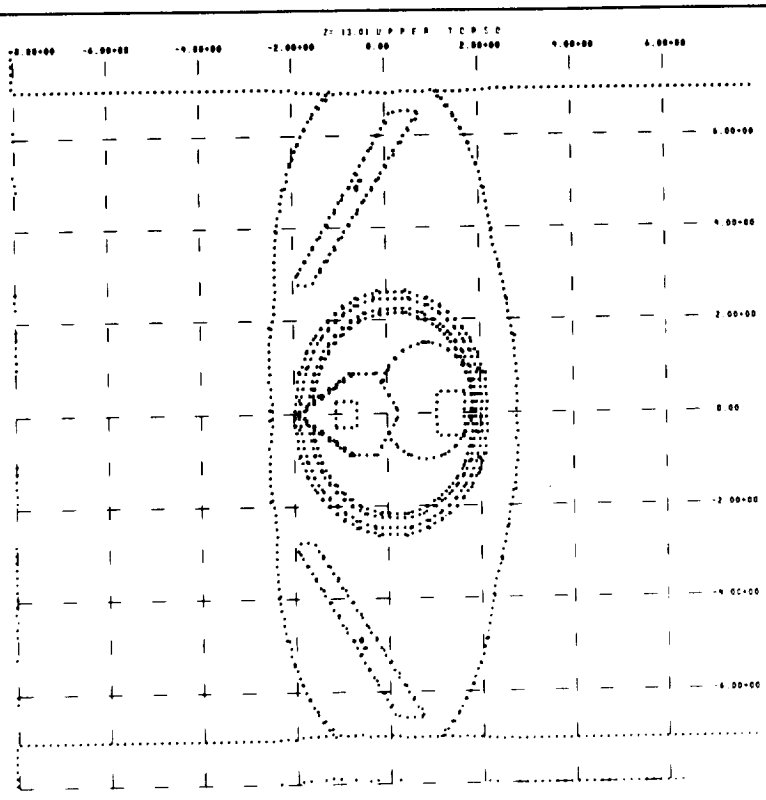

Figure 26. Horizontal Cross Section Through the Upper Torso at z = 13.01

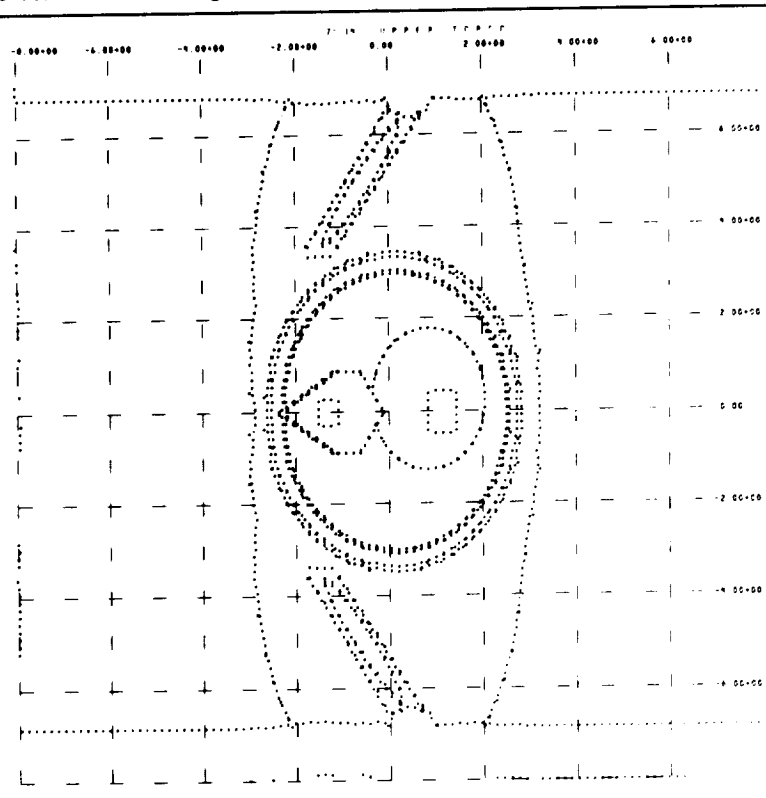

Figure 27. Horizontal Cross Section Through the Upper Torso at z - 14

CR145

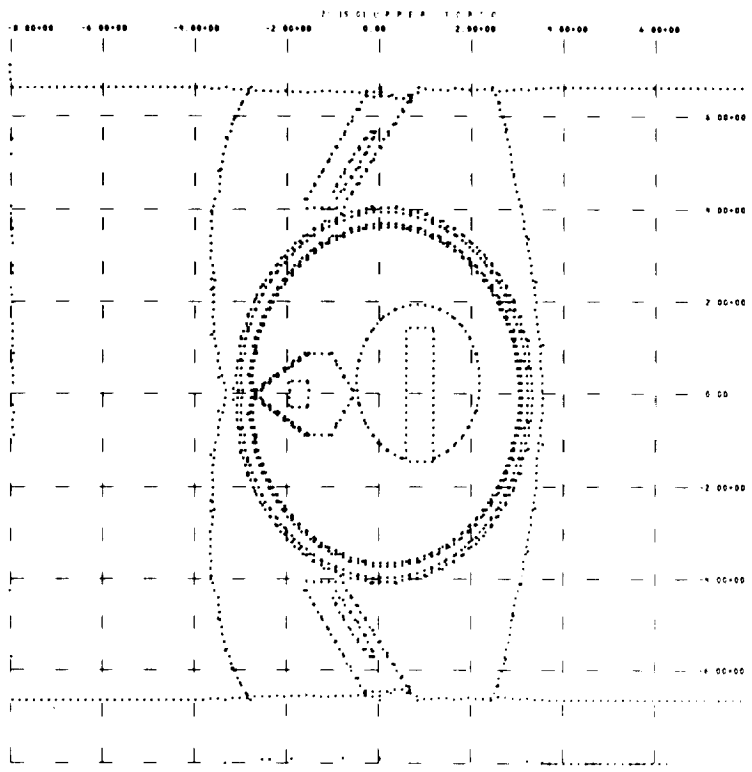

Figure 28. Horizontal Cross Section Through the Upper Torso at z = 15.01

CR145

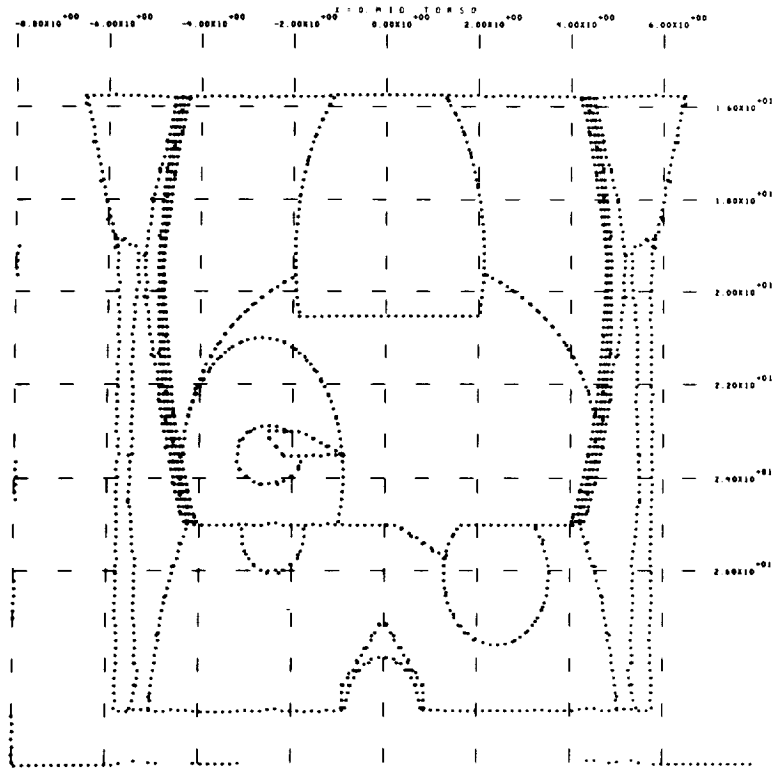

Figure 29. Vertical Cross Section Through the Mid Torso at x = 0

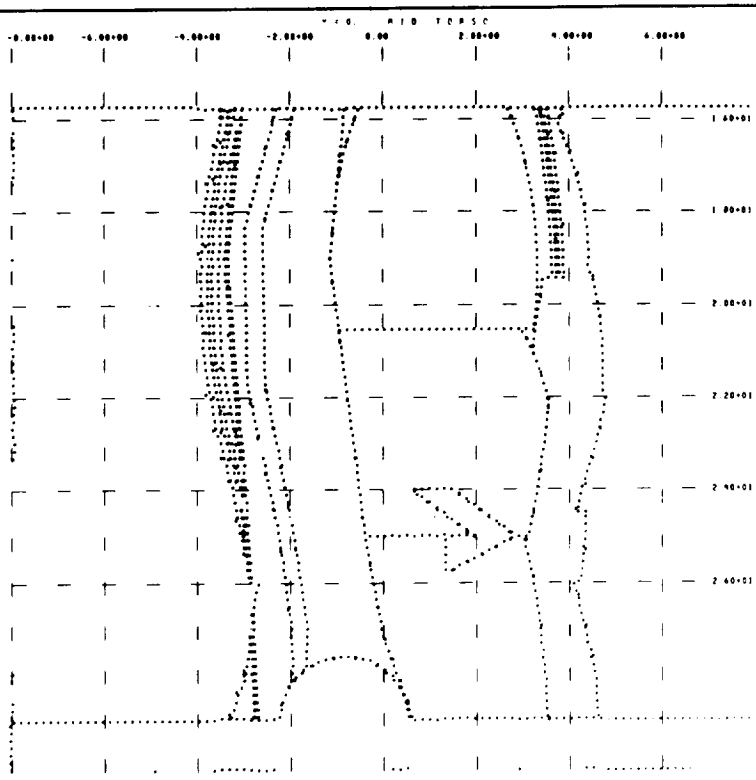

Figure 30. Vertical Cross Section Through the Mid Torso at y = 0

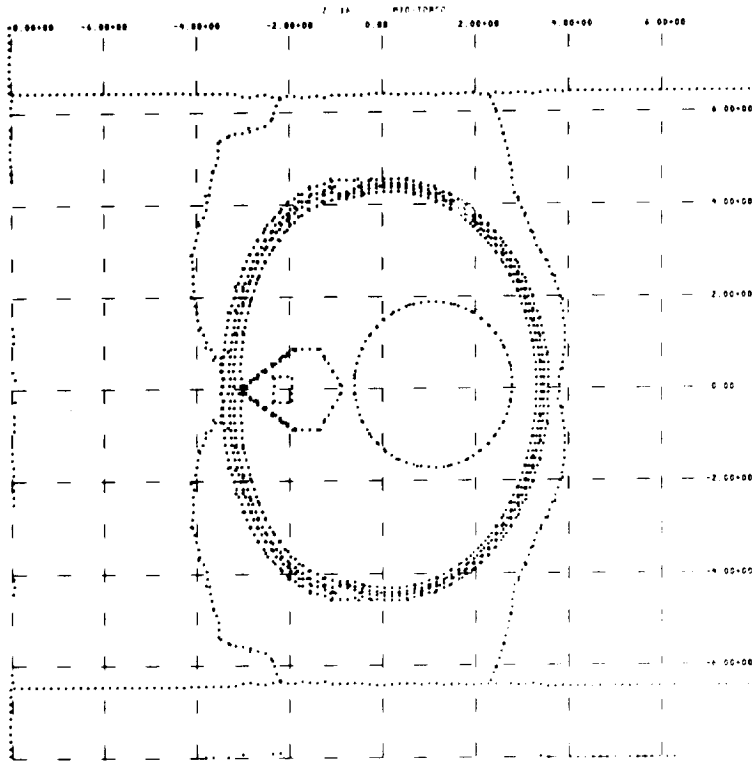

Figure 31. Horizontal Cross Section Through the Mid Torso at z = 16

CR145

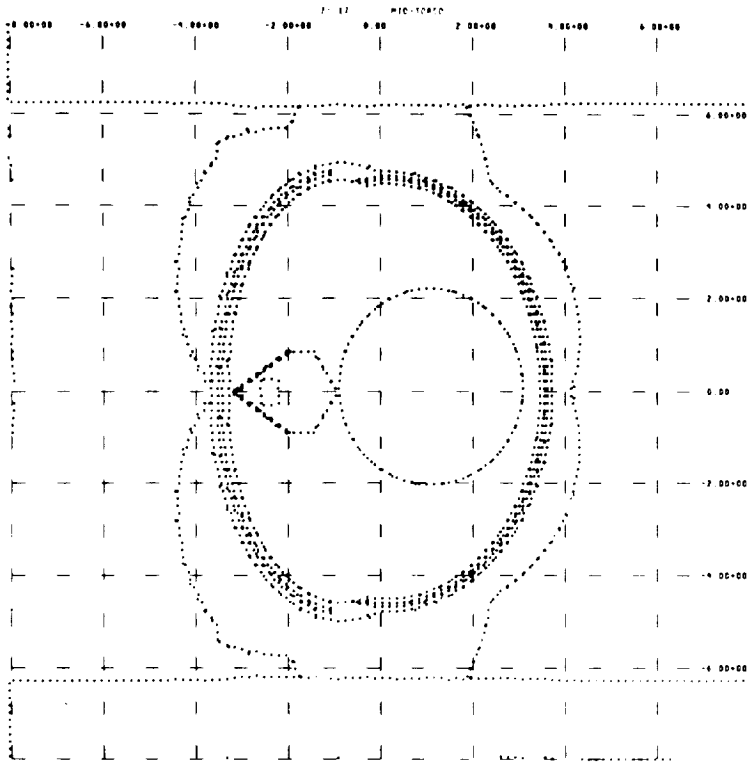

Figure 32. Horizontal Cross Section Through the Mid Torso at z = 17

CR145

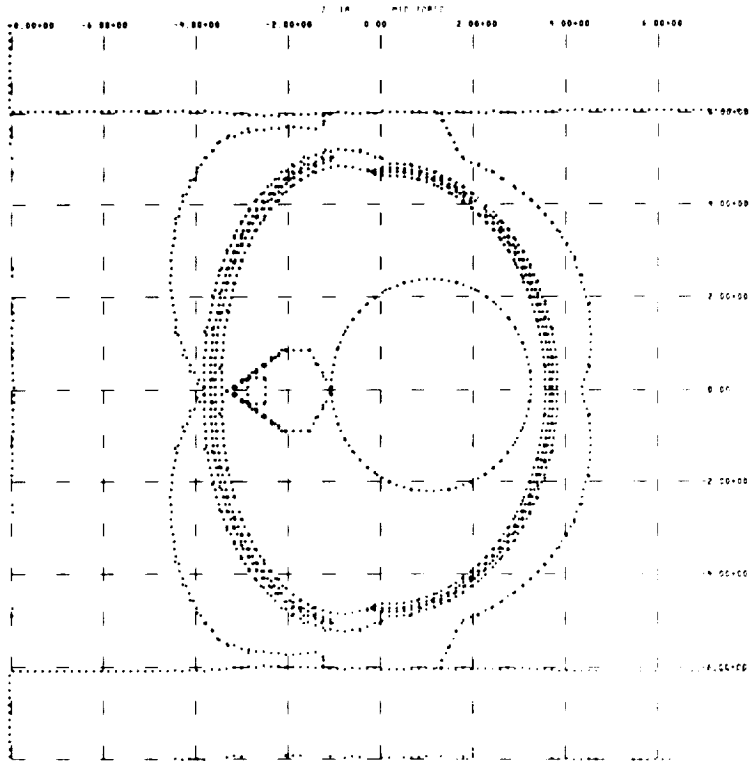

Figure 33. Horizontal Cross Section Through the Mid Torso at z = 18

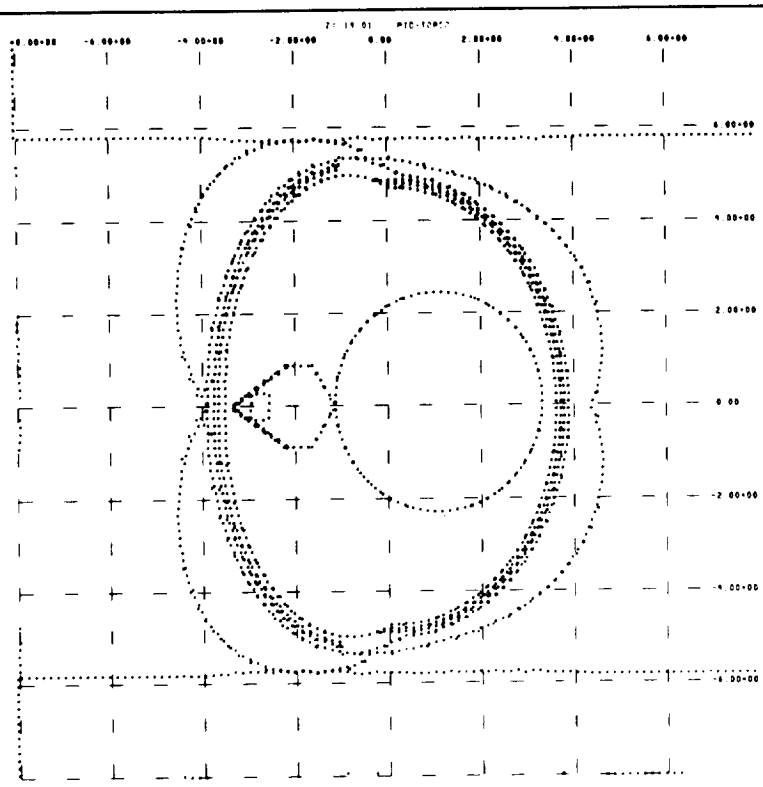

Figure 34. Horizontal Cross Section Through the Mid Torso at z = 19.01

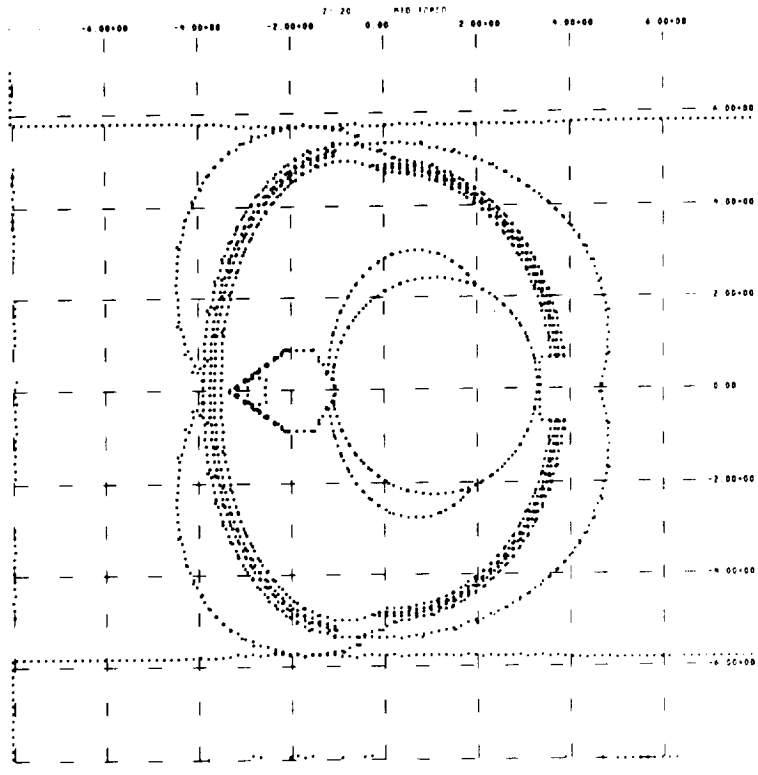

Figure 35. Horizontal Cross Section Through the Mid Torso at z = 20

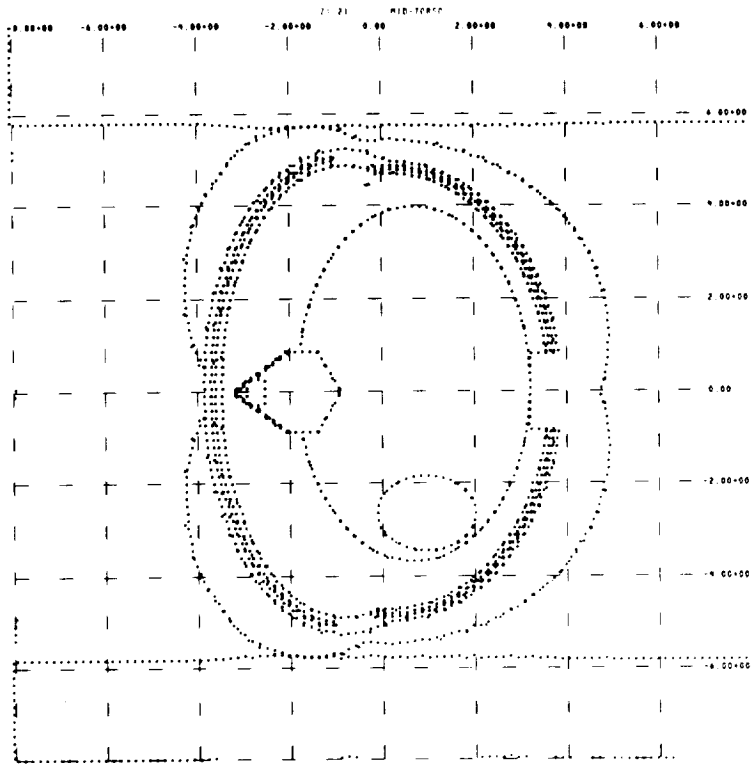

Figure 36. Horizontal Cross Section Through the Mid Torso at z = 21

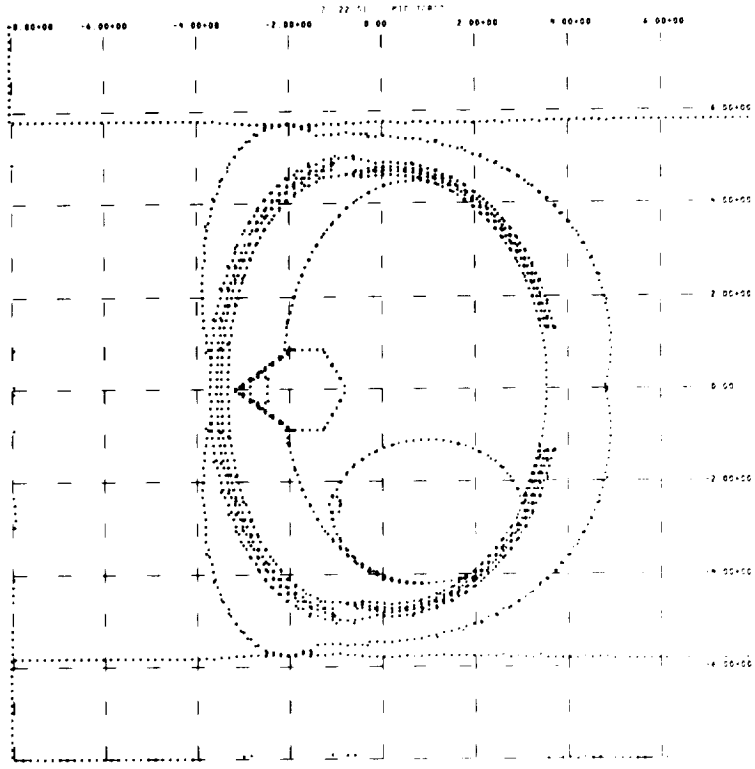

Figure 37. Horizontal Cross Section Through the Mid Torso at z = 22.01

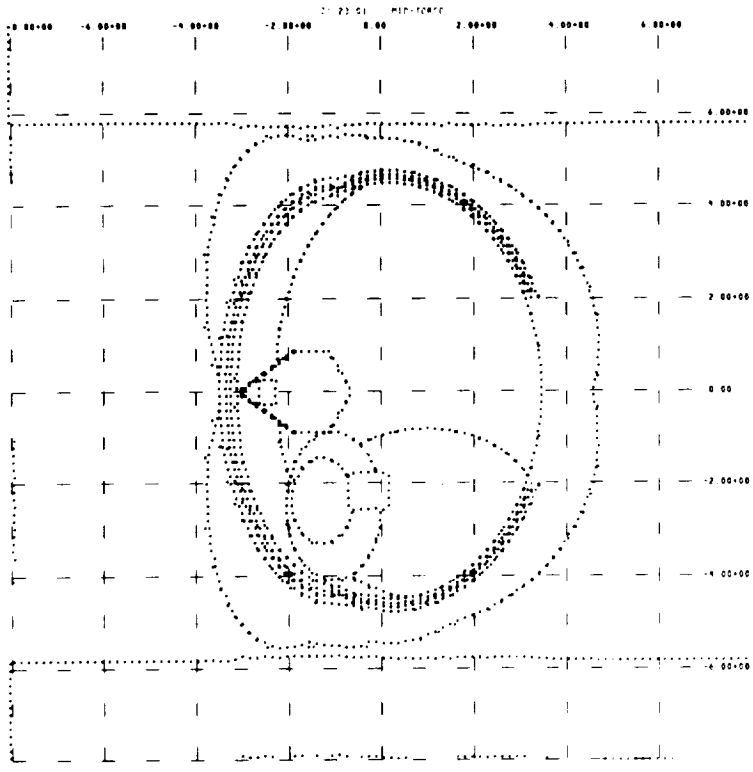

Figure 38. Horizontal Cross Section Through the Mid Torso at z = 23.01

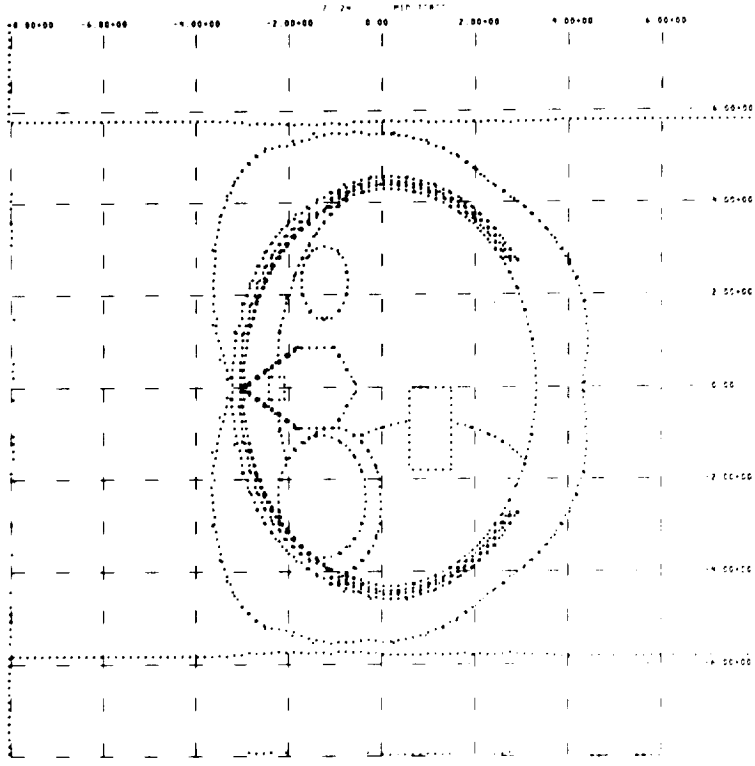

Figure 39. Horizontal Cross Section Through the Mid Torso at z = 24

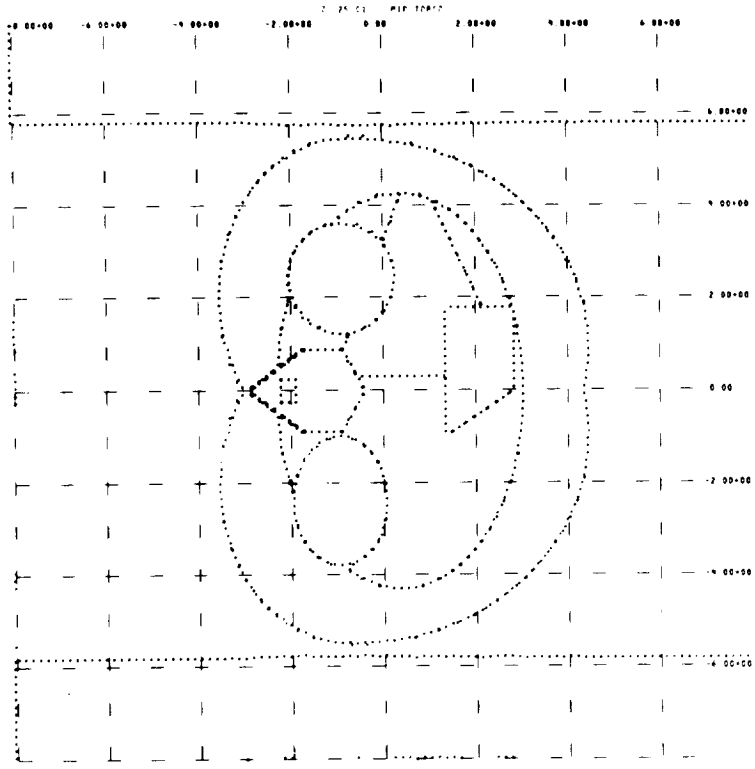

Figure 40. Horizontal Cross Section Through the Mid Torso at z = 25.01

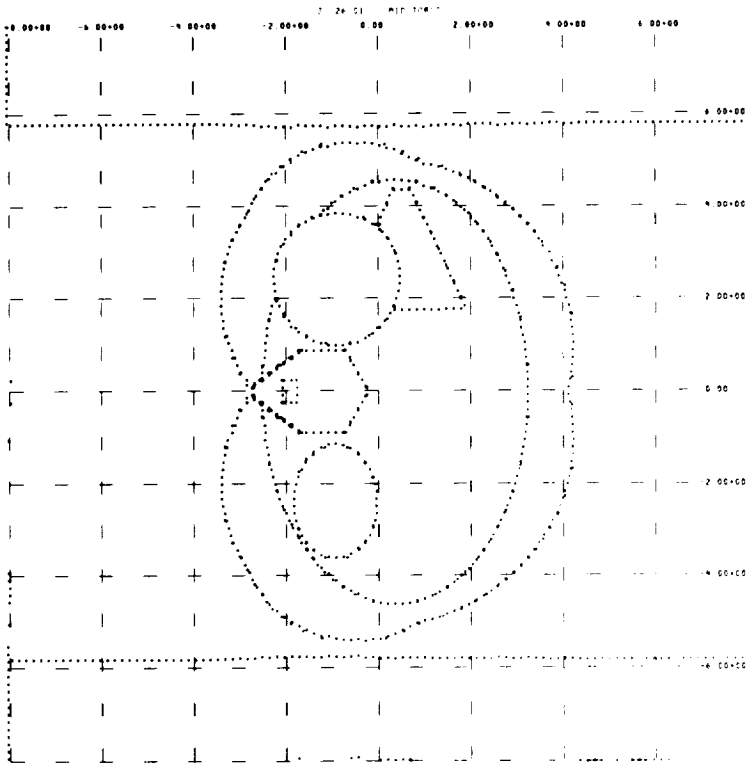

Figure 41. Horizontal Cross Section Through the Mid Torso at z = 26.01

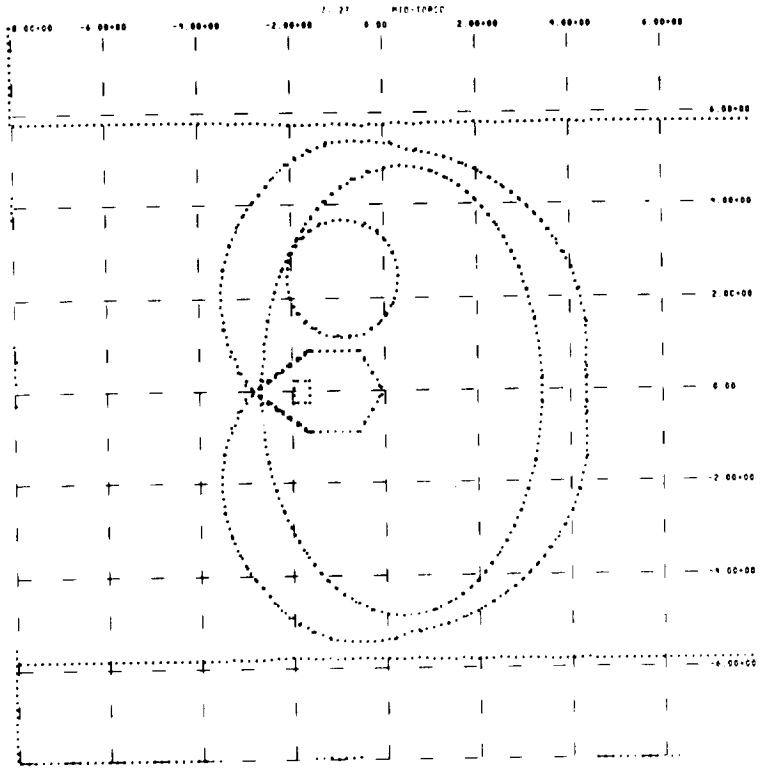

Figure 42. Horizontal Cross Section Through the Mid Torso at z = 27

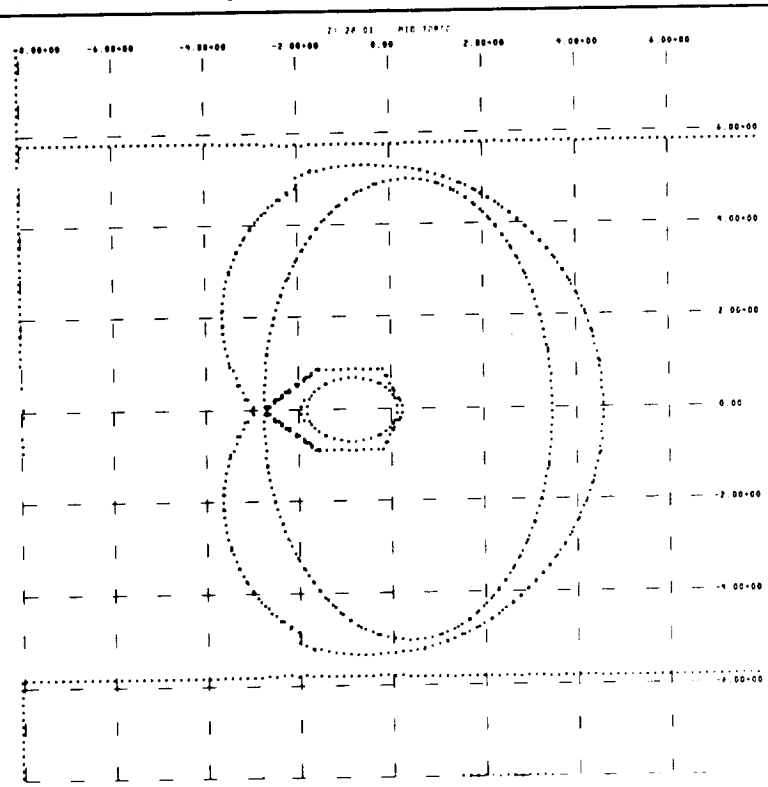

Figure 43. Horizontal Cross Section Through the Mid Torso at z = 28.01

CR145

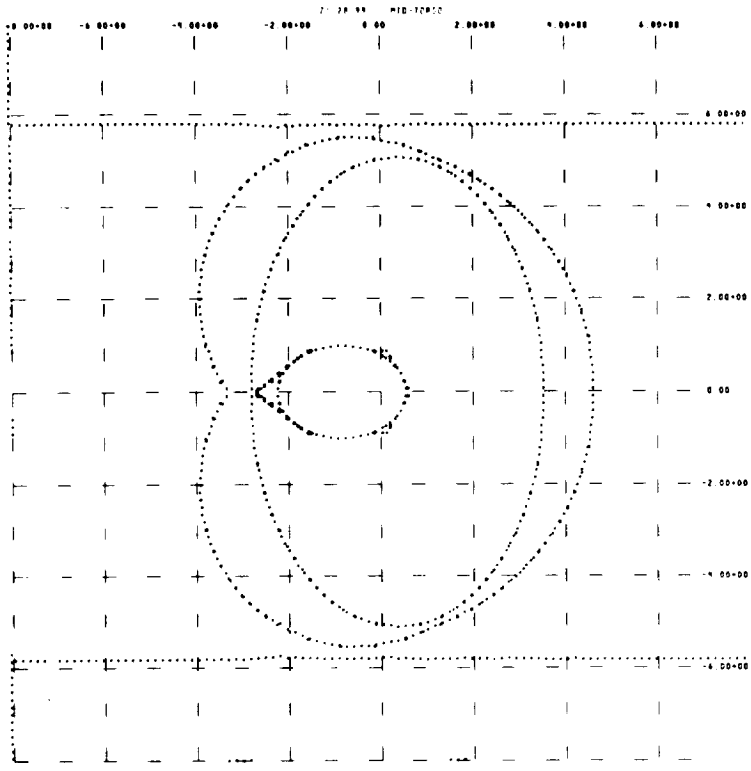

Figure 44. Horizontal Cross Section Through the Mid Torso at z = 28.99

CR145

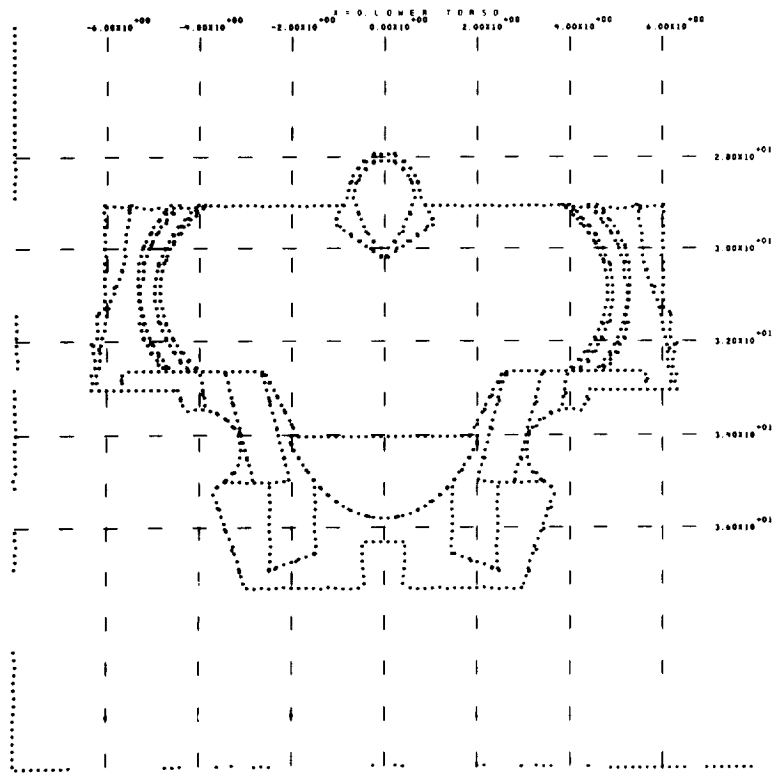

Figure 45. Vertical Cross Section Through the Lower Torso at x = 0

CR145

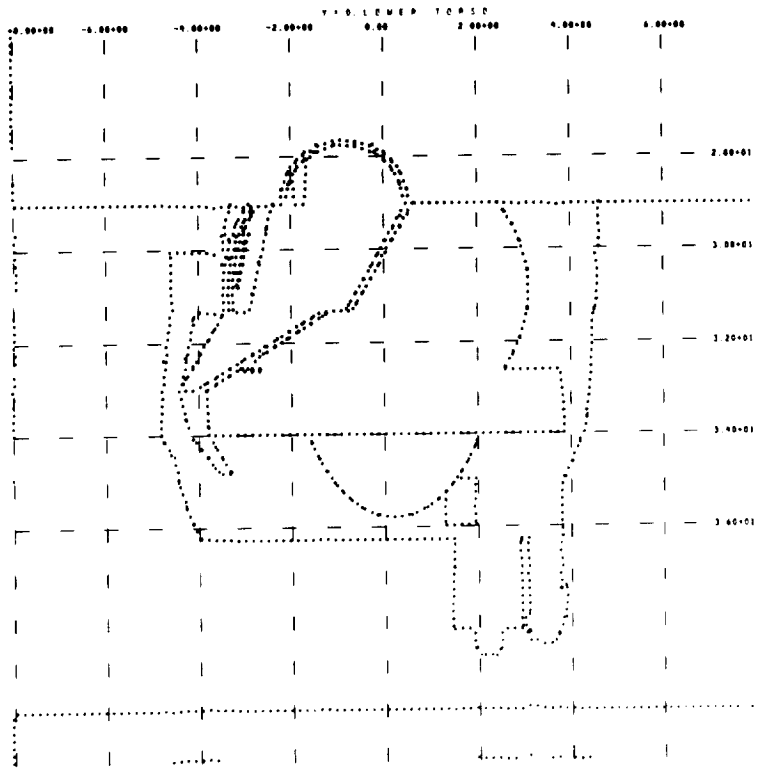

Figure 46. Vertical Cross Section Through the Lower Torso at y = 0

CR145

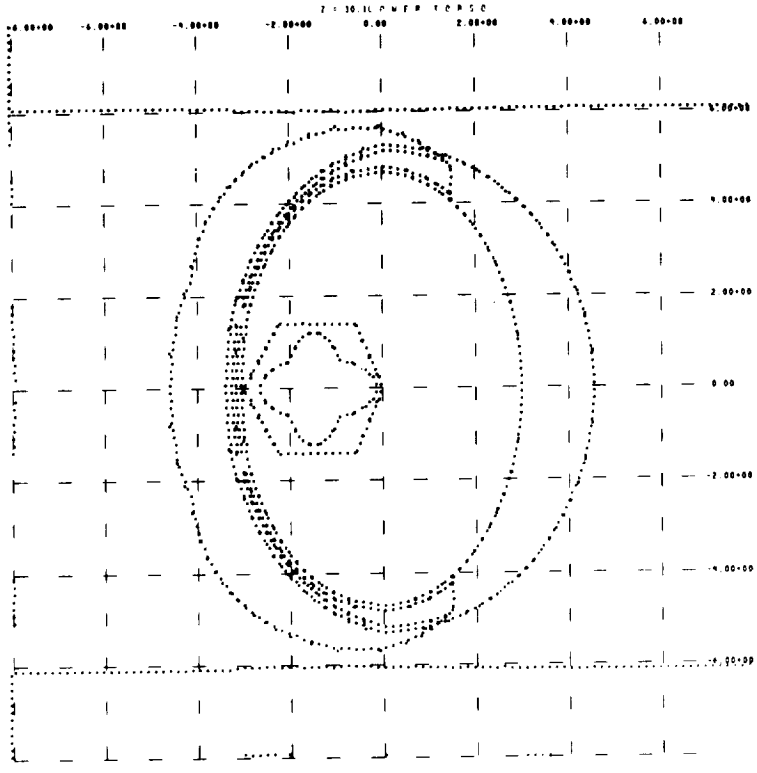

Figure 47. Horizontal Cross Section Through the Lower Torso at z = 30.1

CR145

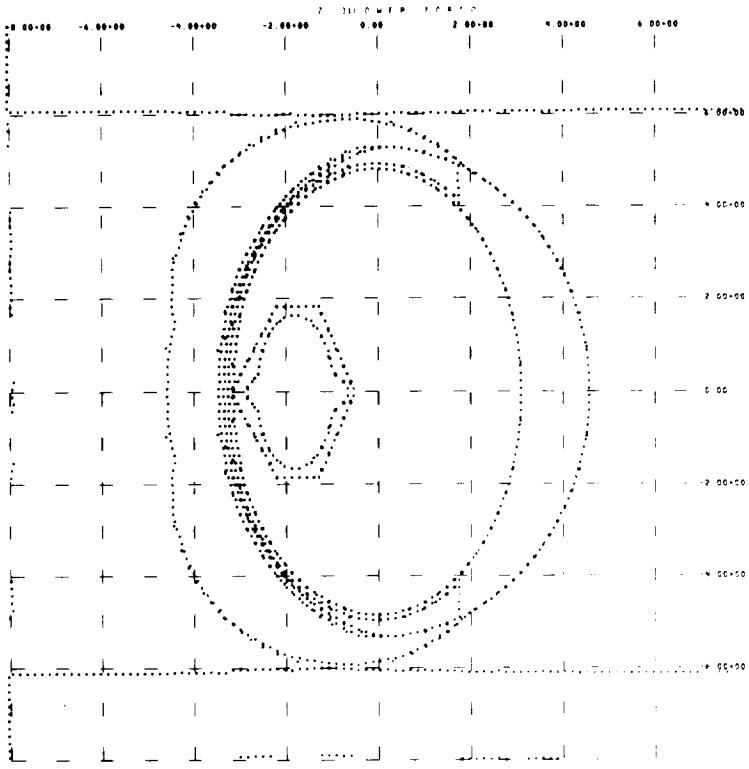

Figure 48. Horizontal Cross Section Through the Lower Torso at z = 31

CR145

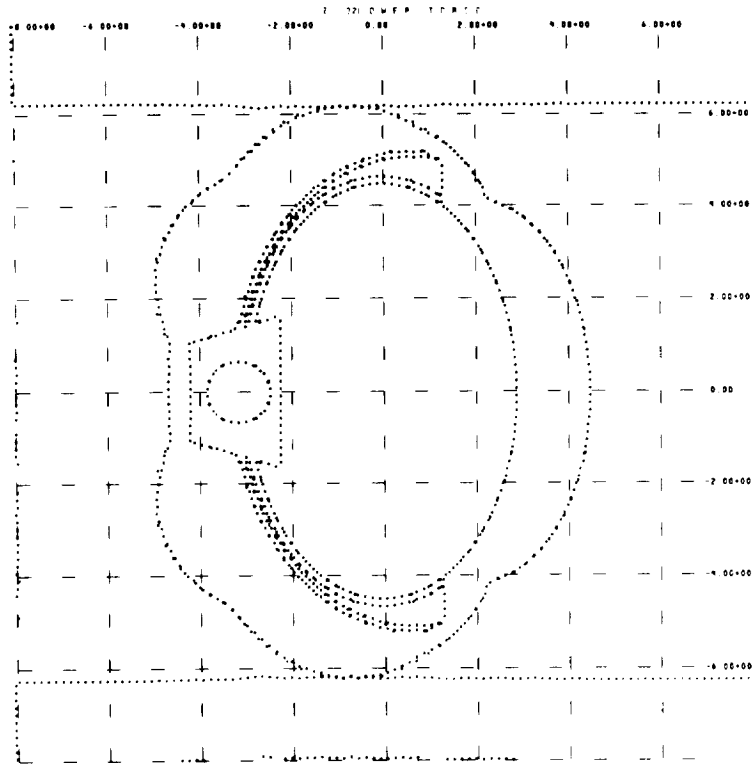

Figure 49. Horizontal Cross Section Through the Lower Torso at z = 32

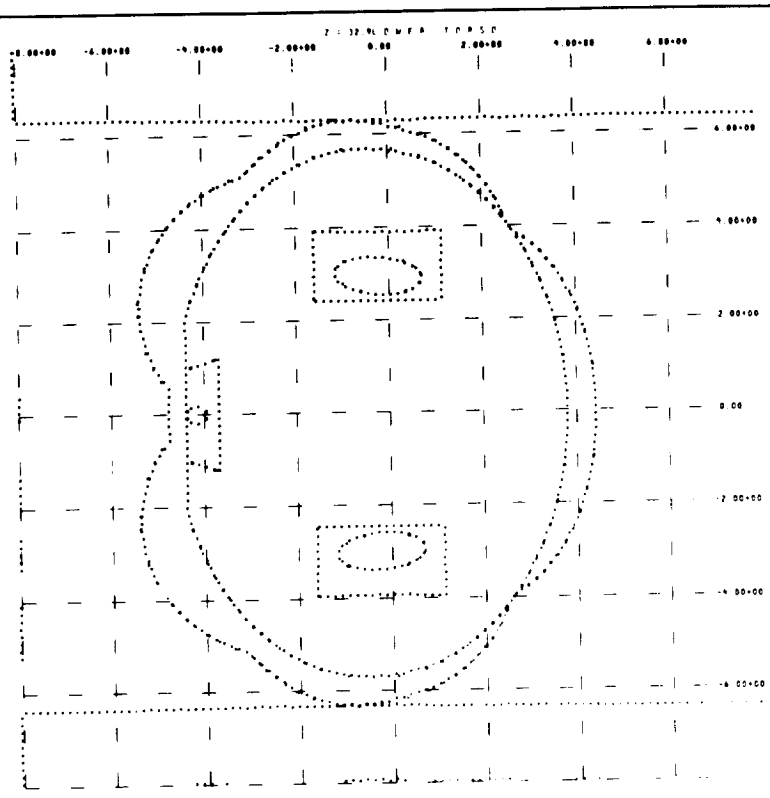

Figure 50. Horizontal Cross Section Through the Lower Torso at z = 32.9

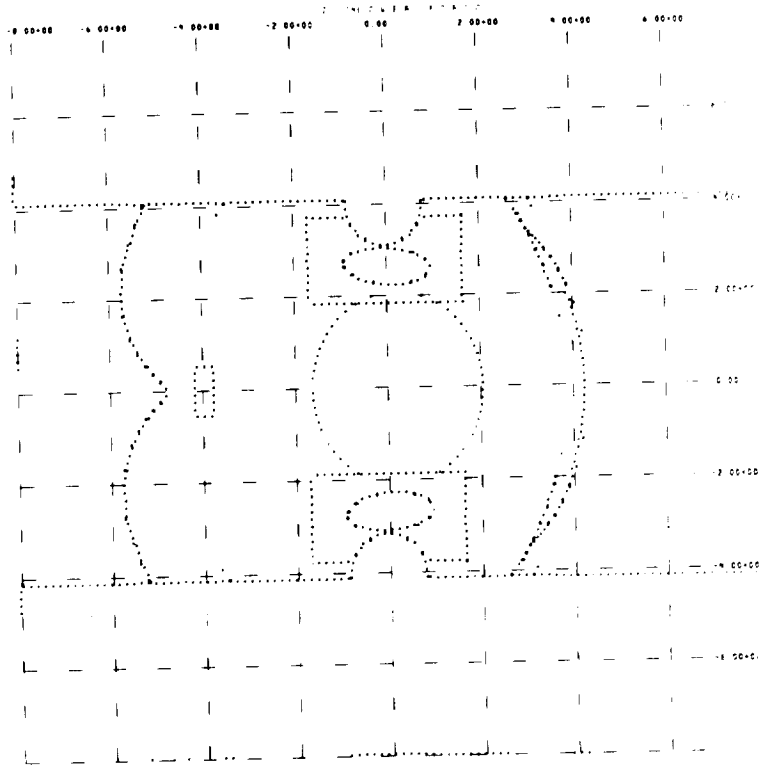

Figure 51. Horizontal Cross Section Through the Lower Torso at z = 34

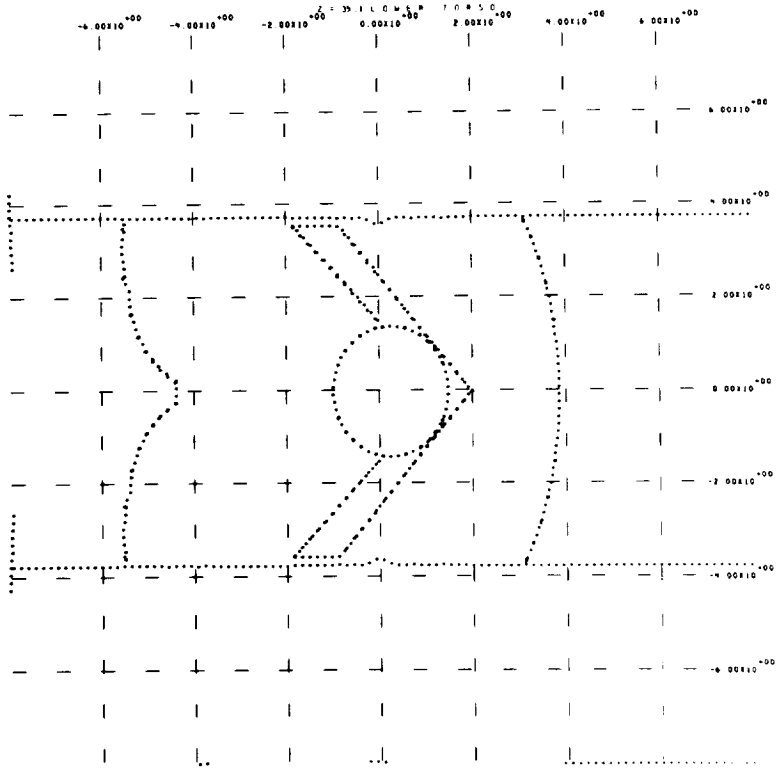

Figure 52. Horizontal Cross Section Through the Lower Torso at z = 35

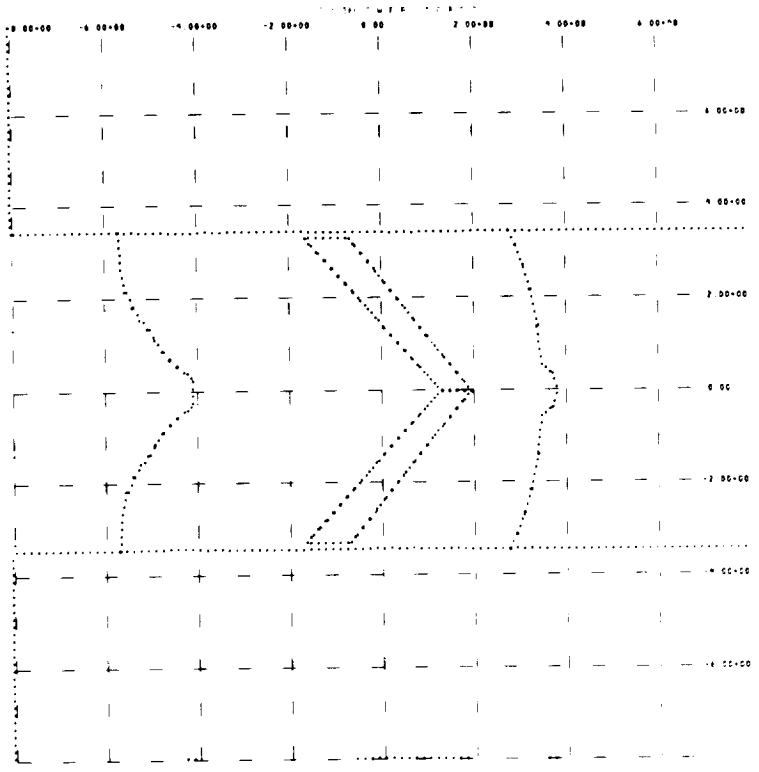

Figure 53. Horizontal Cross Section Through the Lower Torso at z = 36

CR146

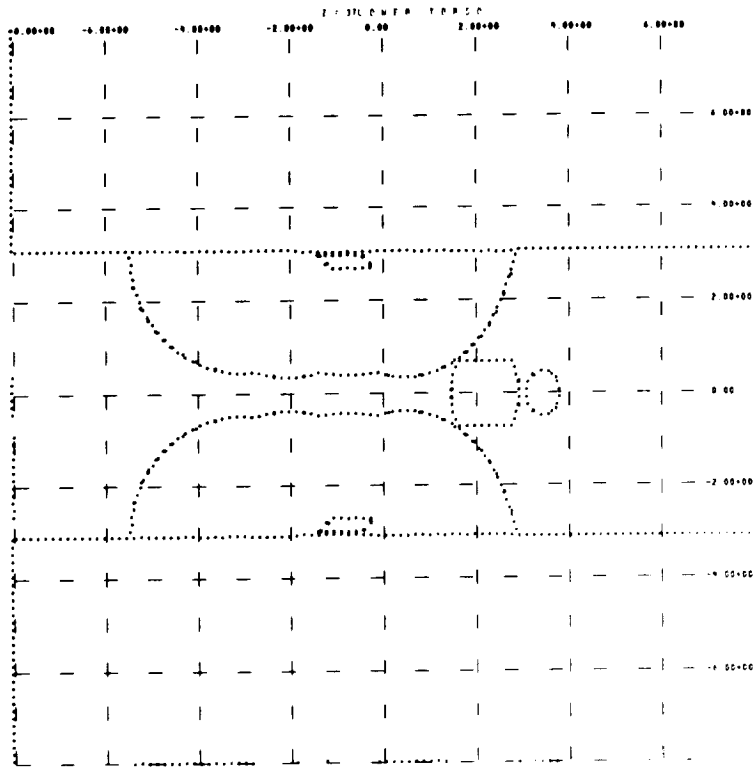

Figure 54. Horizontal Cross Section Through the Lower Torso at z = 37

CR145

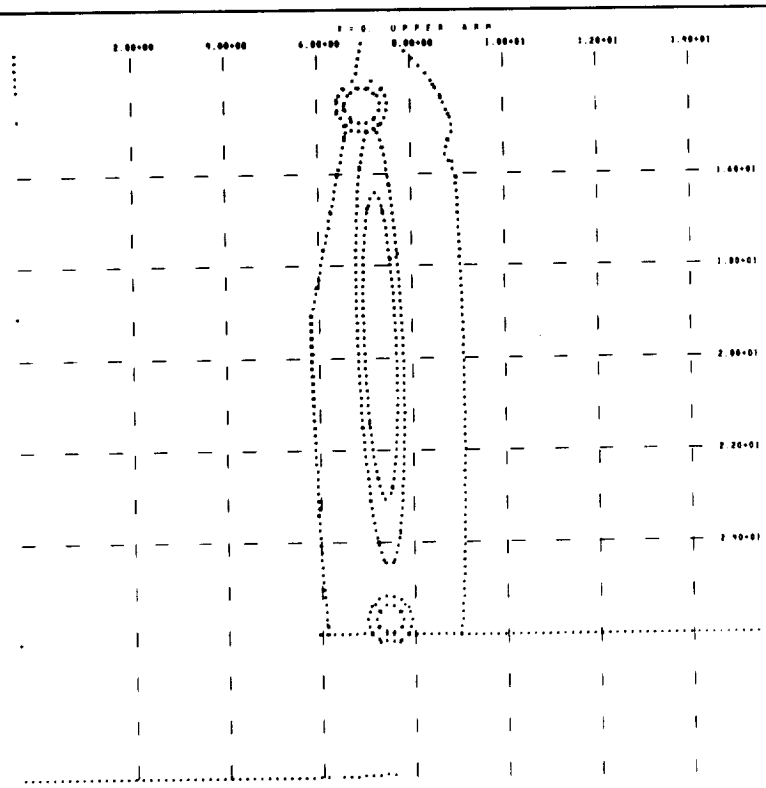

Figure 55. Vertical Cross Section Through the Upper Arm at x = 0

CR145

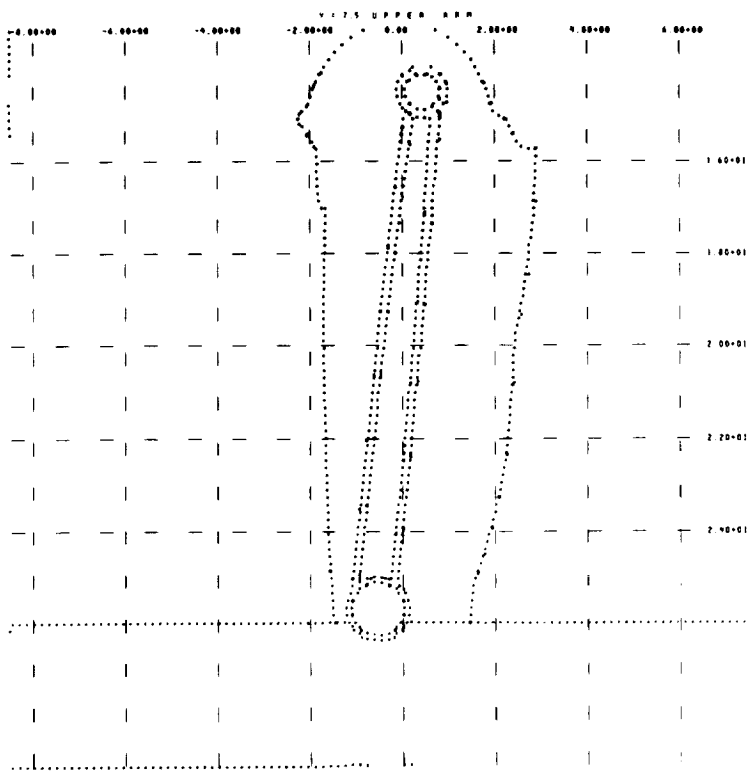

Figure 56. Vertical Cross Section Through the Upper Arm at y = 7.5

CR145

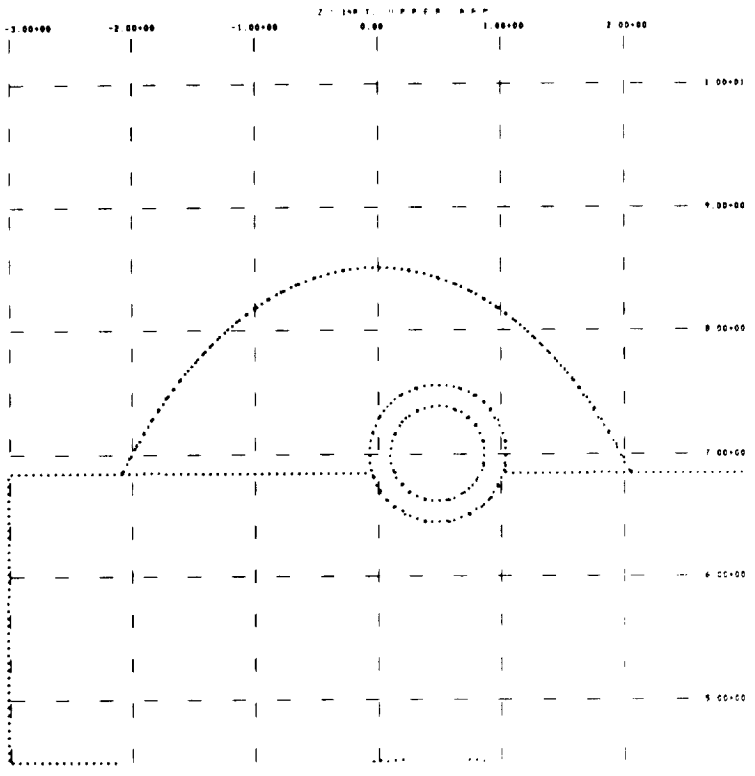

Figure 57. Horizontal Cross Section Through the Upper Arm at z = 14

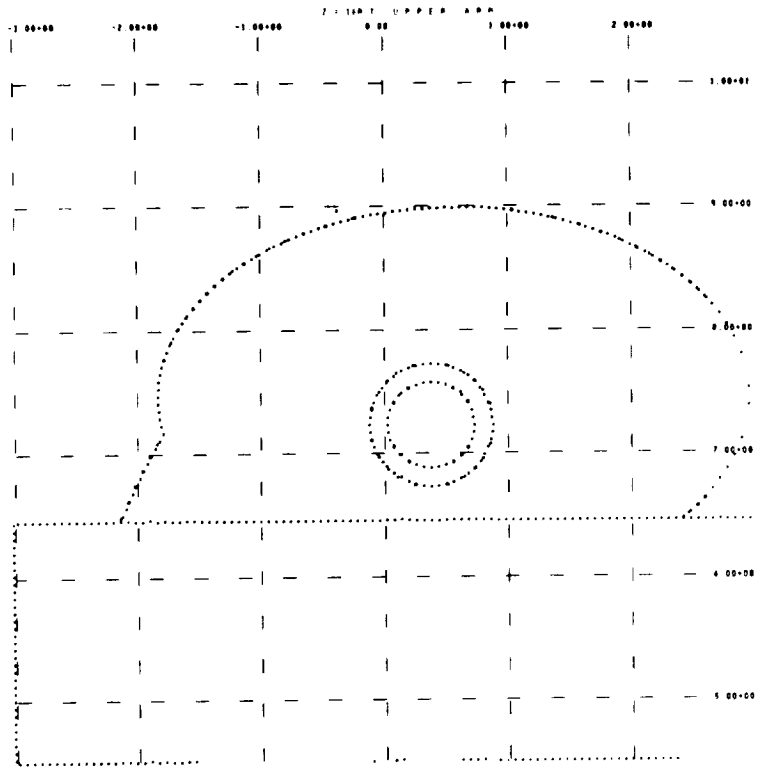

Figure 58. Horizontal Cross Section Through the Upper Arm at z = 16

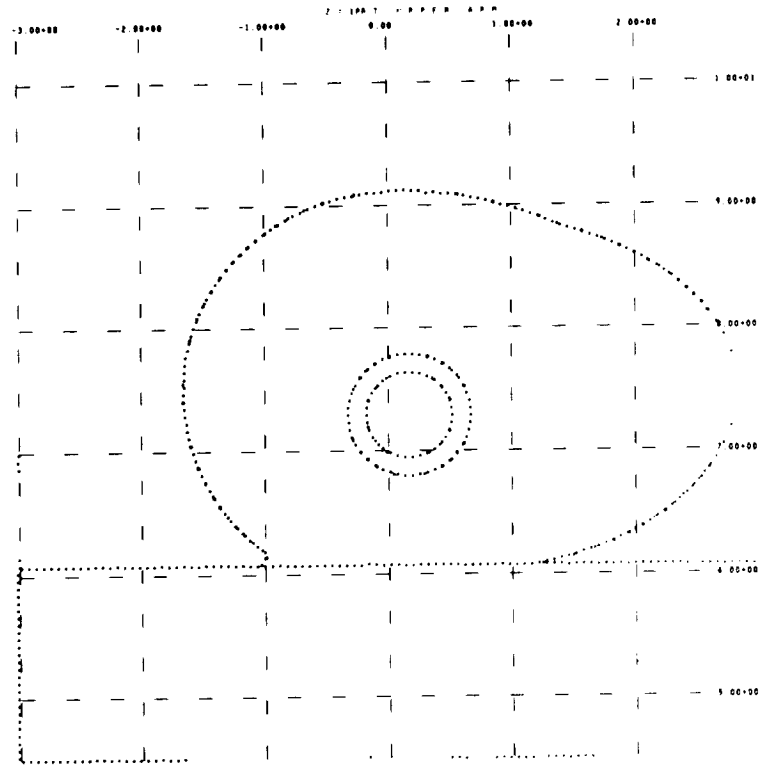

Figure 59. Horizontal Cross Section Through the Upper Arm at z = 18

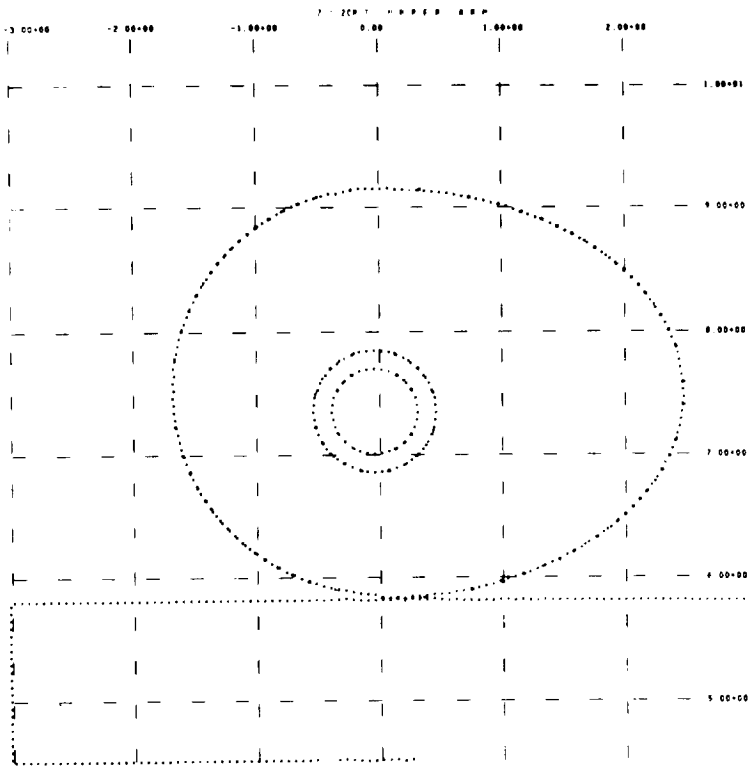

Figure 60. Horizontal Cross Section Through the Upper Arm at z = 20

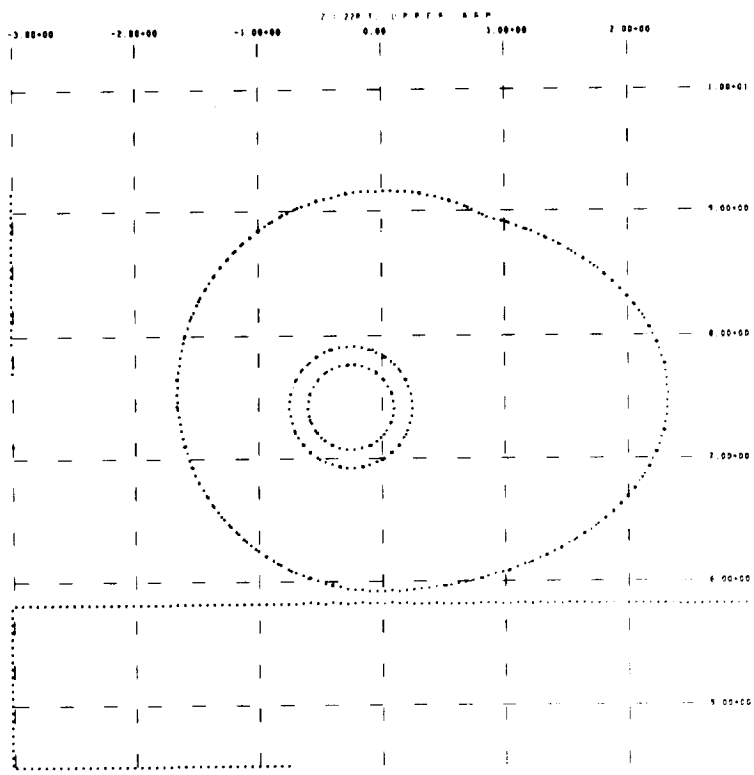

Figure 61. Horizontal Cross Section Through the Upper Arm at z = 22

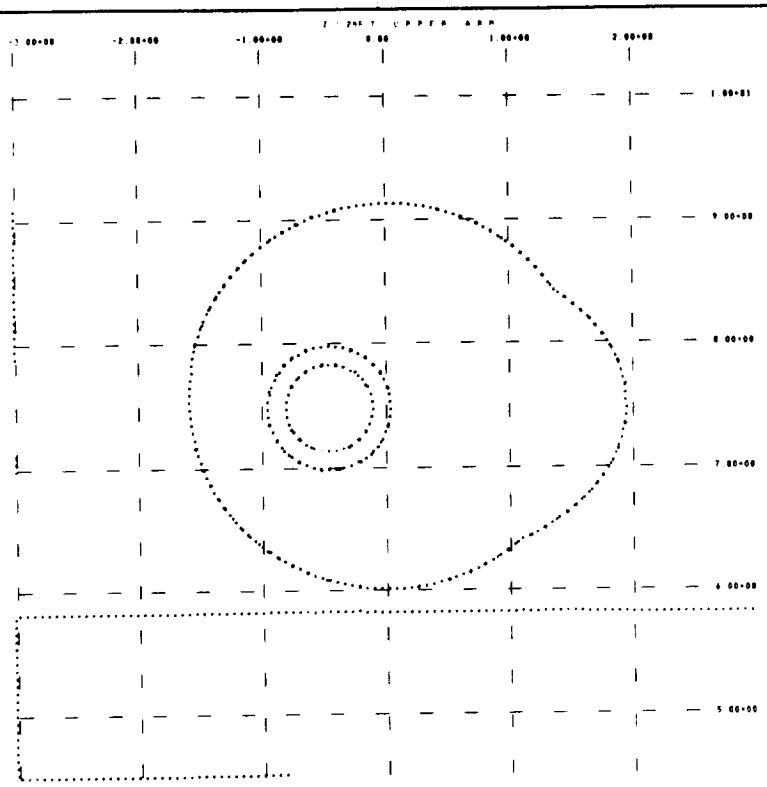

Figure 62. Horizontal Cross Section Through the Upper Arm at z = 24

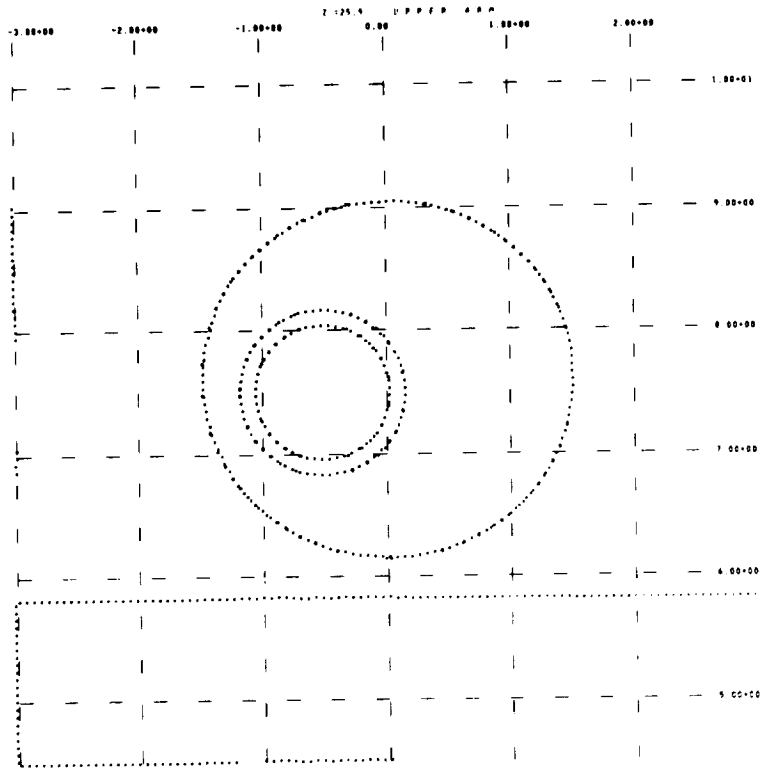

Figure 63. Horizontal Cross Section Through the Upper Arm at z = 25.9

CR145

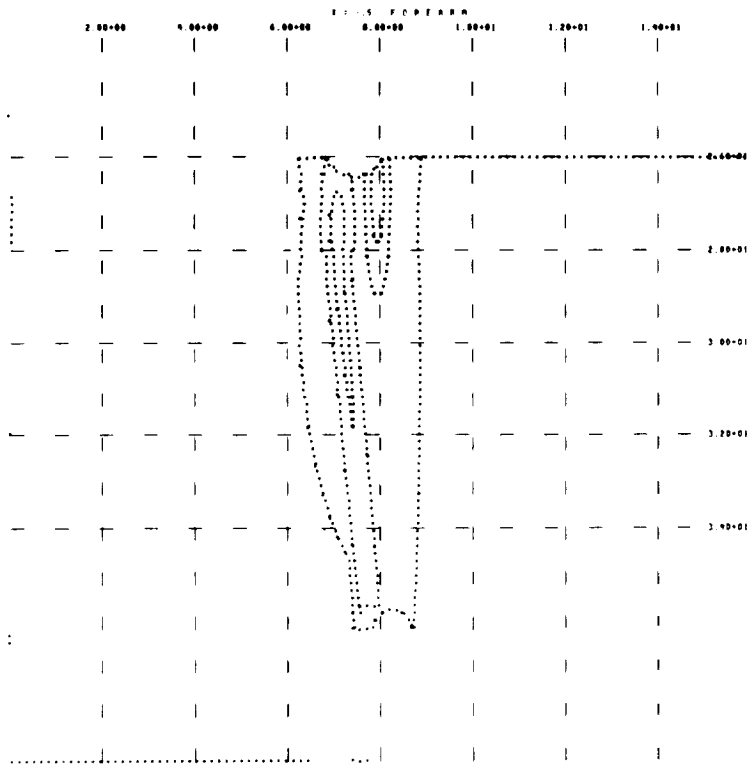

Figure 64. Vertical Cross Section Through the Forearm at x =-0.5

CR145

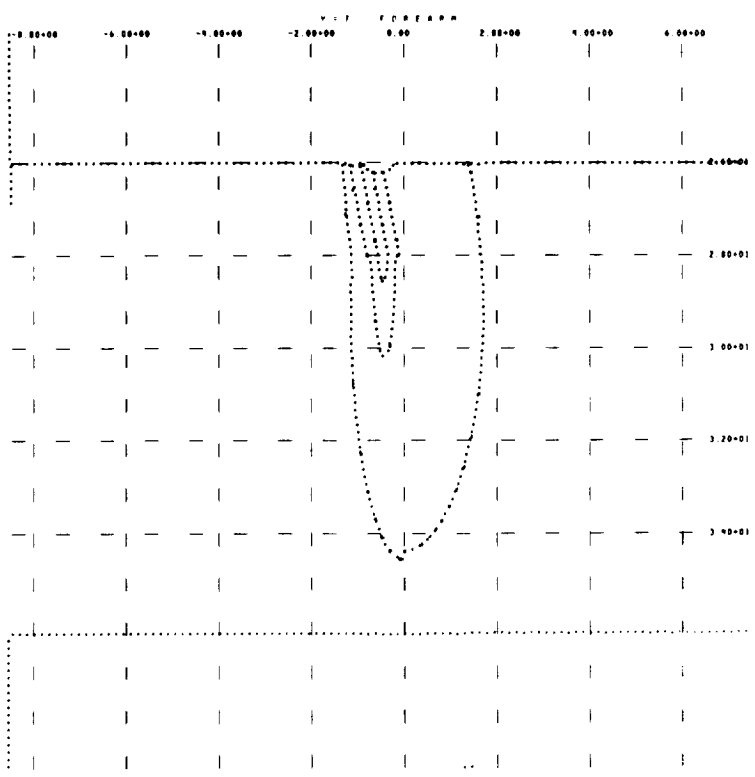

Figure 65. Vertical Cross Section Through the Forearm at y = 7

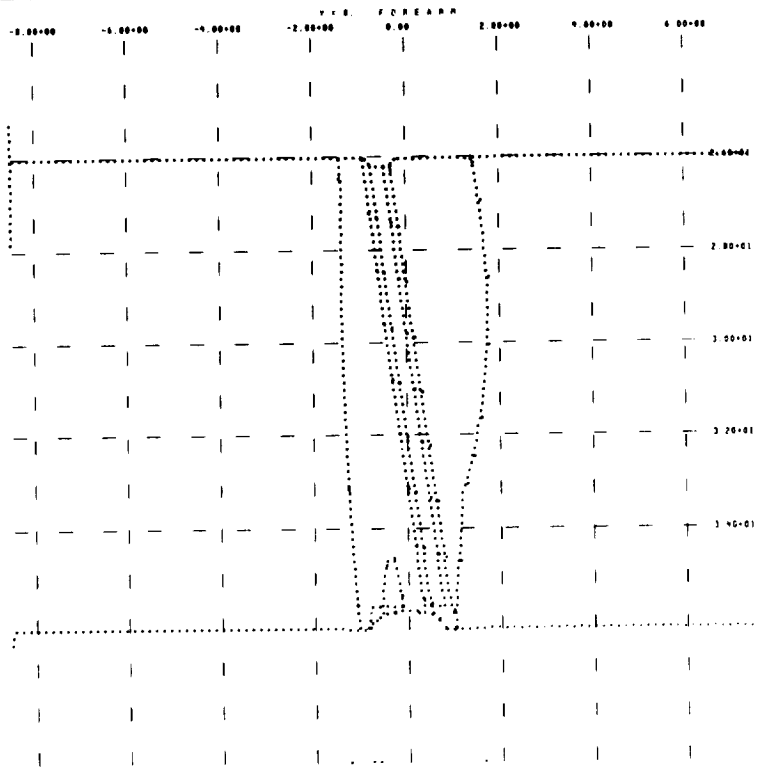

Figure 66. Vertical Cross Section Through the Forearm at y = 8

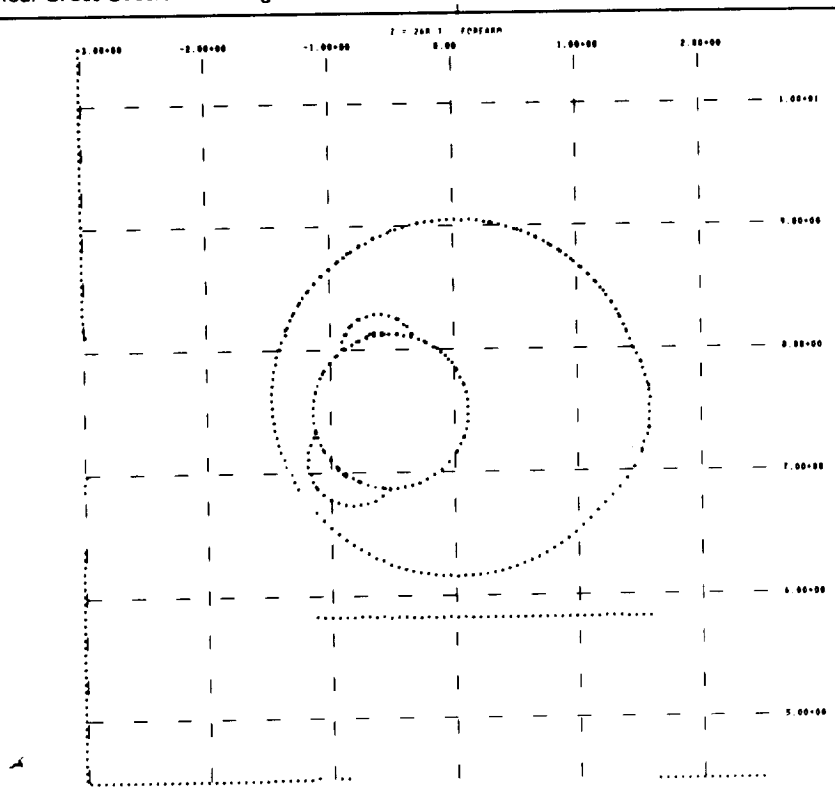

Figure 67. Horizontal Cross Section Through the Forearm at z = 26

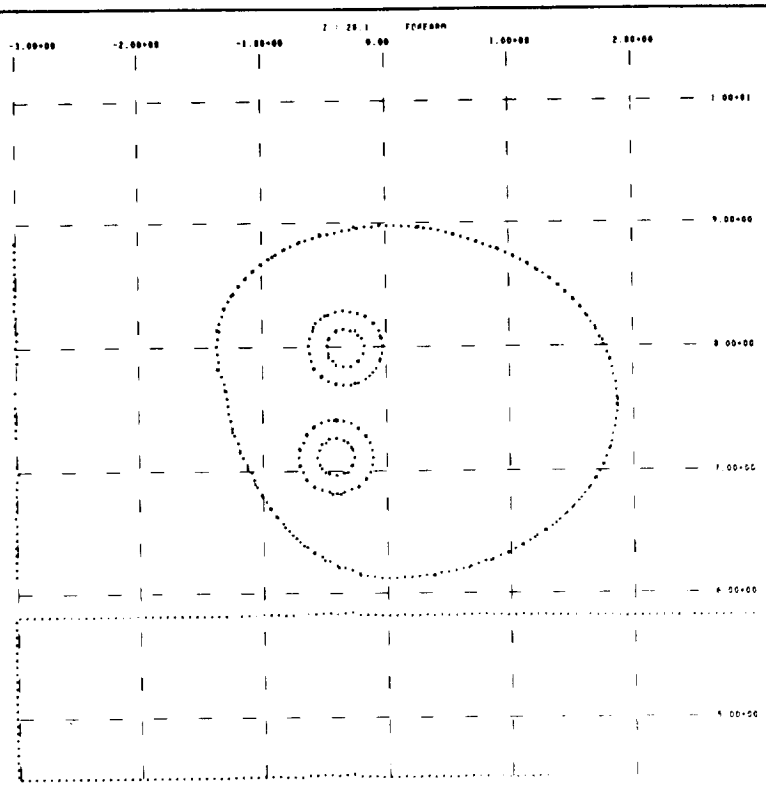

Figure 68. Horizontal Cross Section Through the Forearm at z = 28.1

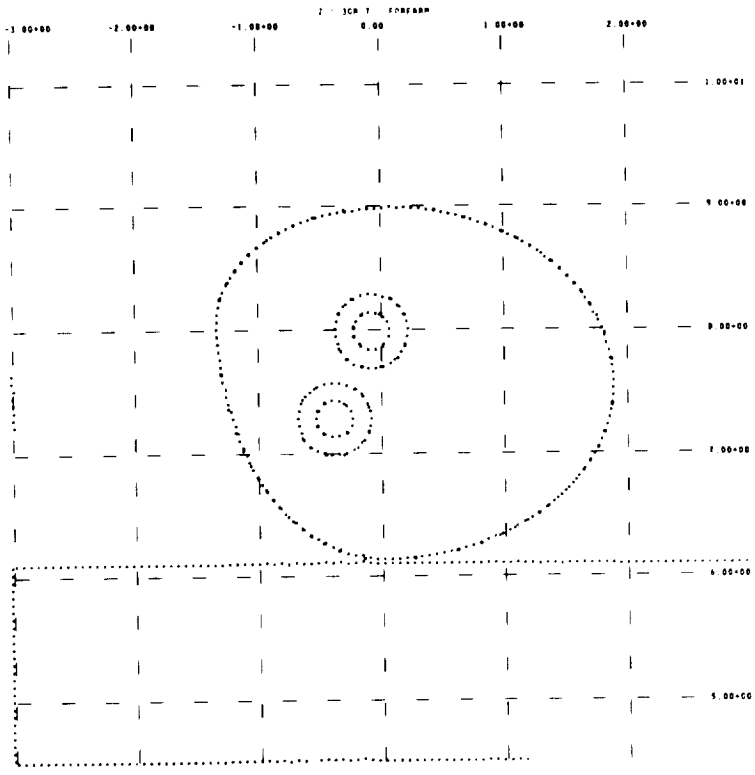

Figure 69. Horizontal Cross Section Through the Forearm at z = 30

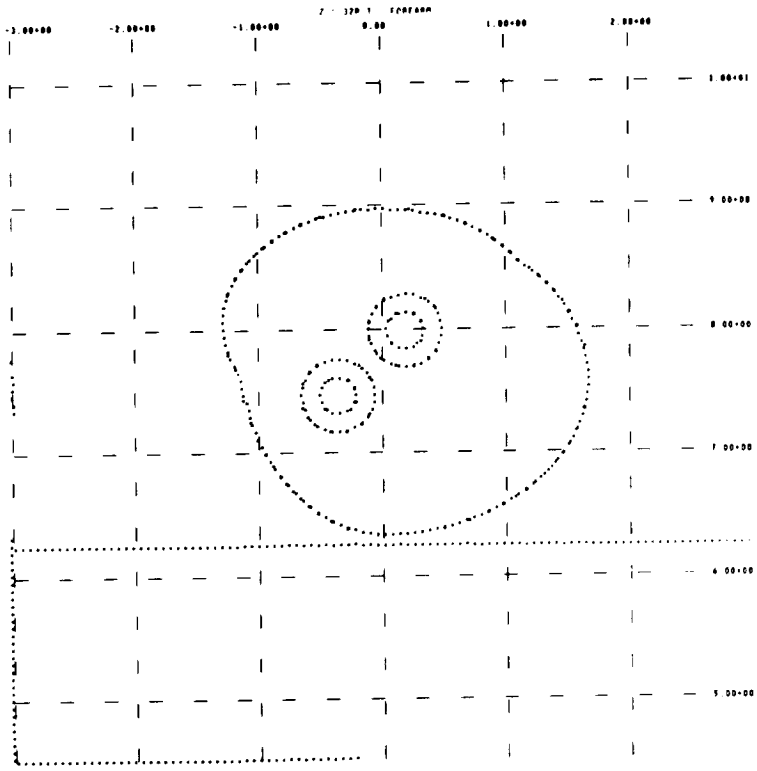

Figure 70. Horizontal Cross Section Through the Forearm at z = 32

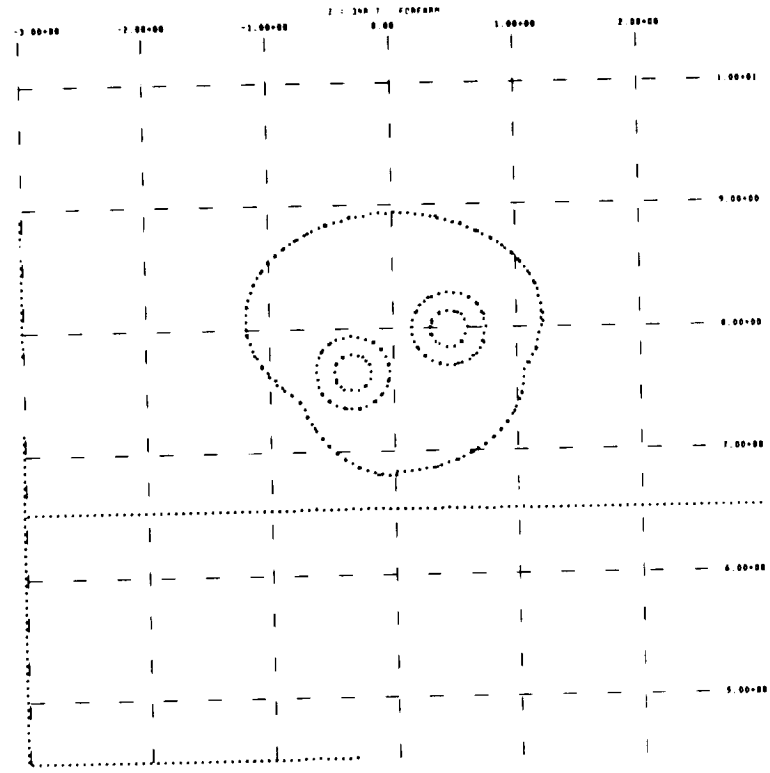

Figure 71. Horizontal Cross Section Through the Forearm at z = 34

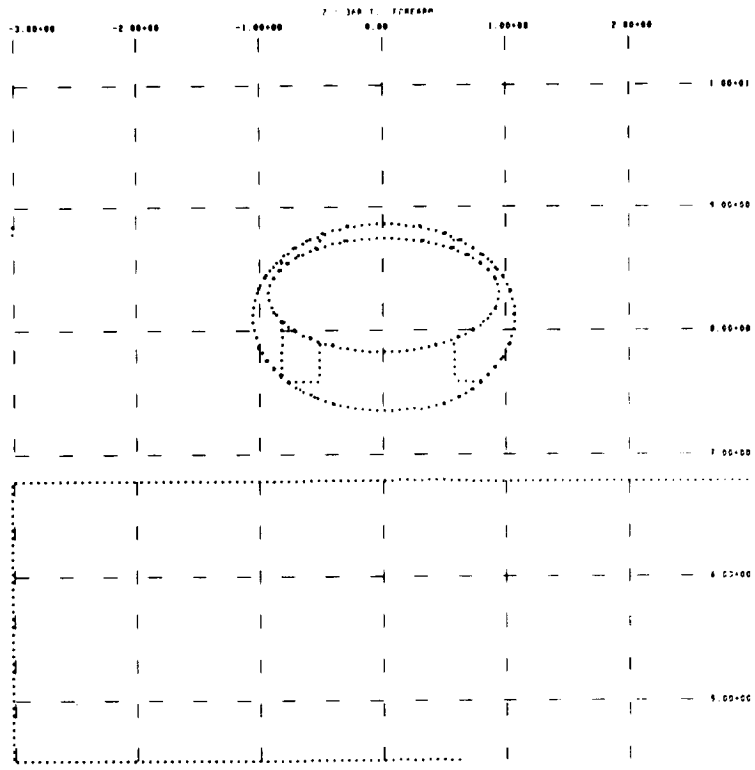

Figure 72. Horizontal Cross Section Through the Forearm at z = 36

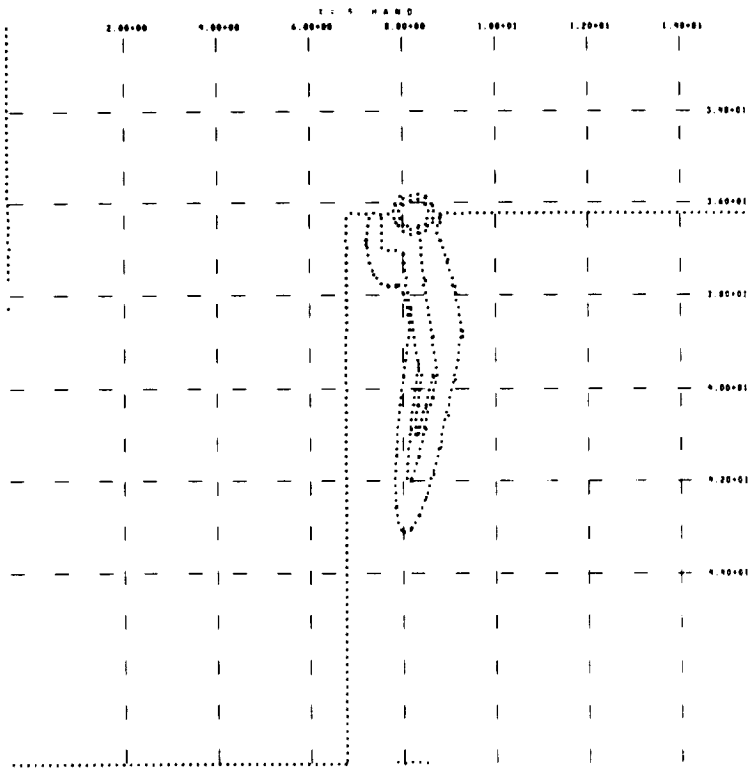

Figure 73. Vertical Cross Section Through the Hand at x = 0.5

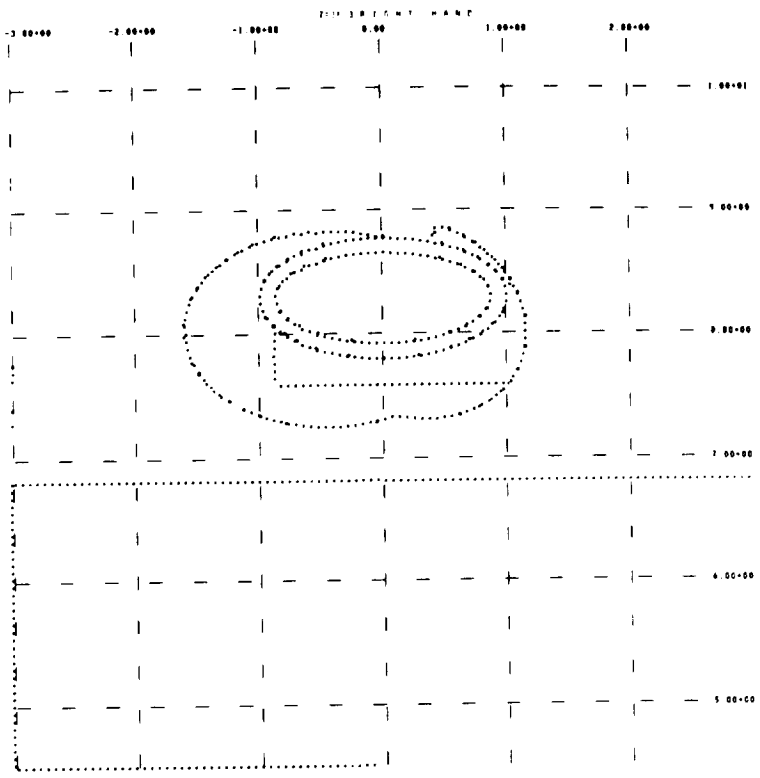

Figure 74. Horizontal Cross Section Through the Hand at z = 36.3

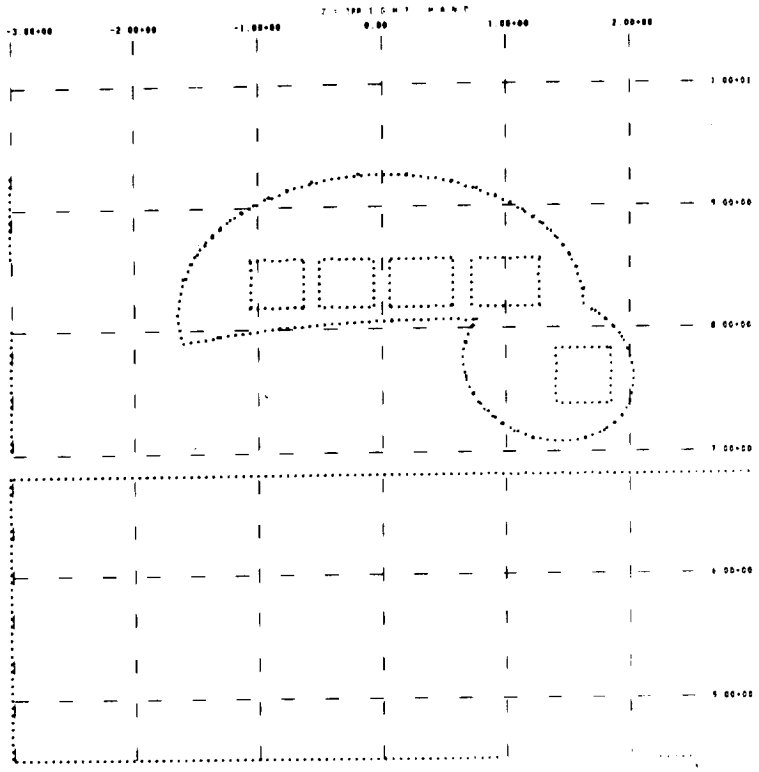

Figure 75. Horizontal Cross Section Through the Hand at z = 38

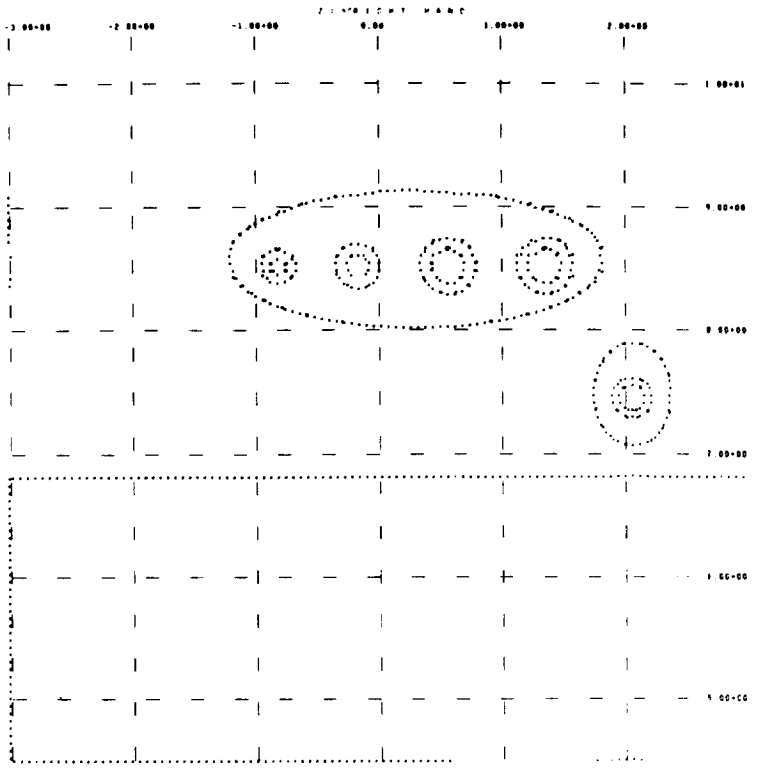

Figure 76. Horizontal Cross Section Through the Hand at z = 40

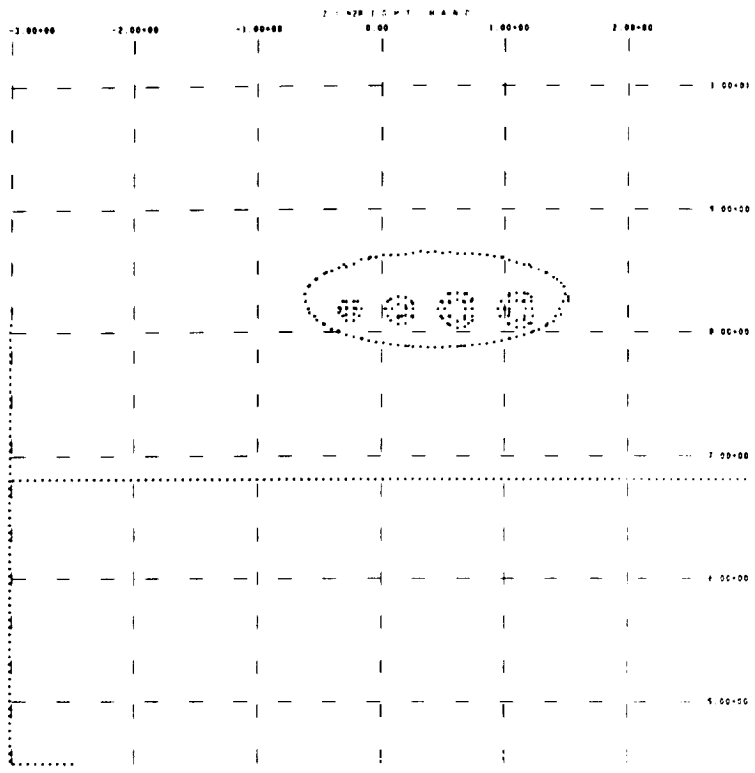

Figure 77. Horizontal Cross Section Through the Hand at z = 42

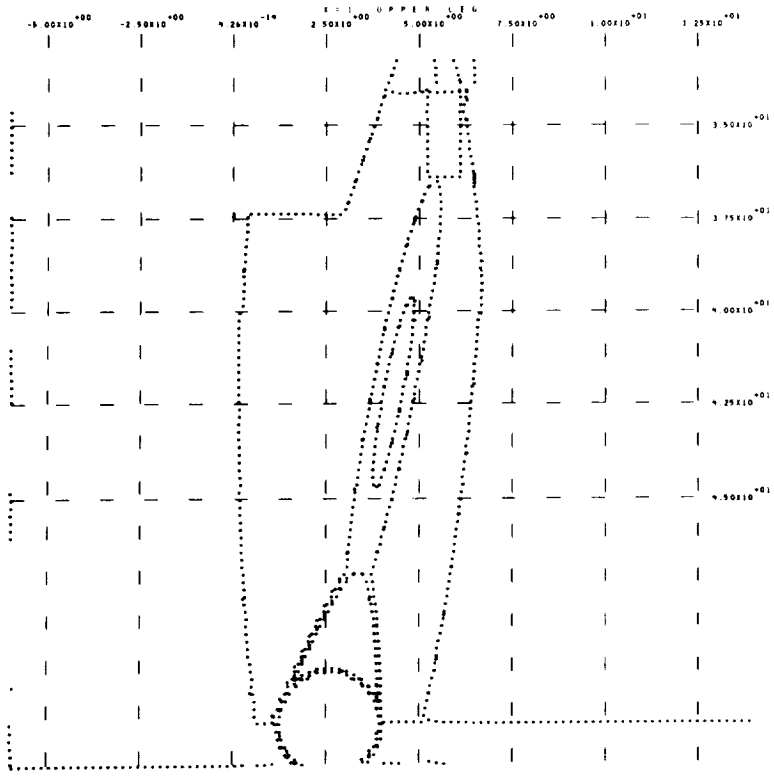

Figure 78. Vertical Cross Section Through the Upper Leg at x = 1.0

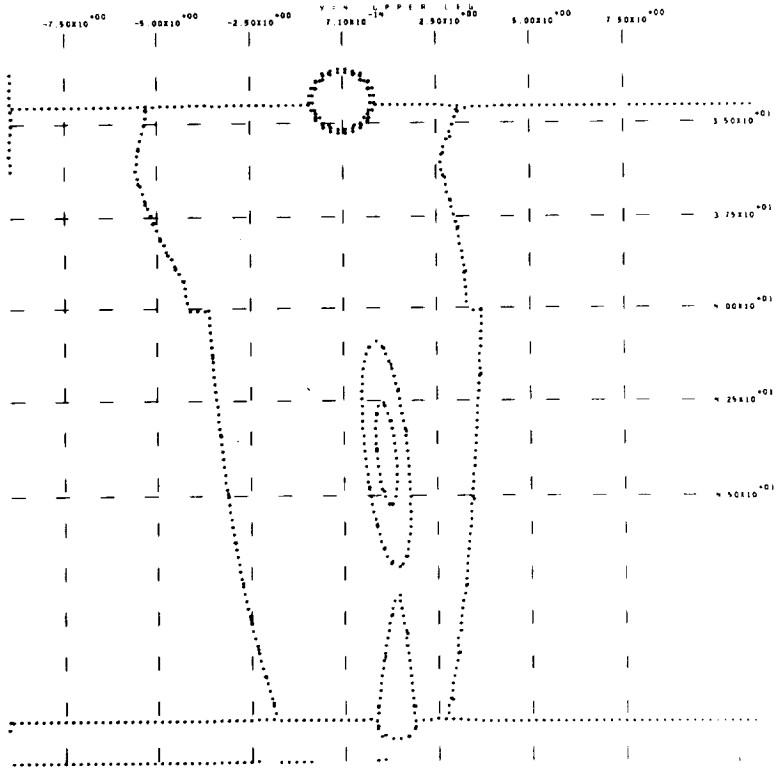

Figure 79. Vertical Cross Section Through the Upper Leg at y = 4

CR145

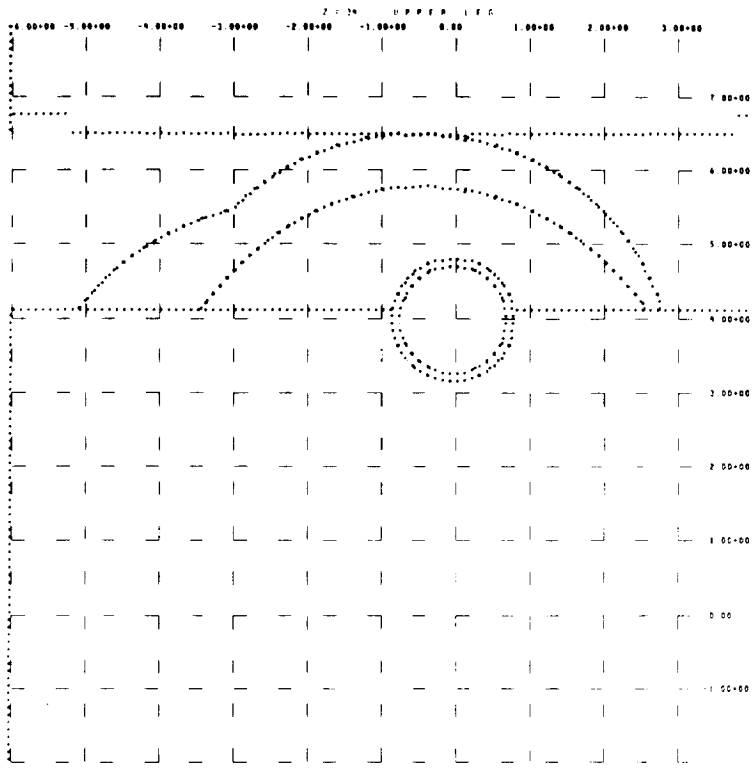

Figure 80. Horizontal Cross Section Through the Upper Leg at z = 34

CR145

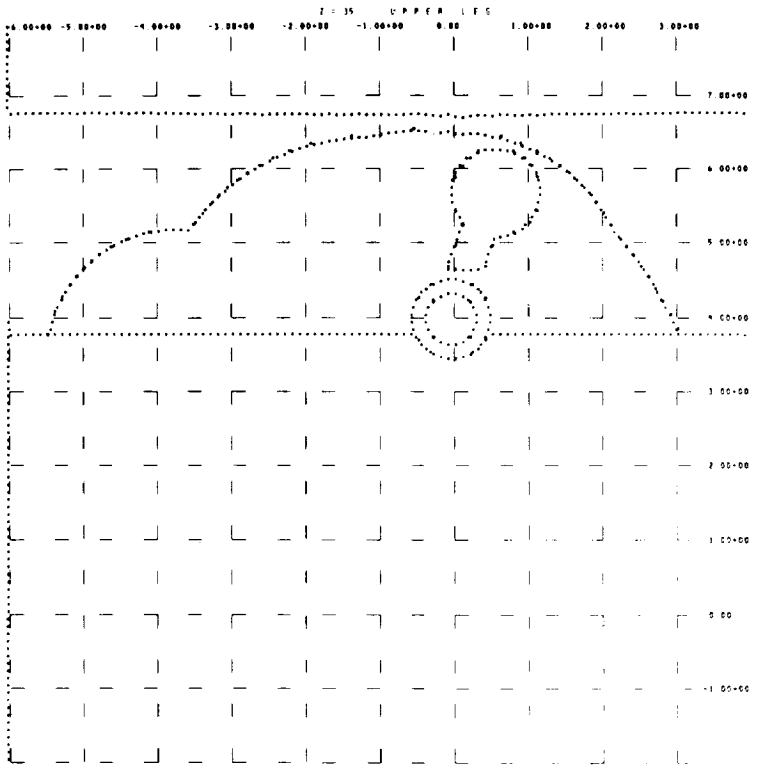

Figure 81. Horizontal Cross Section Through the Upper Leg at z = 35

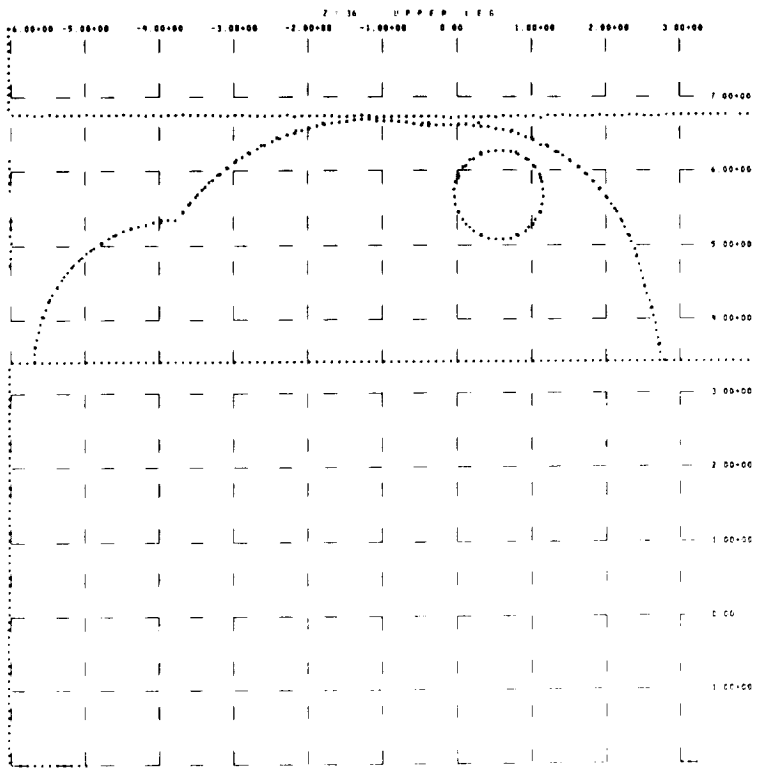

Figure 82. Horizontal Cross Section Through the Upper Leg at z = 36

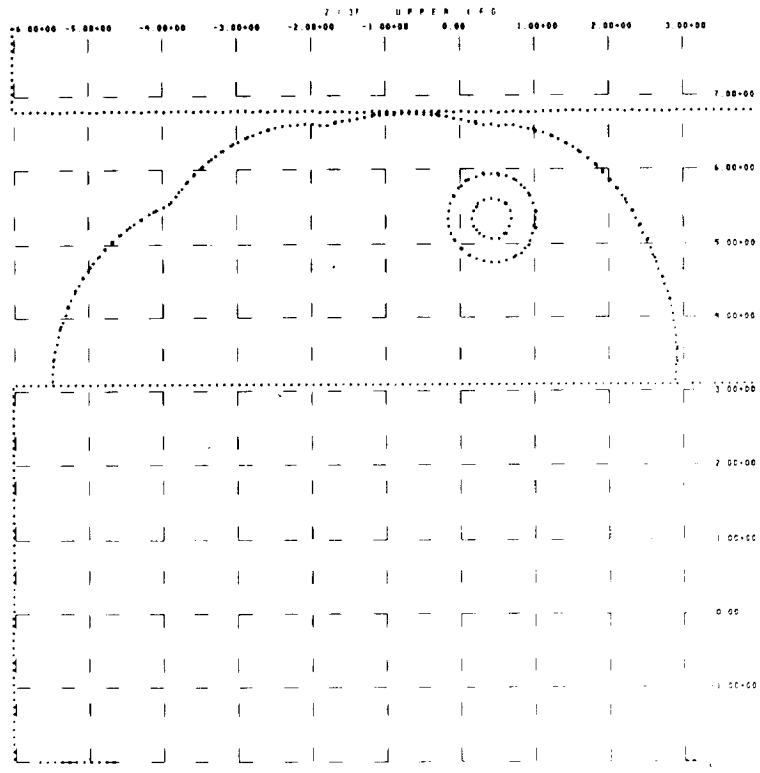

Figure 83. Horizontal Cross Section Through the Upper Leg at z = 37

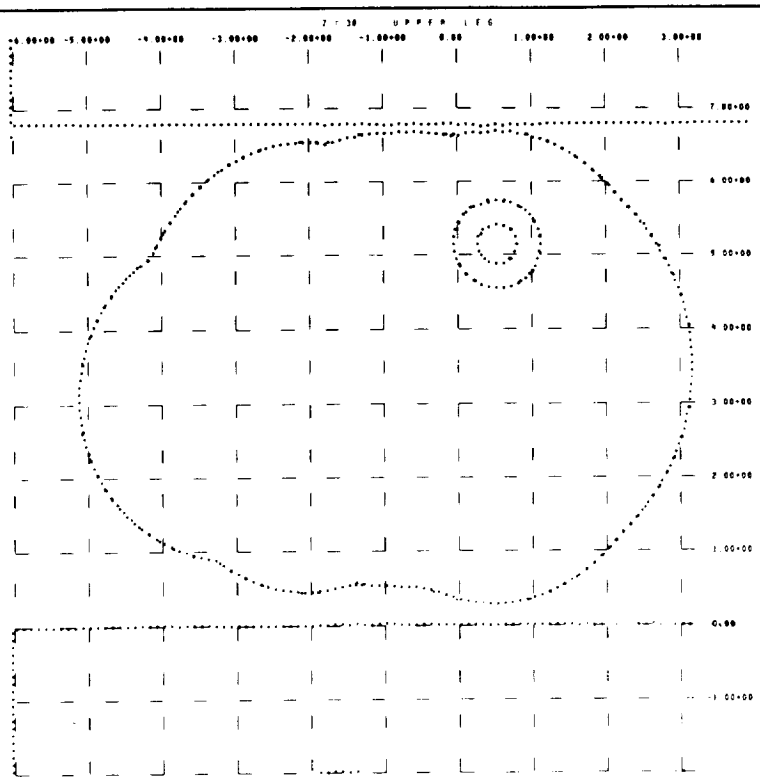

Figure 84. Horizontal Cross Section Through the Upper Leg at z = 38

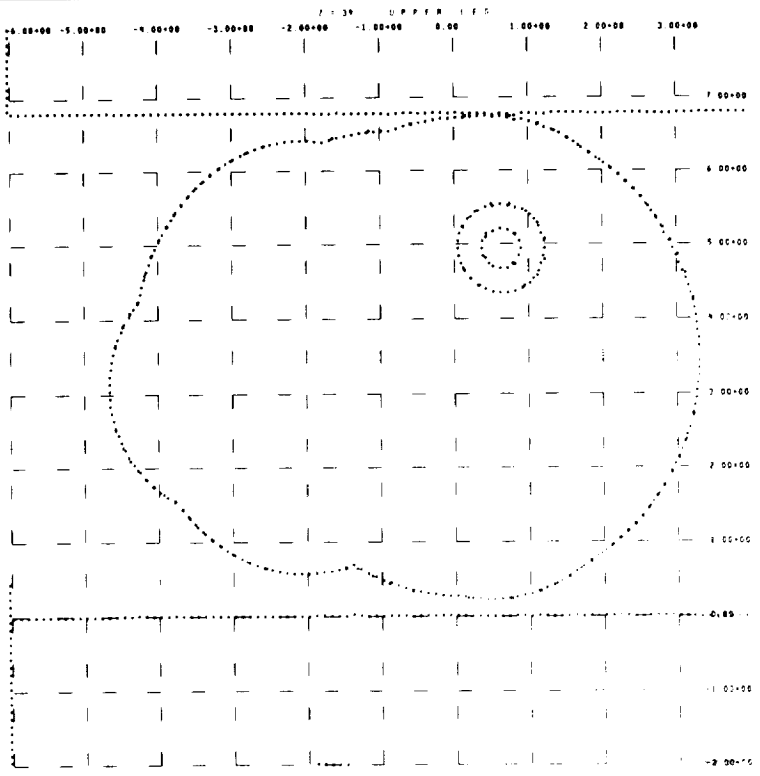

Figure 85. Horizontal Cross Section Through the Upper Leg at z = 39

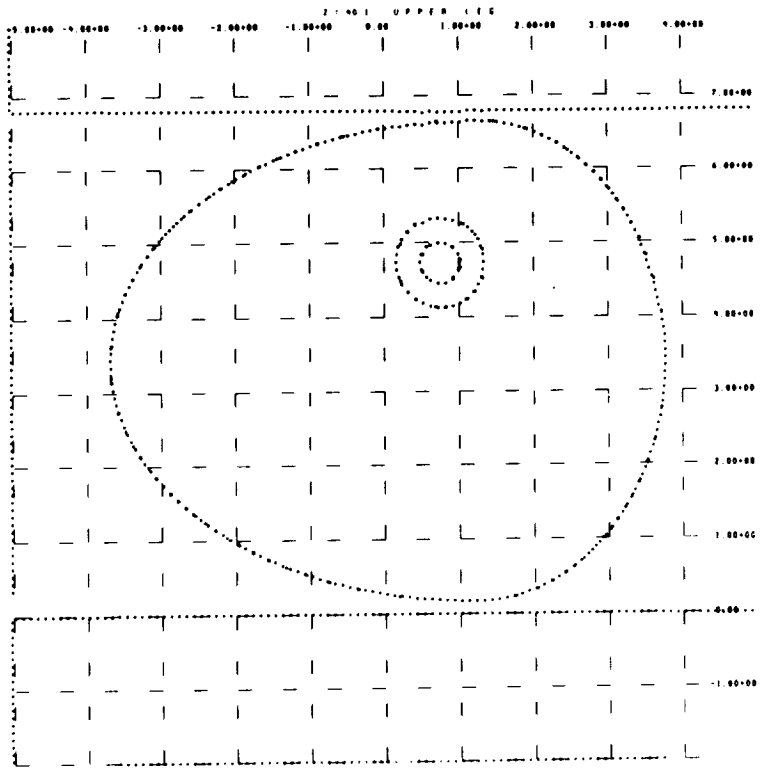

Figure 86. Horizontal Cross Section Through the Upper Leg at z = 40.1

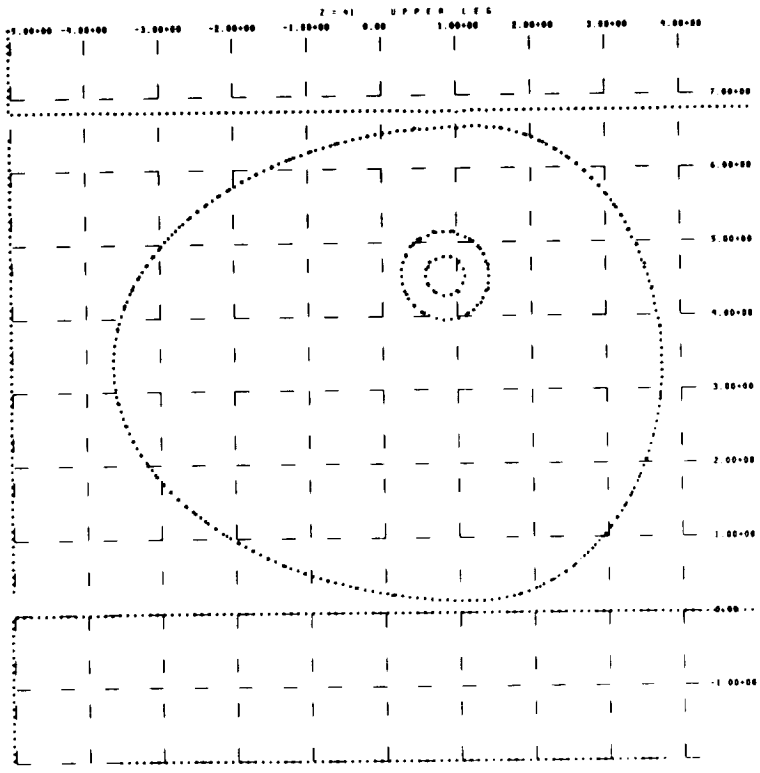

Figure 87. Horizontal Cross Section Through the Upper Leg at z = 41

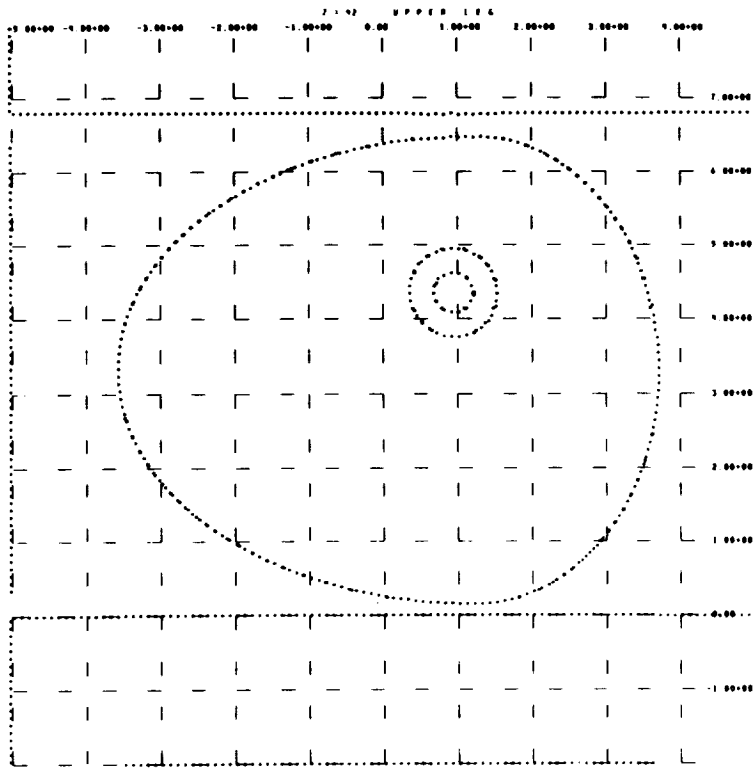

Figure 88. Horizontal Cross Section Through the Upper Leg at z = 42

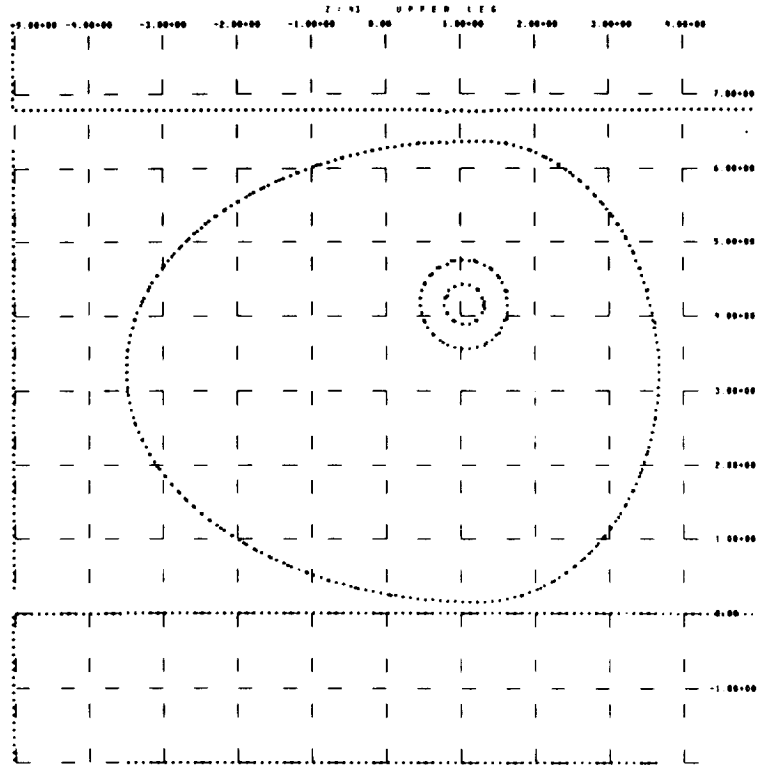

Figure 89. Horizontal Cross Section Through the Upper Leg at z = 43

CR145

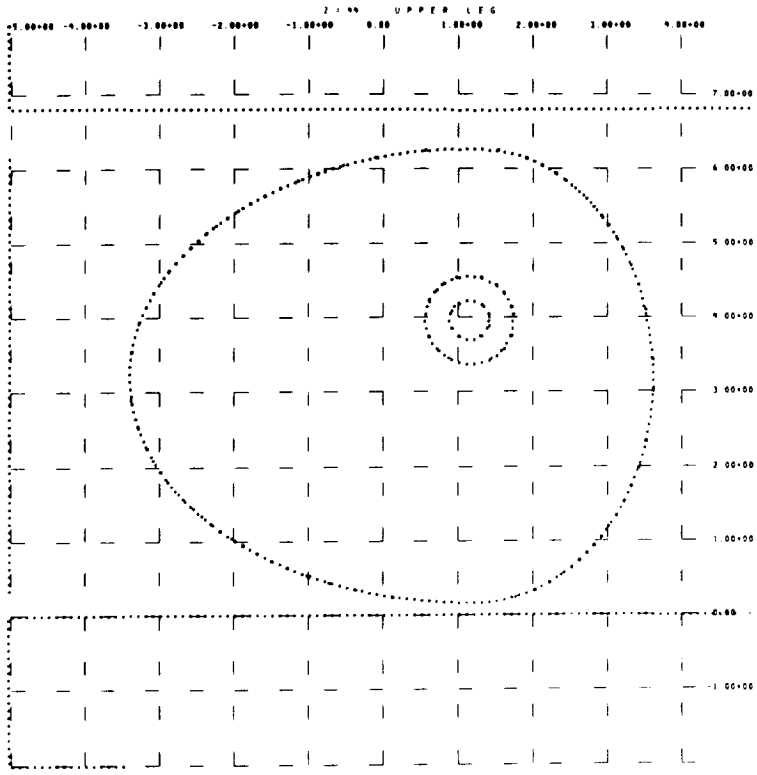

Figure 90. Horizontal Cross Section Through the Upper Leg at z = 44

CR145

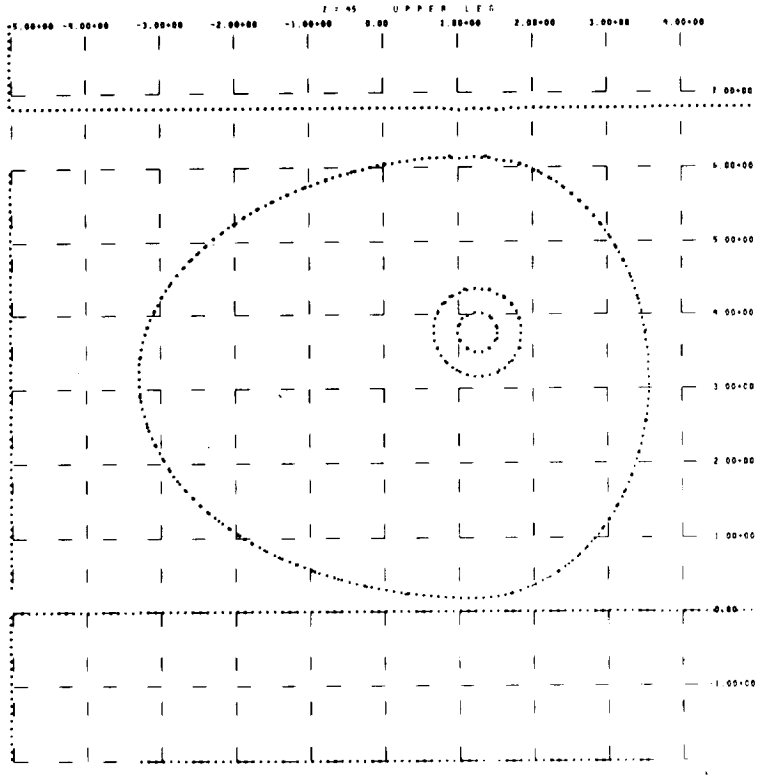

Figure 91. Horizontal Cross Section Through the Upper Leg at z = 45

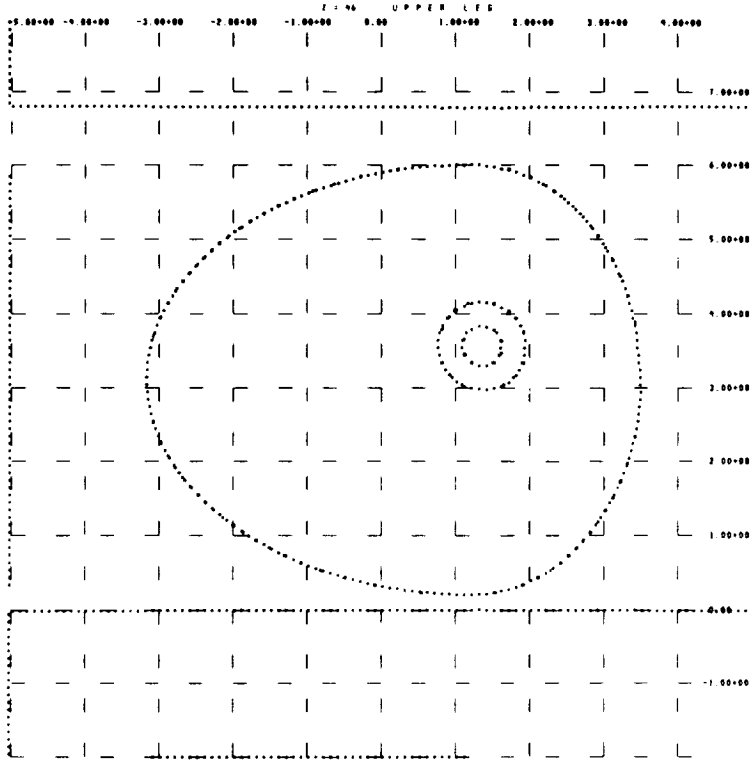

Figure 92. Horizontal Cross Section Through the Upper Leg at z = 46

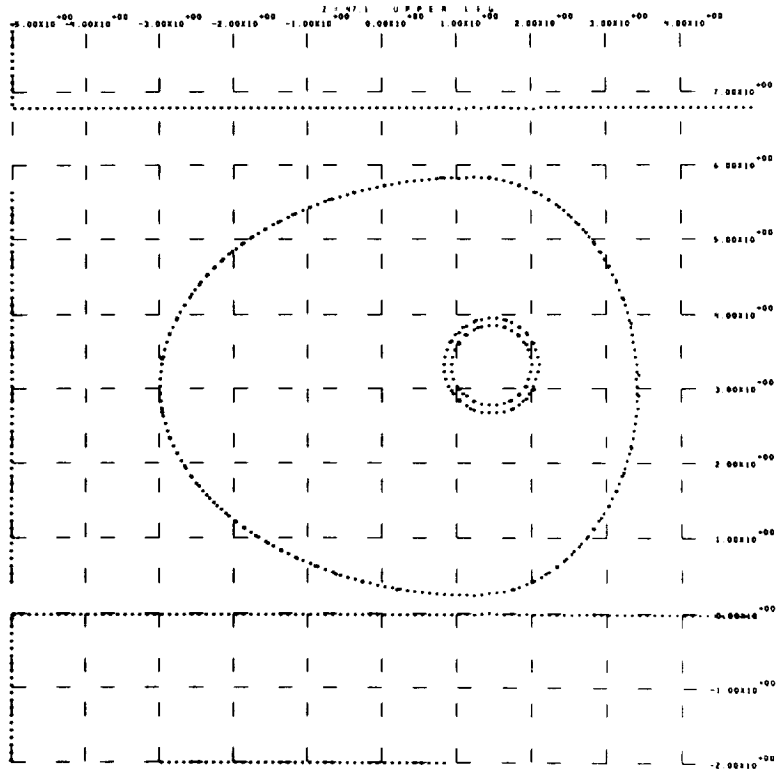

Figure 93. Horizontal Cross Section Through the Upper Leg at z = 47.1

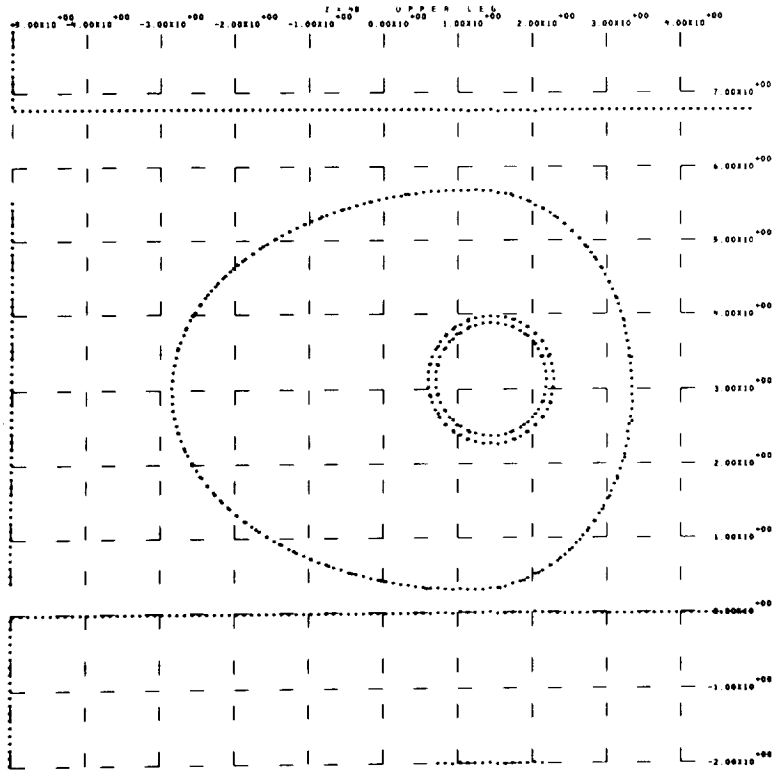

Figure 94. Horizontal Cross Section Through the Upper Leg at z = 48

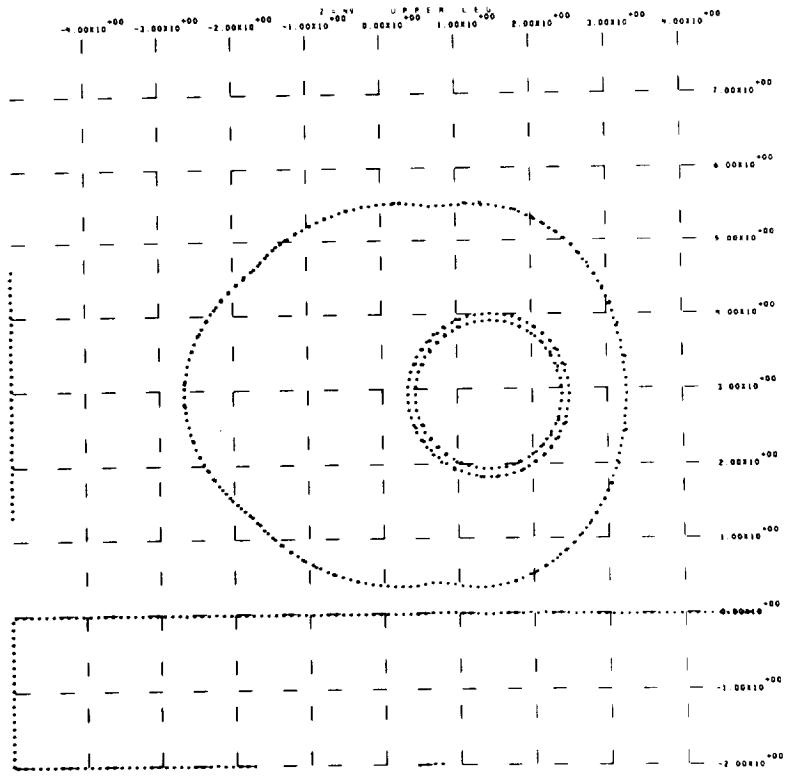

Figure 95. Horizontal Cross Section Through the Upper Leg at z = 49

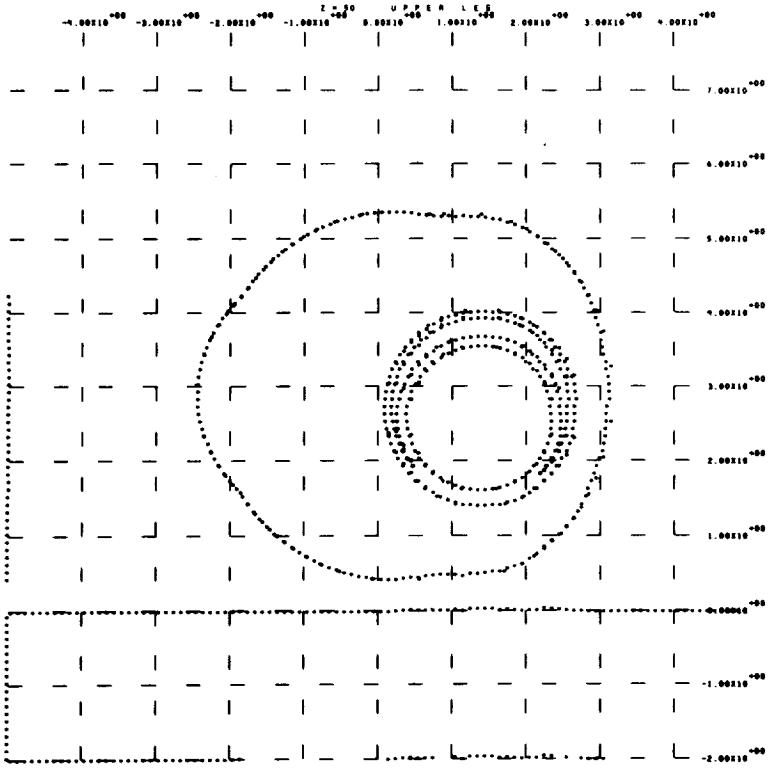

Figure 96. Horizontal Cross Section Through the Upper Leg at z = 50

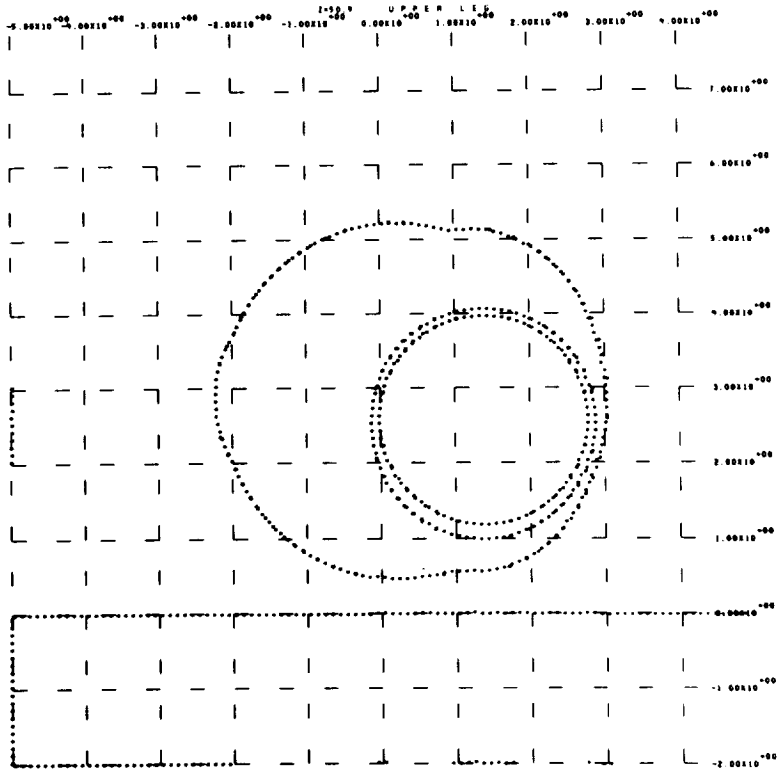

Figure 97. Horizontal Cross Section Through the Upper Leg at z = 50.9

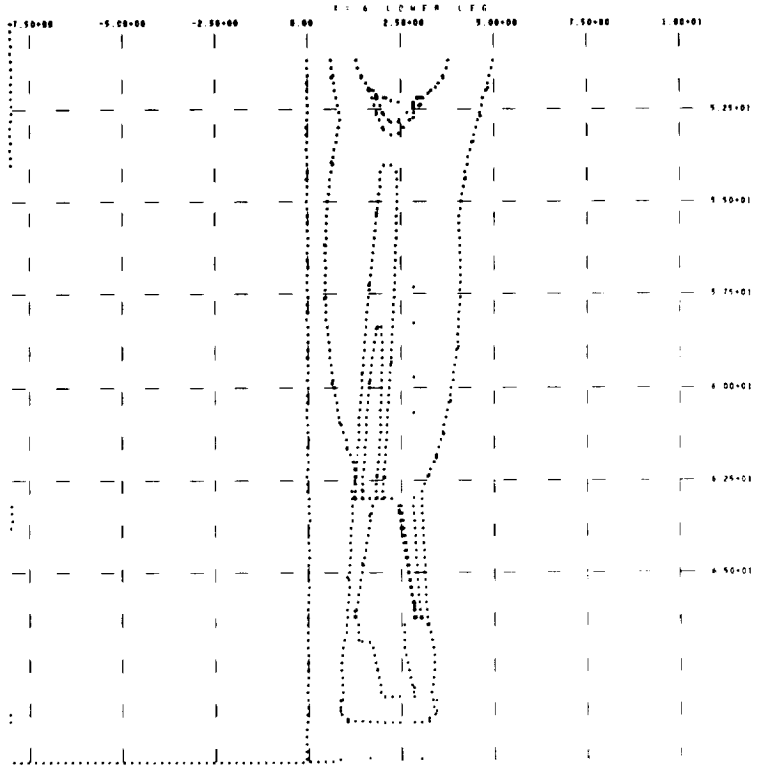

Figure 98. Vertical Cross Section Through the Lower Leg at x = 0.6

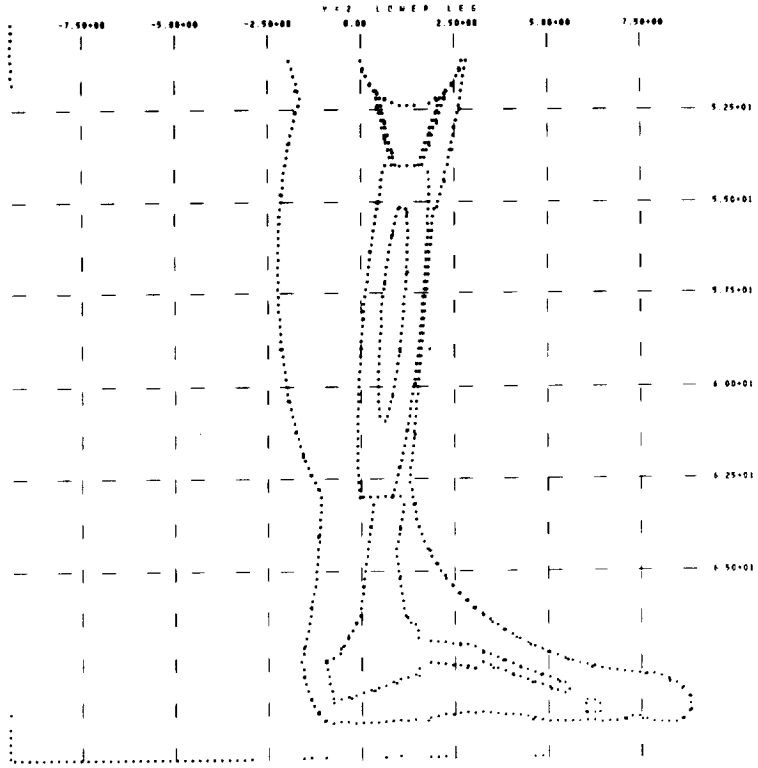

Figure 99. Vertical Cross Section Through the Lower Leg at y = 2

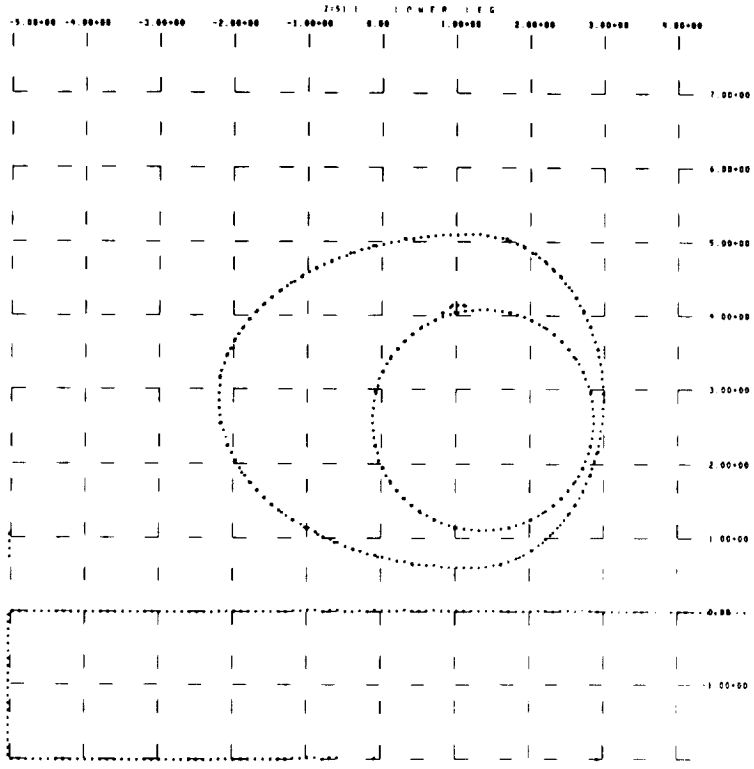

Figure 100. Horizontal Cross Section Through the Lower Leg at z = 51.1

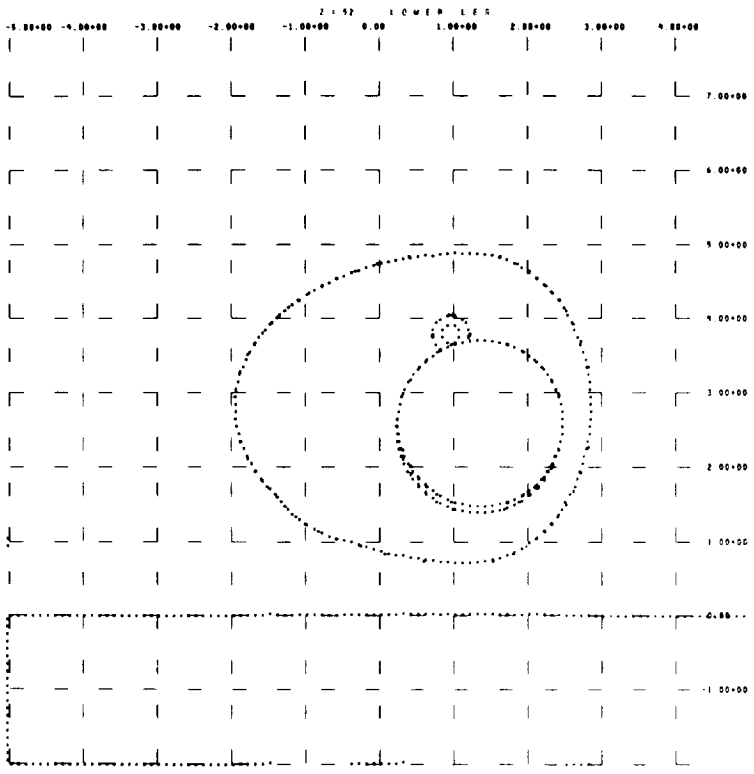

Figure 101. Horizontal Cross Section Through the Lower Leg at z = 52

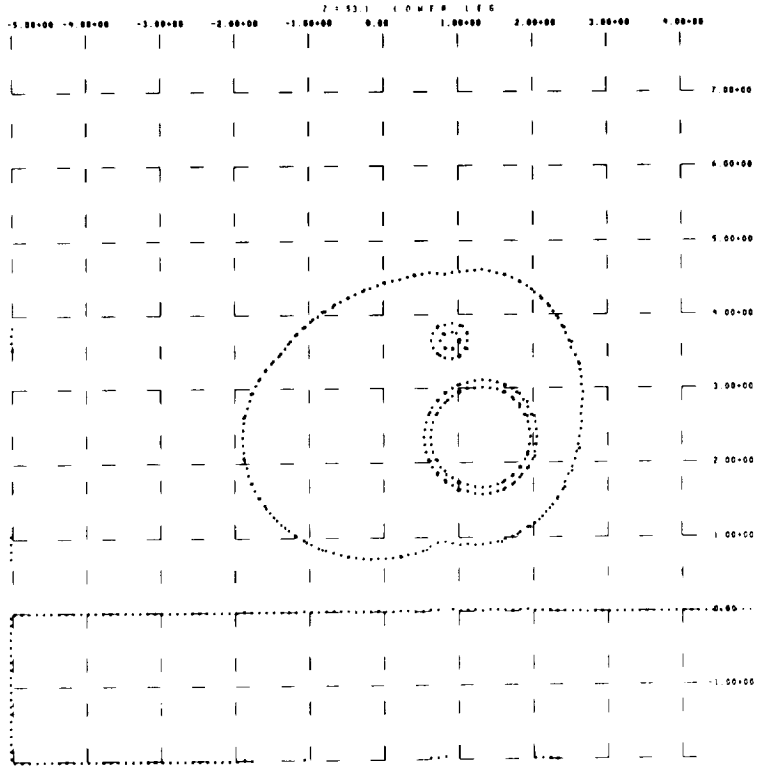

Figure 102. Horizontal Cross Section Through the Lower Leg at z = 53.1

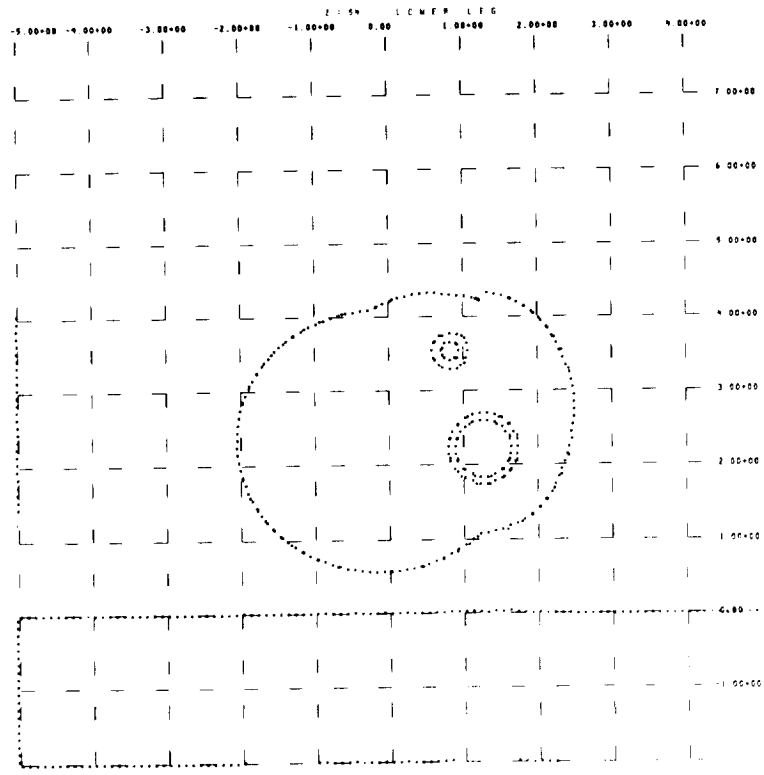

Figure 103. Horizontal Cross Section Through the Lower Leg at z = 54

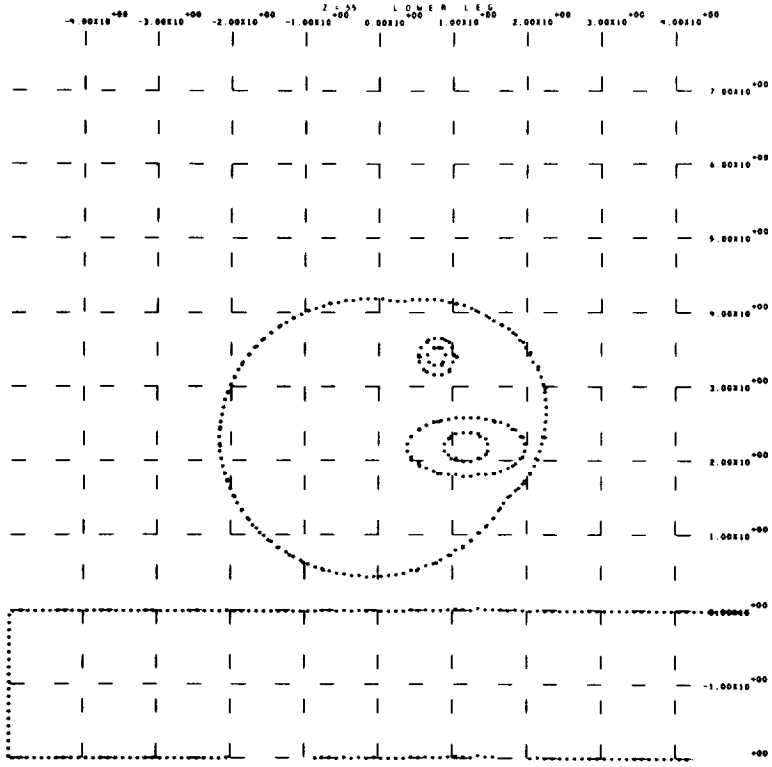

Figure 104. Horizontal Cross Section Through the Lower Leg at z = 55

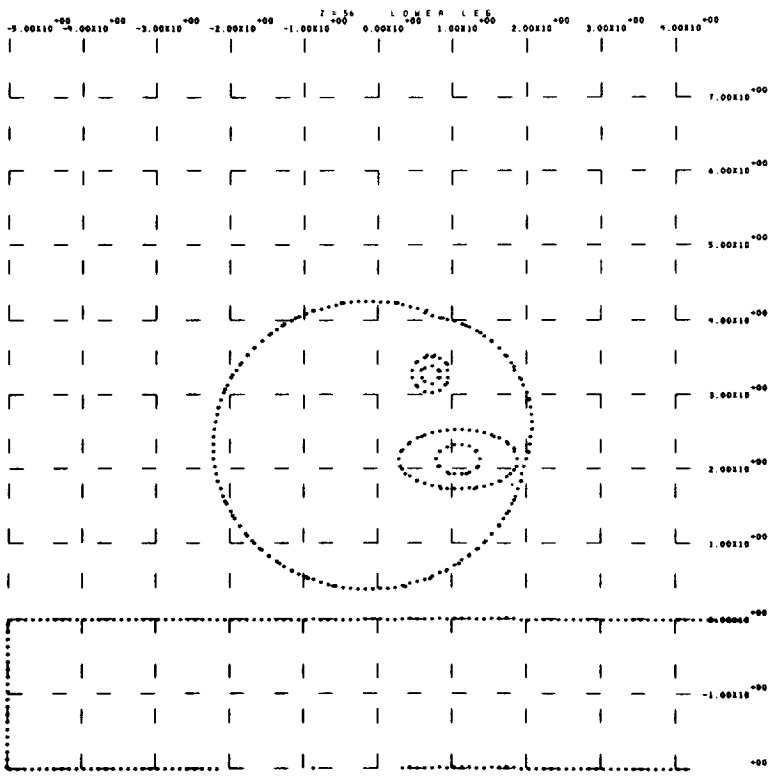

Figure 105. Horizontal Cross Section Through the Lower Leg at z = 56

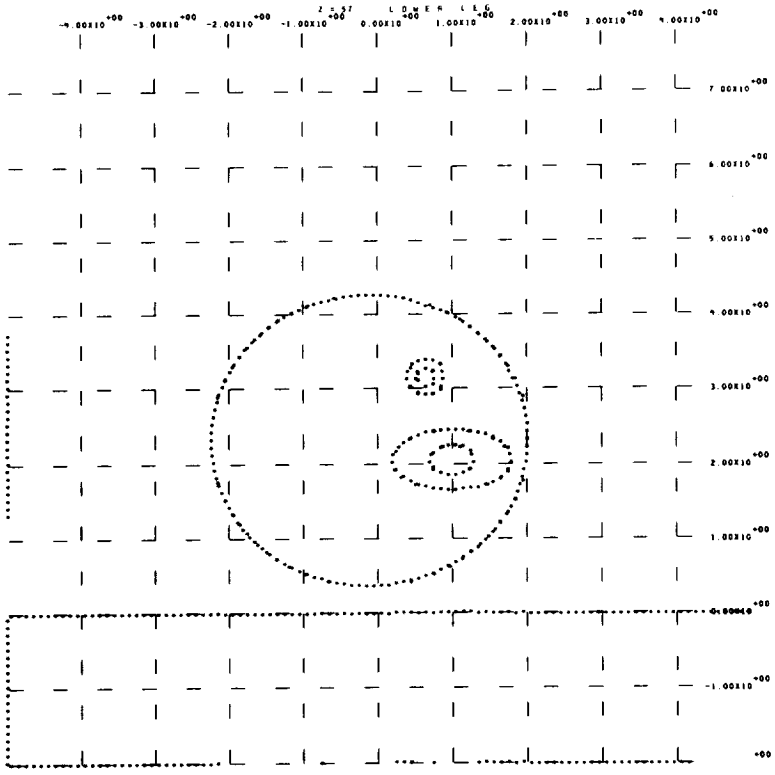

Figure 106. Horizontal Cross Section Through the Lower Leg at z = 57

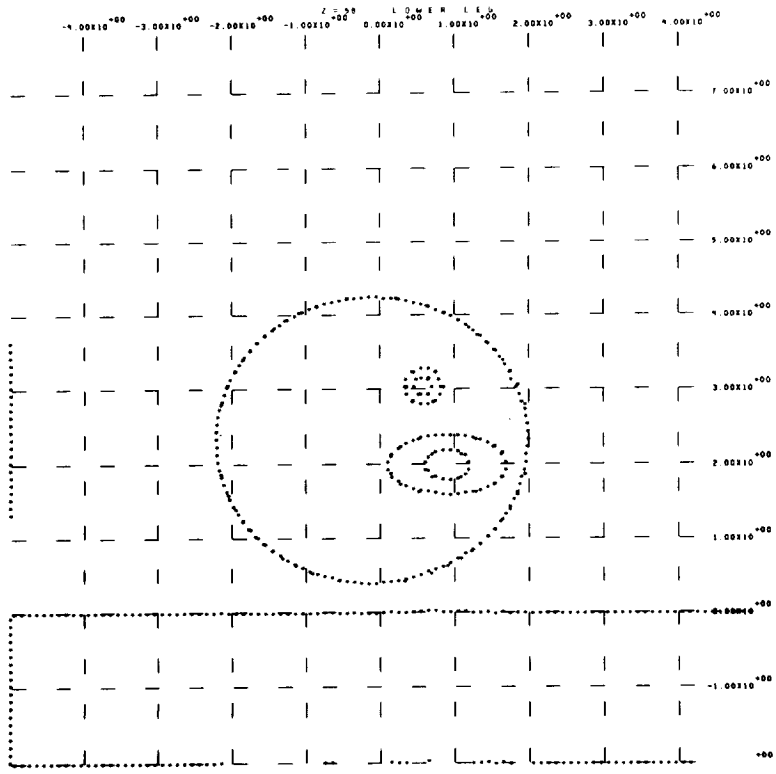

Figure 107. Horizontal Cross Section Through the Lower Leg at z = 58

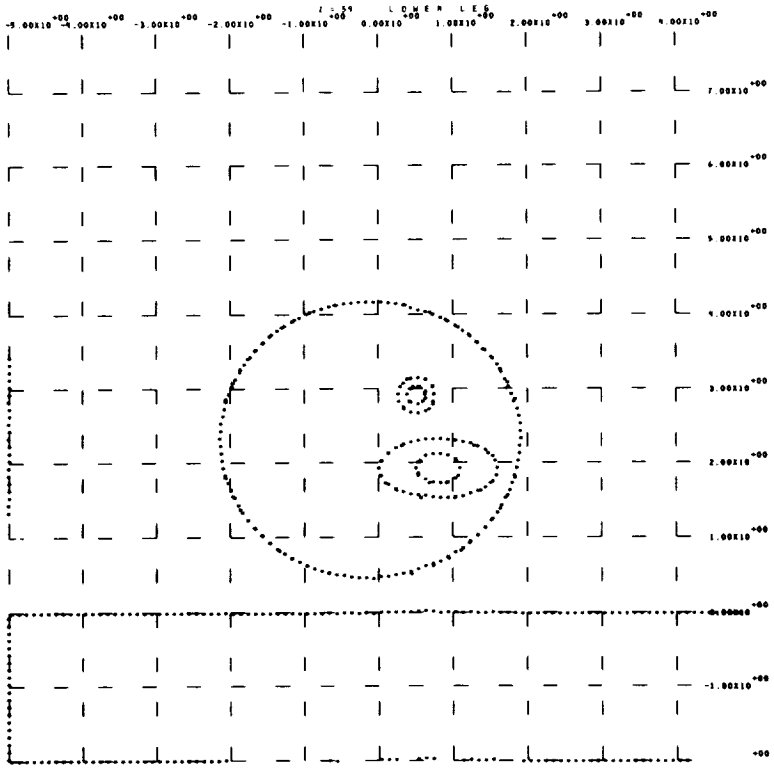

Figure 108. Horizontal Cross Section Through the Lower Leg at z = 59

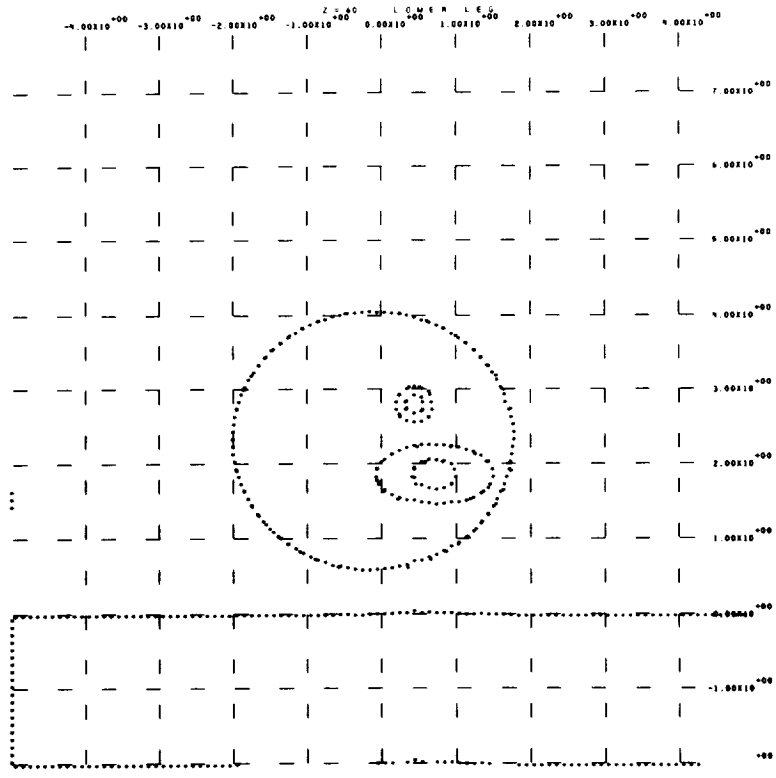

Figure 109. Horizontal Cross Section Through the Lower Leg at z = 60

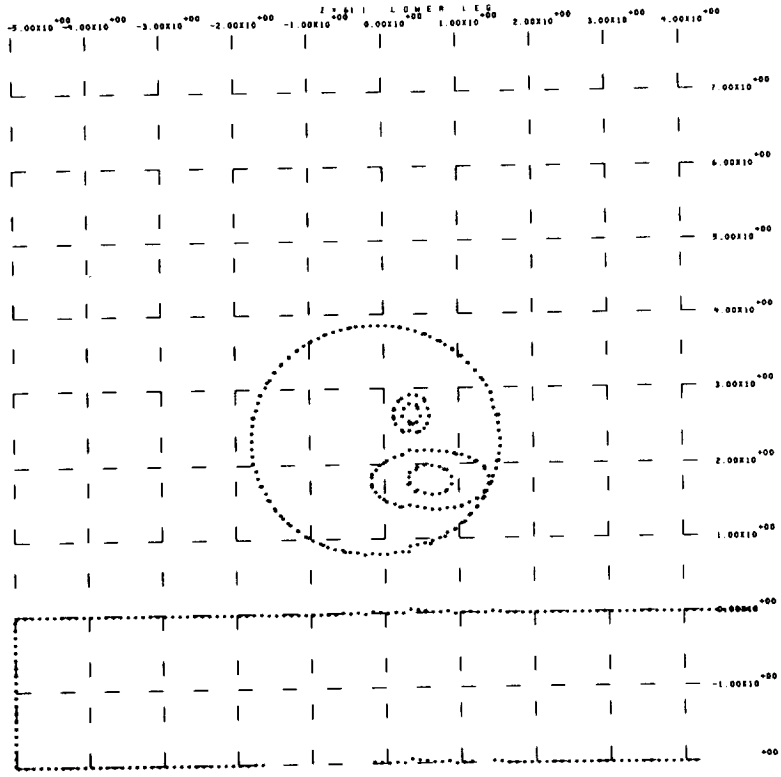

Figure 110. Horizontal Cross Section Through the Lower Leg at z = 61.1

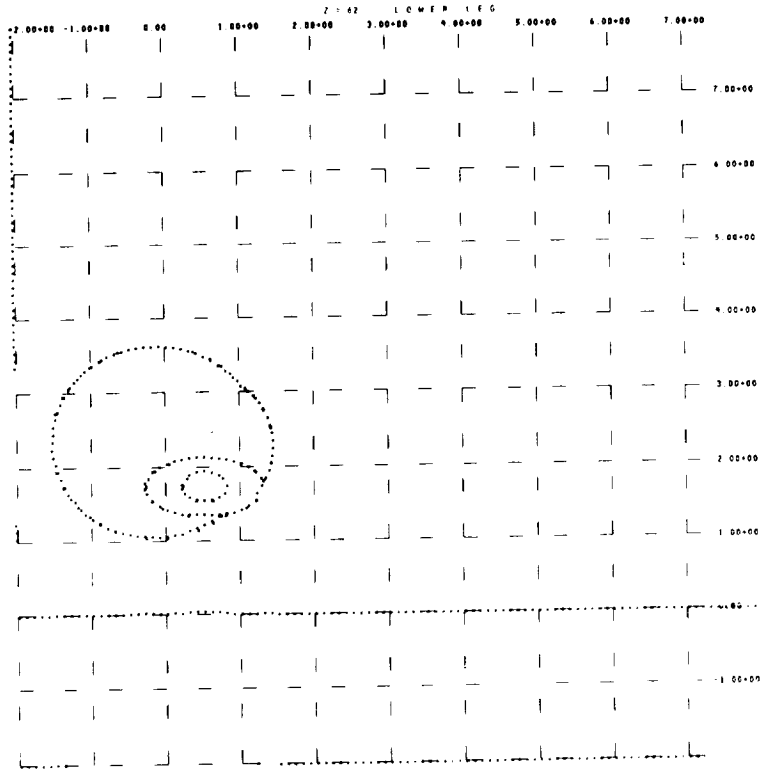

Figure 111. Horizontal Cross Section Through the Lower Leg at z = 62

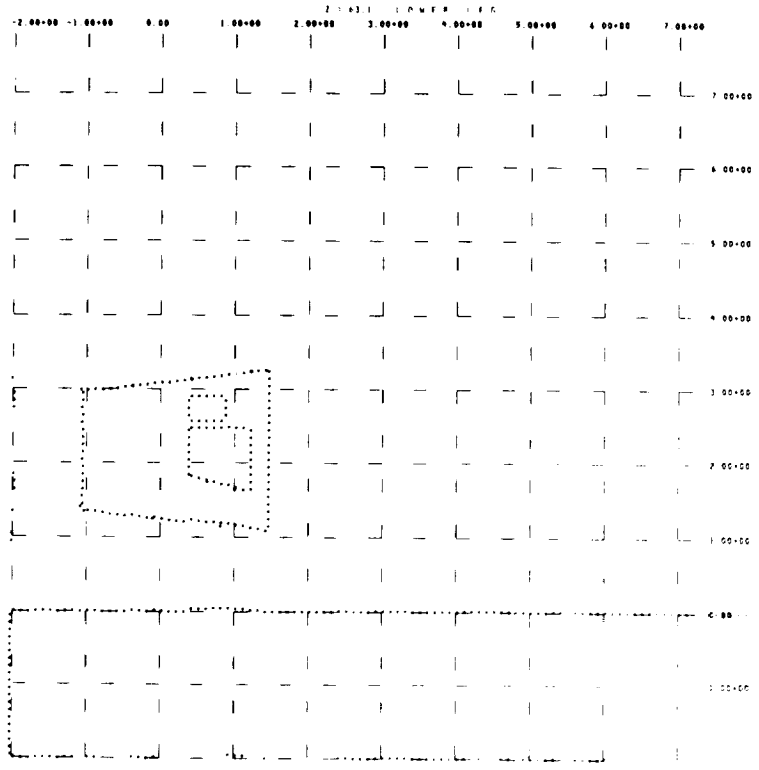

Figure 112. Horizontal Cross Section Through the Lower Leg at z = 63.1

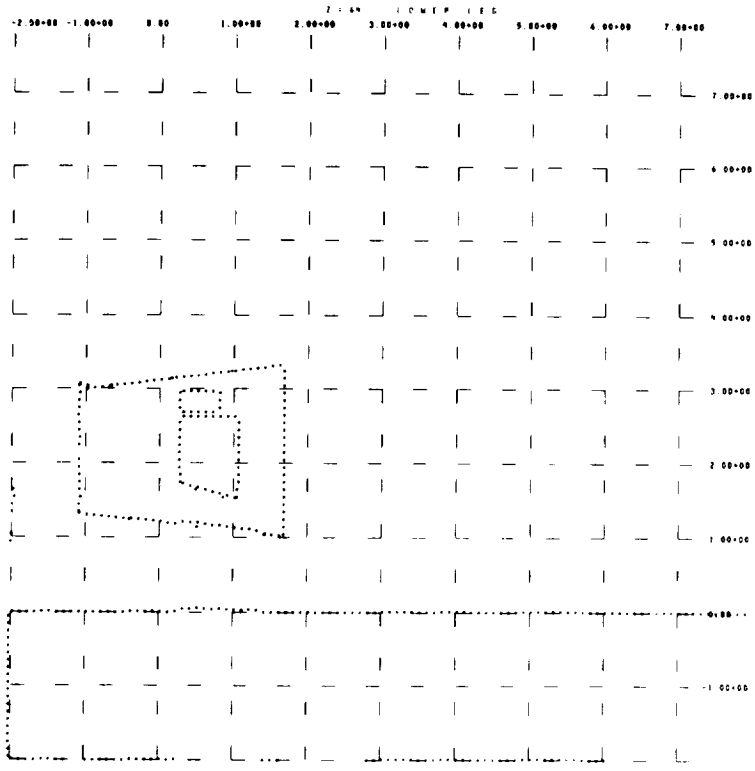

Figure 113. Horizontal Cross Section Through the Lower Leg at z = 64

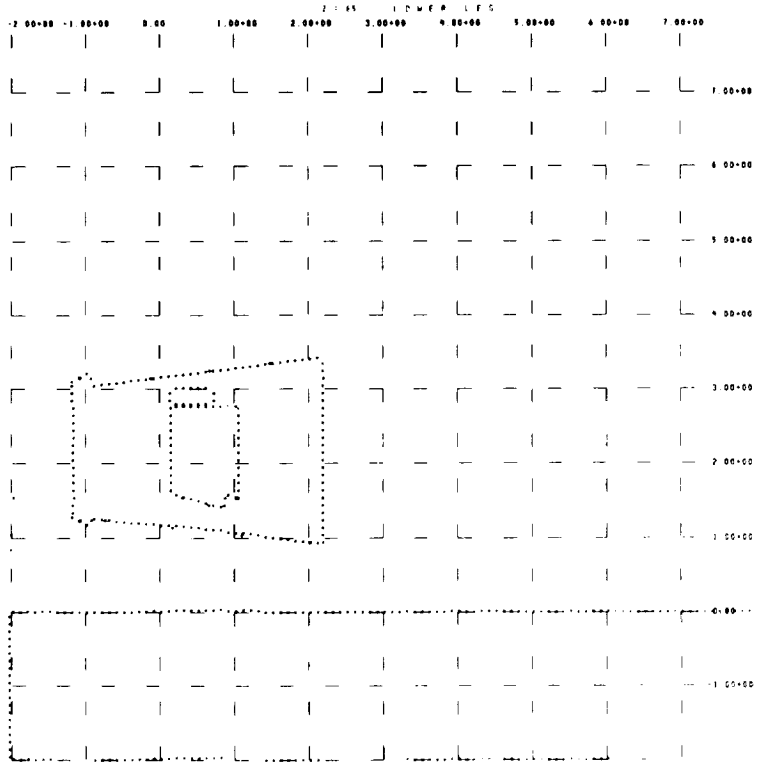

Figure 114. Horizontal Cross Section Through the Lower Leg at z = 65

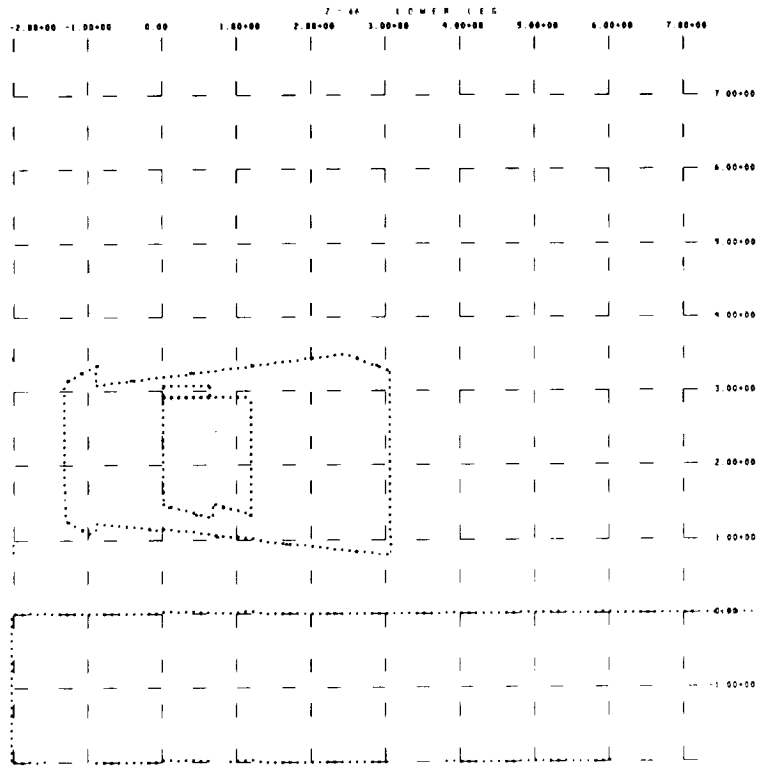

Figure 115. Horizontal Cross Section Through the Lower Leg at z = 66

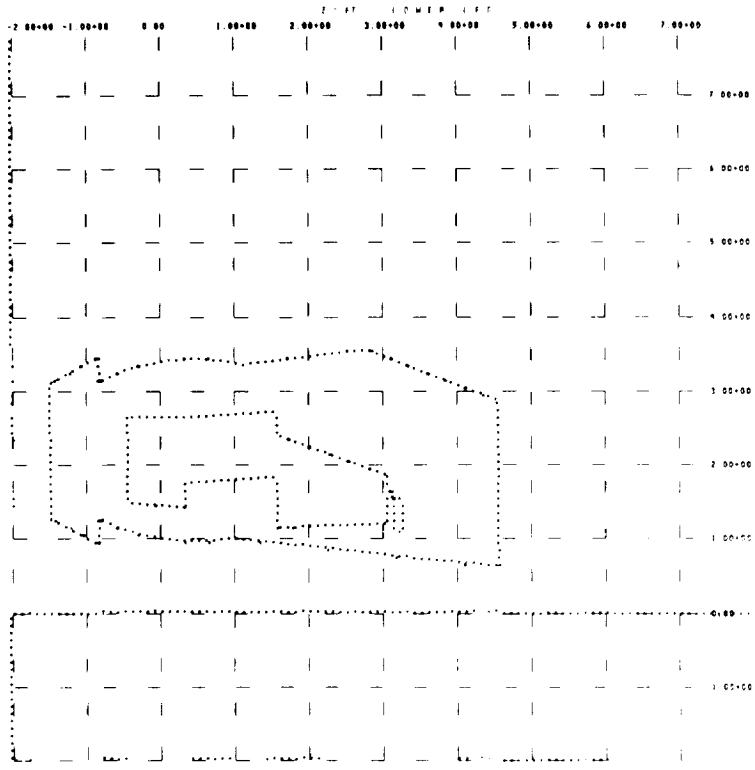

Figure 116. Horizontal Cross Section Through the Lower Leg at z = 67

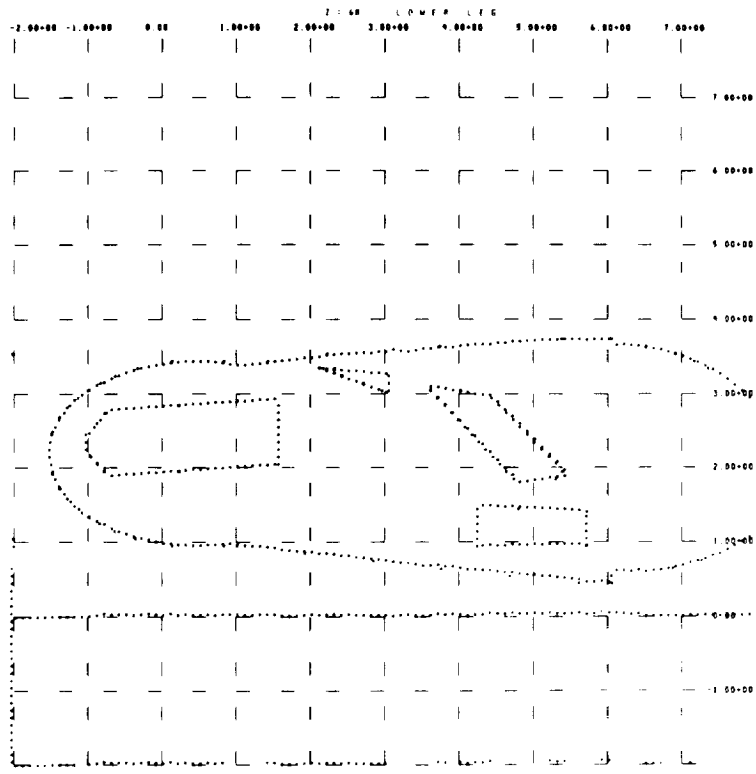

Figure 117. Horizontal Cross Section Through the Lower Leg at z = 68

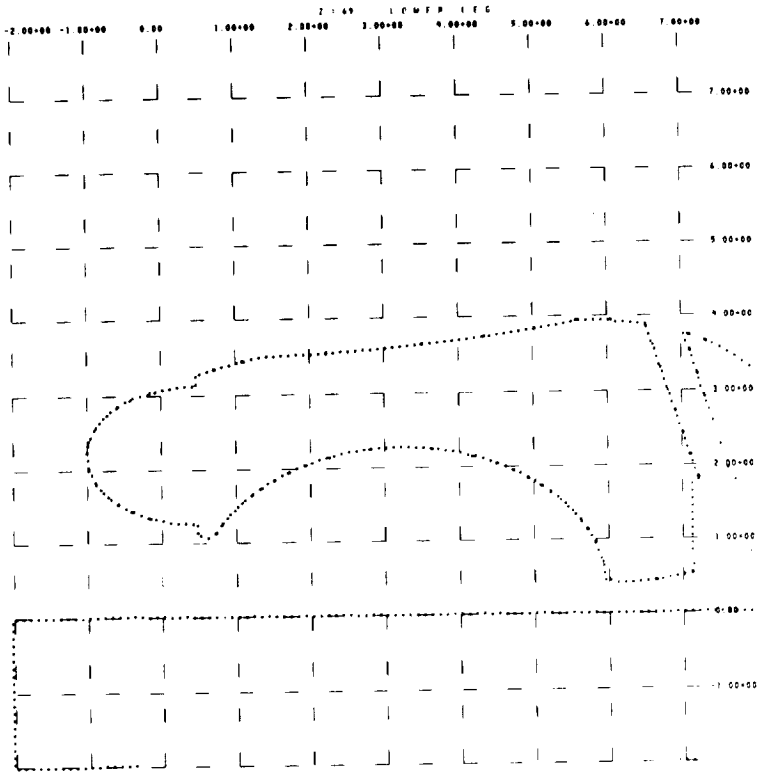

Figure 118. Horizontal Cross Section Through the Lower Leg at z = 69

legs and at two-inch intervals in arms and hands. Some of the z-sections are not precisely at one-inch intervals in order to avoid location of the view on a plane surface used in the model description.

Head

Figures 4-15 indicate the detail incorporated in the head model, including representation of the jawbone, teeth, nasal passages, eyes, ears, etc. The model for the joint at the head/neck interface is partially indicated by the views through the neck "socket" in Figures 4 and 6.

Neck

Views through the neck section are included in Figures 16-21. The ball of the ball-and-socket neck joint model is shown in Figures 16 and 17, as is the plane interface with the upper torso model. The neck section actually includes some of the upper shoulders as illustrated by Figures 16 and 21.

Upper Torso

Figures 22-28 show that interfaces of the upper torso with the neck and mid-torso sections are planes, with no joints being modeled at these locations. These figures also show the manner in which the shoulder joints were modeled, the interface between the shoulder and arm being the ball and socket region and a plane slightly inclined from the vertical. The upper portion of the rib cage is shown to be modeled as a layer of homogenized bone and bone marrow (i.e., skeleton) between layers of bone. This "sandwich" is a continuous curved sheet; no material has been removed to approximate the separation between individual ribs.

Mid-Torso

Cross sections through the mid-torso are given as Figures 29-44. The lower interface of this body section (with the lower torso) is shown in Figures 29 and 30 to incorporate a pseudo-joint that permits some flexing of the model at the waist.

Lower Torso

The lower torso has a number of interfaces with other body parts, as shown in Figures 45-54. The interface with the mid-torso section is relatively simple, but the junctions with the upper legs are the most complex of all the joint models. There are three common plane surfaces between each upper leg section and the lower torso, in lieu of the single plane surface required at other joints, because the hip ball-and-socket joint is offset. This model results in a fairly realistic approximation to body mass distribution in the vicinity of the hip for any realistic leg position.

Upper Arm

The upper arm section is illustrated in Figures 55-63. The balls of the ball-and-socket joints at either end of the section are shown in both Figures 55 and 56. In Figure 55, the ball associated with the elbow joint appears considerably smaller than in Figure 56 because the plane of the cross section does not cut through the ball center. The angle between cross section plane and the axis of the humerus is also responsible for the apparent discontinuity between the elbow and the humerus. The large marrow region typical of the long bones of the body is clearly shown in all views.

Forearm

Cross sections through the forearm, given in Figures 64-72, again show the marrow regions within both the radius and ulna. These bones are shown to terminate in a wrist joint, which is represented as a non-spherical ball-and-socket joint.

Hand

The wrist joint is further illustrated in views of the hand in Figures 73-77. As shown in Figure 75, the bones of the hand are square in cross section, as in the original CAM model. However, the bones of the fingers have been rounded and some marrow included in them.

Upper Leg

The upper leg is depicted in Figures 78-97. As in the views through the upper arm, shown in Figures 78 and 79, the cross section planes cut diagonally across the femur itself and of the ball joints. A small offset (about 0.25 in.) in the leg skin line is evident at Z=40. This offset existed in the original CAM model and has not yet been corrected; the leg contour changes abruptly across the plane, as indicated in Figures 85 and 86 by views above and below the plane.

Lower Leg

The lower leg and foot are shown in Figures 98-118. Below the plane Z = 63, the geometry is as in the original version, the only changes having been to debug the geometric data. Above this plane extensive remodeling was done, especially to improve the knee geometry and to reshape and incorporate marrow in the long bones; hence, there is a small offset or discontinuity in the long bones at Z = 63.

3.2 MATERIALS AND MASSES

The material composition for each region is indicated by assigning the index of a standardized set of materials. While there exist several sets of body material compositions in the literature, no attempt has been made to research these data and the compositions that have been assumed are those in the original CAM report. These compositions are reproduced in Table 4.

Table 4

MATERIAL COMPOSITIONS

Chemical Element	Fractional Composition by Weight									
	Code No.									
	1	2	3	4	5	6	7	8	9	10
	Name									
	Void	Lung	Organ	Intestine	Muscle	Bone	Marrow (fat)	Skeleton	Tissue	Water
	Density (gm/cm^3)									
	0.000	0.257	1.058	0.451	1.060	1.75	0.918	1.499	1.000	1.000
Hydrogen (H)		0.0980	0.0980	0.0980	0.1020	0.064	0.122	0.082	0.1000	0.1119
Carbon (C)		0.1450	0.1450	0.1450	0.1230	0.278	0.761	0.423	0.1800	---
Nitrogen (N)		0.0380	0.0380	0.0380	0.0350	0.027	---	0.019	0.0300	---
Oxygen (O)		0.7070	0.7070	0.7070	0.7290	0.410	0.117	0.322	0.6500	0.8881
Sodium (Na)		0.0015	0.0015	0.0015	0.0008	---		---	0.0015	
Magnesium (Mg)		0.0002	0.0002	0.0002	0.0002	0.002		0.001	0.0005	
Phosphorous (P)		0.0030	0.0030	0.0030	0.0020	0.070		0.049	0.0100	
Sulfur (S)		0.0018	0.0018	0.0018	0.0050	0.002		0.001	0.0025	
Potassium (K)		0.0026	0.0026	0.0026	0.0030	---		---	0.0020	
Calcium (Ca)		0.0009	0.0009	0.0009		0.147		0.103	0.0015	
Chlorine (Cl)		0.0020	0.0020	0.0020					0.0015	
Stopping power relative to Aluminum for 50 Mev protons		1.281	1.281	1.281	1.287	1.202	1.348	1.247	1.262	1.299

As noted in Section 3.1, the last digit of the material index defines the composition. It should be noted that the model is dependent on the assumed chemical compositions only to the extent that the density specified for each region is consistent with Table 4; no other material composition data is built into the model and use of an alternative set of elemental compositions in radiation transport calculations based on the model should be simple to implement. A value for the stopping power of the material for 50 MEV protons, relative to that of aluminum, is also given; these data can be used to convert true areal density along rays through the CAM model to equivalent aluminum densities.

Ray tracing calculations have been employed to construct tabular data defining the masses, areas, etc. of various portions of the model. These data, presented as Tables 5-7, give the masses and skin areas for each of the 15 body sections, and the masses of each organ (as distinguished by the material code).

The data in Table 7 also show the relationship among the spatial distributions of BFO mass as incorporated in the model and as measured by various investigators. Using the Ellis BFO mass distribution data as a reference, it is evident that CAM model generally underestimates BFO mass for all sites other than the sternum and ribs. Some underestimation would be expected because all BFO sites are not explicitly modeled. There is also the possibility that the number of rays used to produce these mass values was too few for adequate convergence, and that due to the highly irregular shapes of the sites, the tendency is toward low values. The overestimation of BFO mass in the sternum and rib sites is due to the rib being mdeled as a continuous sheet, with no separation between ribs.

The procedure for computing mass and skin area involves tracing N rays randomly in the 4π solid angle about a specified point, observing the distances along the path to the entrance and exit points to each region or subsection of interest and adding mass or area increments to the running summation for each geometric piece of interest. Formally, if the ith region

Table 5

VOLUME, MASS AND SKIN AREA OF BODY SECTIONS

Section	Volume cm^3	Mass kg	Skin Area cm^2
Head	4.10(3	4.58	1.36(3
Neck	0.93(3	1.05	0.40(3
Upper Torso	4.55(3	4.52	0.83(3
Mid Torso	17.93(3	15.76	2.96(3
Lower Torso	10.49(3	9.74	2.01(3
Right Upper Arm	2.21(3	2.37	0.83(3
Right Forearm	0.83(3	0.94	0.56(3
Right Hand	0.63(3	0.44	0.35(3
Right Upper Leg	8.96(3	9.65	2.19(3
Right Lower Leg	3.16(3	3.50	1.81(3
Left Upper Arm	2.21(3	2.37	0.83(3
Left Forearm	0.88(3	0.94	0.56(3
Left Hand	0.36(3	0.44	0.35(3
Left Upper Leg	8.96(3	9.65	2.19(3
Left Lower Leg	3.16(3	3.50	1.81(3
Total:	69.14(3	69.45	19.04(3

Table 6

MASS DISTRIBUTION BY MATERIAL AND BODY SECTION

Body Section	Mass (kg)							Total Mass	
	2 Lung	3 Organ	4 Intestine	5 Muscle	6 Bone	7 Marrow	8 Skeleton	kg	lb
Head	0	1.38	0	2.19	0.74	0	0.27	4.58	10.10
Neck	0	0.048	0	0.67	0.28	0	0.051	1.05	2.32
Upper Torso	0.22	0.26	0	2.86	0.62	0	0.56	4.52	9.97
Mid Torso	0.84	4.72	1.24	5.94	1.77	0	1.25	15.76	34.75
Lower Torso	0	0.22	1.63	5.57	1.48	0	0.84	9.74	21.48
Right Upper Arm	0	0	0	2.27	0.048	0.009	0.046	2.37	5.23
Right Forearm	0	0	0	0.85	0.060	0.034	0	0.94	2.07
Right Hand	0	0	0	0.27	0.046	0	0.12	0.44	0.97
Right Upper Leg*	0	0	0.077	8.75	0.14	0.004	0.68	9.65	21.28
Right Lower Leg	0	0	0	3.04	0.071	0.005	0.38	3.50	7.72
Left Upper Arm	0	0	0	2.27	0.048	0.009	0.046	2.37	5.23
Left Forearm	0	0	0	0.85	0.060	0.034	0	0.94	2.07
Left Hand	0	0	0	0.27	0.046	0	0.12	0.44	0.97
Left Upper Leg*	0	0	0.007	8.75	0.14	0.004	0.68	9.65	21.28
Left Lower Leg	0	0	0	3.04	0.071	0.005	0.38	3.50	7.72
Total:	1.06	6.628	3.024	47.59	5.62	0.104	5.41	69.45	153.2

*The leg/torso interface was simplified by including a portion of the intestine in the upper leg model.

Table 7

COMPARISON OF MARROW DISTRIBUTION
IN CAM WITH EXPERIMENTAL DATA

Site	Bone Marrow Mass (Grams)		
	Ellis	Hashimoto	CAM*
Cranium and Mandible	136	53	62
Upper Limb Girdle	84	53	23
Sternum and Ribs	105	130	270
Cervical Vertebrae	42	23	
Head			19
Neck			15
Thoracic Vertebrae	146	100	
Upper Torso			46
Mid Torso			146
Lumbar Vertebrae and Sacrum	261	153	
Mid Torso			57
Lower Torso			126
Lower Limb Girdle	272	252	126
Total Active (Red)	(1046)	(764)	(890)
Upper Limbs			186
Lower Limbs			654
Total (Red and Yellow)			(1730)

*Marrow mass estimated as 30 percent of skeleton mass (Material 8) plus 100 percent of marrow mass (Material 7).

is traversed by the ray, the distance to the entrance and exit penetration being r_m and r_{m+1}, respectively

$$\Delta M_i = \frac{4\pi\rho_i}{3N}\left(r_{m+1}^3 - r_m^3\right)$$

Also, if this region is an external region such that the outer surface is a skin location, the area is estimated by

$$\Delta A_i = \frac{4\pi}{\mu N} r_{m+1}^2$$

where μ is the cosine of the angle between the ray and the normal to the skin surface.

3.3 DOSE POINT LOCATIONS

To facilitate use of the CAM model in performing radiation analyses, the locations of internal dose points in various body organs have been determined. The coordinates of these points as well as the region identification and material index, are given in Tables 8-11. These locations have been verified as to their location within the organ they are stated to represent. Their use by various investigators should provide consistency of dose results that may not be evidenced if points were selected independently by each user.

For several body organs of interest in radiobiological studies, point locations are quite satisfactory because the spatial extent of the organs is limited. Hence point locations are presented in Table 8 for the lens of eye, testes, heart, hypothalamus, and thyroid, adrenal and pituitary glands.

Dose point locations in the spatially distributed BFO and gastrointestinal tract are given in Tables 9 and 10. These locations were selected randomly by techniques summarized in Section 2.6. However, there is is an order built into the listing of these points because they were obtained by sampling from body sections separately, rather than from the whole man. The relative weights of the points in each body section are approximately the same, but do differ because the sampling densities (i.e., the number of

Table 8

DOSE POINT LOCATIONS FOR VARIOUS ORGANS

Site	Coordinates (in.)		
	X	Y	Z
Right Eye, Lens	3.404	1.245	4.30
Right Eye, Retina at Optic Nerve	2.278	1.245	4.30
Right Testicle	2.25	0.55	38.25
Left Testicle	2.25	-0.55	38.50
Heart	1.71	0.14	17.60
Thyroid Gland	2.125	0.0	11.4
Pituitary Gland	1.4	0.0	3.4
Adrenal Glands	-0.8	-2.4	22.9
	-0.7	2.3	23.9
Hypothalamus	0.90	0.0	4.10

points per unit mass of BFO) differ for each section. The weights to be associated with each dose point are listed in Table 12 and were obtained by prorating the fraction of the organ in the section among the several points used to represent it.

The use of fewer points than are listed to represent any organ would require adjustment of the dose point weights from the values found in the table. Also, if a mass distribution for the BFO other than the one modeled, as specified in Tables 6 and 7, is preferred, the weights can be adjusted accordingly.

Dose point locations for the skin are given in Table 11. These locations were selected by the technique described in Section 2.6, using the assembled model, and hence they have uniform weights. Because the rays used to select these points can penetrate the body several times (e.g., entry and exit of upper arm, followed by entry and exit of upper torso) the penetration number is also noted in the table. It is likely that some of these points are

Table 9 (Page 1 of 2)

DOSE POINT LOCATIONS FOR BONE MARROW

X(IN.)	Y(IN.)	Z(IN.)	REGION I.D.	MATERIAL
3.024408E+00	-8.902859E-01	6.380068E+00	HDSKBF34	8
2.420503E+00	-8.157519E-01	6.499583E+00	HDSKBF34	8
-1.116720E+00	-1.422792E+00	5.513416E+00	HDSKBF30	8
2.680207E+00	-1.430791E+00	2.828930E+00	HDSKBF10	8
1.209184E+00	-1.006380E-02	4.087204E+00	HDSKBF33	8
-7.160909E-01	1.108629E-01	1.045724E+01	NKSBF006	8
1.174010E-01	-8.081106E-01	1.134202E+01	NKSBF011	8
-6.617771E-01	3.247597E+00	1.404661E+01	UTRBF001	8
-2.848661E-01	-7.102887E-01	1.303650E+01	UTSBF005	8
-4.805325E-01	-4.784578E+00	1.360597E+01	UTOBF004	8
1.325192E-01	1.377036E-01	1.236354E+01	UTSBF001	8
-1.439266E+00	8.516540E-01	1.555344E+01	UTSBF002	8
-2.872203E+00	-5.221478E-01	1.509778E+01	UTRBF004	8
-1.925754E+00	1.318068E-02	1.413423E+01	UTSBF003	8
1.993821E+00	2.655915E+00	1.457758E+01	UTRBF001	8
-7.366612E-01	3.812638E+00	1.535332E+01	UTRBF001	8
-1.302073E+00	2.789686E-01	1.271345E+01	UTSBF003	8
-2.429280E+00	2.777714E-01	2.023321E+01	MTTVER14	8
-1.318100E+00	-2.525972E-01	1.647978E+01	MTTVER01	8
-1.671411E+00	-4.853780E+00	2.084014E+01	MTRBF009	8
-1.271770E+00	7.795977E-01	2.403729E+01	MTTVER22	8
2.736849E+00	3.537505E+00	1.970338E+01	MTRBF002	8
-1.140002E+00	-4.047064E+00	2.377156E+01	MTRBF009	8
-1.533947E+00	7.008566E-01	2.638441E+01	MTLVER04	8
2.263407E+00	4.007944E+00	1.938197E+01	MTRBF001	8
-9.916122E-01	1.932821E-01	2.630033E+01	MTLVER02	8
-2.701057E+00	2.549259E-01	2.266330E+01	MTTVER24	8
-1.065064E+00	-1.590949E-02	2.034666E+01	MTTVER13	8
-2.601354E-01	4.364946E+00	2.405222E+01	MTRBF004	8
-1.463894E+00	3.233955E-01	2.291397E+01	MTTVER22	8
-1.600678E+00	5.751758E-01	2.691455E+01	MTLVER04	8
-1.434756E+00	-5.457801E-02	1.916538E+01	MTTVER13	8
-1.111456E+00	-4.685074E+00	2.233324E+01	MTRBF009	8
-9.097623E-01	3.118157E-01	2.600319E+01	MTLVER04	8
-1.798347E+00	8.510987E-01	1.819333E+01	MTTVER04	8
-1.065825E+00	-5.461984E-01	2.482650E+01	MTTVER21	8
-1.168863E+00	-4.598708E-01	2.429830E+01	MTTVER21	8
-8.725048E-02	7.562285E+00	2.253087E+01	RUABF002	17
4.449368E-02	7.236762E+00	1.688708E+01	RUABF002	17
-7.451644E-01	-7.446651E+00	2.609339E+01	LUABF003	18
4.714665E-01	-7.126461E+00	1.676128E+01	LUABF002	17
-7.735195E-01	-2.801519E+00	3.669041E+01	LTPBF017	8
-3.872055E-02	5.032853E+00	3.146490E+01	LTPBF011	8
-1.266091E+00	2.247152E-02	2.961736E+01	LTSBF001	8
-3.053492E+00	1.447406E+00	3.157397E+01	LTPBF012	8
9.917892E-01	4.989018E+00	3.123776E+01	LTPBF007	8
-1.014684E+00	-6.431966E-01	2.887229E+01	LTLVER02	8
-2.585730E+00	-3.108971E+00	3.113242E+01	LTPBF008	8
-2.443143E+00	8.858117E-01	3.139482E+01	LTSBF003	8
1.390081E+00	-4.066142E-01	3.538740E+01	LTPBF017	8

Table 9 (Page 2 of 2)

DOSE POINT LOCATIONS FOR BONE MARROW

X(IN.)	Y(IN.)	Z(IN.)	REGION I.D.	MATERIAL
-9.624029E-01	-3.974816E-02	2.897189E+01	LTLVER02	8
-2.104693E+00	6.673627E-01	3.090373E+01	LTSBF001	8
-3.454303E+00	-2.601852E-01	3.241035E+01	LTSBF003	8
-1.071803E+00	2.740581E+00	3.543757E+01	LTPBF016	8
-3.308095E+00	-3.380643E-01	3.229979E+01	LTSBF003	8
-3.002394E-01	1.516318E-01	3.023119E+01	LTSBF002	8
-5.458063E-01	7.190898E+00	2.669745E+01	RFABF002	17
9.282897E-02	8.055300E+00	3.013457E+01	RFABF001	17
-6.832250E-01	-6.986903E+00	2.651046E+01	LFABF002	17
-4.938237E-01	-7.156764E+00	2.812107E+01	LFABF003	17
1.715605E-01	7.997020E+00	3.602680E+01	RHNBF001	18
2.080082E+00	7.509076E+00	4.045430E+01	RHNBF002	18
-3.031141E-01	-8.598113E+00	3.908587E+01	LHNBN401	18
1.191579E+00	-8.255145E+00	4.199860E+01	LHNBF003	18
-1.291701E-01	4.495308E+00	3.392374E+01	RULBF001	18
1.414047E+00	3.713350E+00	4.464421E+01	RULBF002	17
8.971446E-01	1.423087E+00	5.072317E+01	RULBF003	18
2.058036E+00	3.559454E+00	4.984537E+01	RULBF004	18
1.978723E+00	2.007118E+00	4.930649E+01	RULBF004	18
1.008781E+00	2.844067E+00	4.809235E+01	RULBF004	18
1.522752E+00	3.355810E+00	4.831639E+01	RULBF004	18
1.606378E+00	2.438531E+00	5.231216E+01	RULBF003	18
1.821014E+00	2.982686E+00	4.936166E+01	RULBF004	18
7.589582E-01	5.445607E+00	3.421773E+01	RULBNE02	18
1.183214E+00	-3.666225E+00	4.521944E+01	LULBF002	17
7.007707E-01	-5.219862E+00	3.846345E+01	LULBF002	17
7.508380E-01	-4.742816E+00	3.970318E+01	LULBF002	17
1.134111E+00	-2.342105E+00	5.020987E+01	LULBF003	18
1.272357E+00	-3.852015E+00	5.049163E+01	LULBF003	18
-2.825002E-01	-3.913400E+00	3.487509E+01	LULBF001	18
9.276321E-01	-3.353499E+00	4.868040E+01	LULBF004	18
1.409988E+00	-3.939733E+00	4.938171E+01	LULBF004	18
2.241613E+00	-1.929034E+00	5.014139E+01	LULBF003	18
1.215275E+00	-3.885341E+00	5.110320E+01	LULBF003	18
1.146394E+00	2.220677E+00	5.327471E+01	RLLBF001	18
8.953639E-01	2.052818E+00	6.697610E+01	RLLBNE09	18
2.917729E+00	3.009232E+00	6.795354E+01	RLLBNE06	18
2.975603E-01	2.763621E+00	6.392002E+01	RLLBNE11	18
7.034715E-01	1.784971E+00	6.242232E+01	RLLBF003	17
4.935504E+00	1.011535E+00	6.792136E+01	RLLBNE04	18
2.163081E+00	1.132579E+00	6.732966E+01	RLLBNE05	18
7.489896E-01	3.449235E+00	5.447015E+01	RLLBF002	17
-8.241917E-02	1.750283E+00	6.679622E+01	RLLBNE10	18
8.155524E-01	2.192427E+00	6.669130E+01	RLLBNE10	18
1.067808E+00	-2.169389E+00	6.601659E+01	LLLBNE14	18
1.415350E+00	-2.268528E+00	5.381295E+01	LLLBF001	18
5.796197E+00	-1.255656E+00	6.802044E+01	LLLBNE04	18
3.714954E-01	-1.771087E+00	6.489905E+01	LLLBNE14	18
1.228899E+00	-1.841940E+00	5.276376E+01	LLLBF001	18
2.215343E-01	-1.970502E+00	6.494460E+01	LLLBNE14	18
3.417186E-01	-2.647585E+00	6.449111E+01	LLLBNE13	18
1.109300E+00	-2.140038E+00	5.319622E+01	LLLBF001	18
1.108013E+00	-2.267890E+00	5.499523E+01	LLLBF003	17
-6.350676E-02	-2.606817E+00	6.726758E+01	LLLBNE07	18

Table 10

DOSE POINT LOCATIONS FOR GASTROINTESTINAL TRACT

X(IN.)	Y(IN.)	Z(IN.)	REGION I.D.	MATERIAL
9.581619E-01	-1.858572E+00	2.786689E+01	MTINTS10	4
1.439734E+00	-6.052601E-01	2.727675E+01	MTINTS08	4
4.373922E-01	-4.352442E+00	2.607019E+01	MTINTS10	4
6.434034E-01	4.038131E+00	2.785538E+01	MTINTS14	4
2.304811E-01	3.947268E+00	2.677846E+01	MTINTS14	4
2.097410E+00	-3.560910E+00	2.897975E+01	MTINTS08	4
1.423706E+00	-4.599391E-01	2.896835E+01	MTINTS08	4
2.730778E+00	3.167036E+00	2.868953E+01	MTINTS08	4
1.270096E+00	-1.604914E+00	2.660926E+01	MTINTS10	4
-9.146533E-01	-2.429928E+00	2.739938E+01	MTINTS10	4
3.123350E+00	-5.240075E-01	2.755799E+01	MTINTS08	4
1.410845E+00	-1.486728E+00	2.886928E+01	MTINTS08	4
-3.117554E-01	-4.284921E+00	2.766688E+01	MTINTS10	4
-2.159142E+00	-1.316284E+00	2.568241E+01	MTINTS10	4
2.763858E+00	1.949212E+00	2.830436E+01	MTINTS08	4
8.196615E-01	-3.213659E+00	2.619737E+01	MTINTS10	4
2.367963E+00	2.108163E+00	2.689941E+01	MTINTS08	4
1.141283E+00	-1.565747E+00	2.672266E+01	MTINTS10	4
-1.643305E+00	2.025575E+00	2.815118E+01	MTINTS14	4
1.445120E+00	-1.299999E+00	2.669418E+01	MTINTS08	4
-1.604303E-01	8.641626E-01	3.113129E+01	LTINTS01	4
8.694357E-01	-2.268165E+00	3.202708E+01	LTINTS07	4
-2.852999E+00	-1.612655E+00	3.377517E+01	LTINTS19	4
-8.163661E-01	-1.433093E+00	2.940031E+01	LTINTS05	4
9.693941E-01	-9.519058E-01	3.175162E+01	LTINTS07	4
1.403619E+00	-8.461893E-01	3.294888E+01	LTINTS23	4
-9.315183E-01	4.266001E+00	3.036405E+01	LTINTS02	4
5.746659E-01	-4.080555E-01	2.936882E+01	LTINTS04	4
1.896389E+00	3.039067E+00	2.944340E+01	LTINTS02	4
-5.325139E-01	4.460605E+00	3.105185E+01	LTINTS02	4
-2.014527E+00	-1.906068E+00	2.936691E+01	LTINTS05	4
-1.174317E-01	-3.451386E-01	3.179296E+01	LTINTS07	4
2.418583E+00	4.795363E-01	3.034905E+01	LTINTS01	4
1.471427E+00	3.790446E+00	3.120715E+01	LTINTS02	4
-1.099935E+00	-2.409681E+00	3.084004E+01	LTINTS05	4
-9.191052E-01	3.382678E+00	3.141271E+01	LTINTS07	4
-2.112538E-01	-3.225214E+00	3.127409E+01	LTINTS05	4
-9.634319E-01	-4.107793E+00	3.001239E+01	LTINTS05	4
1.710893E+00	2.086650E+00	3.137095E+01	LTINTS07	4
-1.783067E+00	3.267668E+00	3.060002E+01	LTINTS02	4
4.813042E-01	3.941119E+00	3.257654E+01	LTINTS07	4
1.006929E+00	2.496416E+00	3.269429E+01	LTINTS14	4
2.036543E+00	2.356713E+00	2.951717E+01	LTINTS02	4
1.186983E+00	3.743680E+00	3.110901E+01	LTINTS02	4
-2.535498E+00	2.748806E+00	3.292863E+01	LTINTS12	4
8.885830E-02	-2.734848E+00	3.226088E+01	LTINTS07	4
4.652748E-01	5.004924E+00	3.361447E+01	RULINT01	4
1.240936E+00	5.039225E+00	3.355702E+01	RULINT01	4
-4.532566E-02	-5.011105E+00	3.384288E+01	LULINT01	4
6.484745E-01	-4.617948E+00	3.356672E+01	LULINT01	4

Table 11 (Page 1 of 2)

DOSE POINT LOCATIONS FOR SKIN

X(IN.)	Y(IN.)	Z(IN.)	REGION I.D.	PENETRATION
4.015512E+00	-3.075529E+00	1.746950E+01	MTMUSC11	1
1.031558E+00	5.294690E+00	1.976820E+01	MTMUSC25	2
8.100324E-01	5.923175E+00	1.993794E+01	RUAMUS17	3
-3.359614E-01	9.134174E+00	2.082146E+01	RUAMUS13	4
8.546500E-02	-1.213842E+00	6.365305E+01	LLLMUS51	1
1.495231E+00	-1.722420E+00	6.320164E+01	LLLMUS53	2
2.658573E+00	7.962704E-01	4.519861E+01	RULMUS71	1
-2.234937E+00	2.347637E+00	5.668144E+01	RLLMUS13	2
-3.393465E+00	-1.050996E+00	2.515895E+01	MTMUSC66	1
4.944212E+00	1.960413E+00	2.150266E+01	MTMUSC27	2
-3.750290E-01	4.136752E+00	5.436131E+01	RLLMUS13	1
1.298428E+00	5.185550E-01	5.041577E+01	RULMUS44	2
1.750552E+00	-4.707201E-01	4.934777E+01	LULMUS46	3
3.441656E+00	-4.134371E+00	4.535712E+01	LULMUS71	4
-3.483001E+00	1.021665E+00	5.860470E+00	HDMUS104	1
2.036123E+00	2.450547E+00	2.640556E+00	HDMUSC04	2
3.216928E+00	-3.762820E+00	3.453937E+01	LTMUSC63	1
2.890706E+00	-3.983487E+00	3.400394E+01	LTMUSC63	2
2.860639E+00	-3.999920E+00	3.395767E+01	LTMUSC26	3
6.780295E-01	-5.449038E+00	3.038002E+01	LTMUSC12	4
-1.431844E+00	3.157117E+00	6.718742E+01	RLLMUS61	1
-1.162872E+00	3.106407E+00	6.754606E+01	RLLMUS62	2
-1.000266E+00	3.071102E+00	6.776457E+01	RLLMUS20	3
-6.048090E-03	2.875049E+00	6.909606E+01	RLLMUS22	4
3.991374E+00	6.379995E-02	7.998151E+00	HDMUS234	1
-1.610105E+00	2.689886E+00	5.173608E+00	HDMUSC31	2
-1.146098E+00	-8.260465E+00	3.410418E+01	LEAMUS08	1
2.948790E-01	-8.870805E+00	3.554344E+01	LEAMUS08	2
-1.101295E+00	4.860167E+00	5.071554E+01	RULMUS49	1
1.816127E+00	6.797241E-01	5.084486E+01	RULMUS44	2
3.237156E+00	4.499871E+00	2.110894E+01	MTMUSC25	1
-2.563019E+00	5.584225E+00	2.057110E+01	MTMUSC36	2
-1.836630E+00	-5.220470E+00	2.491496E+01	MTMUSC65	1
4.515731E+00	6.465118E-01	3.132397E+01	LTMUSC21	2
-3.143760E+00	2.528351E-01	2.498432E+01	MTMUSC67	1
4.672535E+00	-9.874179E-01	2.340077E+01	MTMUSC40	2
3.076115E+00	-1.512072E+00	4.714347E+01	LULMUS53	1
9.570842E-01	-2.611573E-01	4.681550E+01	LULMUS38	2
-1.525537E-01	4.020379E-01	4.664391E+01	RULMUS38	3
-2.713793E+00	1.913710E+00	4.624757E+01	RULMUS38	4
-3.727985E+00	-4.203855E-02	2.207189E+01	MTRIBS18	1
-3.258062E+00	5.519128E+00	1.799317E+01	MTMUSC14	2
-1.356085E+00	8.676678E-01	5.488895E+01	RLLMUS13	1
2.950728E+00	2.130207E+00	5.099147E+01	RULMUS43	2
-4.315193E+00	2.757240E+00	3.070581E+01	LTMUSC10	1
1.939273E+00	4.815379E+00	3.007521E+01	LTMUSC20	2
7.254490E+00	3.034990E+00	6.782725E+01	RLLMUS45	1
6.709624E+00	3.957906E+00	6.887807E+01	RLLMUS43	2

Table 11 (Page 2 of 2)

DOSE POINT LOCATIONS FOR SKIN

X(IN.)	Y(IN.)	Z(IN.)	REGION I.D.	PENETRATION
4.455067E+00	-7.910744E-01	1.729588E+01	MTMUSC11	1
3.052677E+00	-4.386118E+00	1.835548E+01	MTMUSC11	2
2.183275E+00	-6.621165E+00	1.901117E+01	LUAMUS15	3
1.279075E+00	-8.934655E+00	1.969535E+01	LUAMUS17	4
-1.484946E+00	8.239892E+00	1.599560E+01	RUAMUS11	1
-1.768919E+00	7.282013E+00	1.687735E+01	RUAMUS12	2
-2.213844E+00	5.788419E+00	1.824371E+01	MTMUSC14	3
-3.680043E+00	8.348200E-01	2.279265E+01	MTMUSC49	4
-3.759373E+00	2.268524E+00	1.548242E+01	UTMUSC54	1
3.772310E-01	-5.508809E+00	2.403204E+01	MTMUSC44	2
7.683447E-01	-6.253575E+00	2.484209E+01	LUAMUS18	3
1.651340E+00	-7.911145E+00	2.667024E+01	LEAMUS04	4
-3.151388E+00	-4.392376E+00	4.299440E+01	LULMUS38	1
-3.040336E+00	-1.994326E+00	4.314725E+01	LULMUS38	2
-2.866024E+00	1.781128E+00	4.338686E+01	RULMUS38	3
-2.723657E+00	4.855746E+00	4.358229E+01	RULMUS38	4
7.317952E+00	-7.538772E-01	6.800124E+01	LLLMUS32	1
5.532503E+00	-1.430001E+00	6.900129E+01	LLLMUS26	2
-2.707944E+00	-1.458275E+00	1.485822E+00	HDMUSC03	1
2.769043E+00	1.368115E+00	1.674200E+00	HDMUSC04	2
-2.291686E+00	4.381929E+00	4.793928E+01	RULMUS36	1
-1.624831E+00	1.340054E+00	5.043296E+01	RULMUS49	2
-1.080222E+00	-1.158320E+00	5.247397E+01	LLLMUS12	3
-4.164354E-01	-4.192199E+00	5.496164E+01	LLLMUS13	4
4.321942E+00	-2.995009E+00	6.707759E+01	LLLMUS60	1
4.434345E+00	-2.648860E+00	6.692188E+01	LLLMUS83	2
9.850835E-01	-6.863194E-01	5.577920E+01	LLLMUS13	1
-2.200815E+00	-2.478002E+00	5.576838E+01	LLLMUS13	2
-4.572803E+00	-4.402696E+00	3.327039E+01	LULMUS03	1
3.896356E+00	3.933005E+00	2.145170E+01	MTMUSC27	2
4.097987E+00	2.263271E+00	3.241070E+01	LTMUSC21	1
-2.180896E+00	4.790759E+00	2.759803E+01	MTMUSC73	2
-1.120936E+00	2.818990E+00	6.834589E+01	RLLMUS20	1
-9.945617E-01	1.583738E+00	6.857735E+01	RLLMUS18	2
2.991783E+00	-3.690312E+00	5.055511E+01	LULMUS43	1
-3.236970E+00	-2.210307E+00	4.200746E+01	LULMUS38	2
-1.282019E+00	7.595540E+00	2.975088E+01	REAMUS07	1
1.883565E+00	7.343836E+00	2.989205E+01	REAMUS09	2
-2.365186E-01	9.152799E+00	2.204502E+01	RUAMUS13	1
-3.509277E-01	5.930388E+00	2.096615E+01	RUAMUS13	2
-3.670680E-01	5.484973E+00	2.082029E+01	MTMUSC25	3
-8.707480E-01	-8.750549E+00	1.606355E+01	LUAMUS13	4
2.835283E+00	-5.183433E+00	4.612720E+01	LULMUS71	1
3.179468E+00	-1.556507E+00	4.584323E+01	LULMUS71	2
-2.500338E+00	5.223359E+00	3.037310E+01	LTMUSC10	1
3.789042E+00	1.334124E+00	3.508229E+01	LTMUSC57	2
3.490362E+00	3.151457E+00	4.655948E+01	RULMUS71	1
2.411415E+00	5.885643E-01	4.520393E+01	RULMUS71	2
2.021048E+00	-3.470332E-01	4.471326E+01	LULMUS71	3
-4.942364E-01	-6.319082E+00	4.155399E+01	LULMUS38	4
-4.795596E+00	-6.176121E-01	3.293534E+01	LTMUSC31	1
2.229495E+00	-4.853264E+00	3.305604E+01	LULMUS02	2

Table 12

DOSE POINT WEIGHTS FOR DISTRIBUTED ORGANS

Body Section	Mass in Section		Dose Points Per Section	Dose Point Weight
	G	Percent		
a) Total Marrow				
Head	81	4.68	5	0.0094
Neck	15	0.87	2	0.0044
Upper Torso	168	9.71	10	0.0097
Mid Torso	374	21.62	20	0.0108
Lower Torso	252	14.57	15	0.0097
Right Upper Arm	23	1.33	2	0.0067
Left Upper Arm	23	1.33	2	0.0067
Right Forearm	34	1.97	2	0.0099
Left Forearm	34	1.97	2	0.0099
Right Hand	36	2.08	2	0.0104
Left Hand	36	2.08	2	0.0104
Right Upper Leg	208	12.02	10	0.0120
Left Upper Leg	208	12.02	10	0.0120
Right Lower Leg	119	6.88	10	0.0069
Left Lower Leg	119	6.88	10	0.0069
	1730		104	
b) Active Marrow				
Head	81	9.10	5	0.0182
Neck	15	1.69	2	0.0085
Upper Torso	168	18.88	10	0.0189
Mid Torso	374	42.02	20	0.0210
Lower Torso	252	28.31	15	0.0189
	890		52	
c) Gastrointestinal Tract				
Mid Torso	1240	41.00	20	0.0205
Lower Torso	1630	53.90	26	0.0207
Right Upper Leg*	77	2.55	2	0.0128
Left Upper Leg*	77	2.55	2	0.0128
	3024		50	

*The leg/torso interface was simplified by including a portion of the intestine in the upper leg model.

substantially more shadowed by the extremities of the body than others and would consequently receive less dose; e.g., as from electrons in EVA. These can be recognized as the dose points associated with all skin penetrations other than the first and last in the list of dose points determined from a single ray.

Section 4
CAMERA PROGRAM DESCRIPTION

The CAMERA program was created to facilitate production use of the CAM model. CAMERA was largely adapted from the MDAC GETRAN program which evolved during activities to convert, evaluate, refine and test the CAM data. GETRAN itself included capabilities from a number of programs: QUAD geometry system as used in various MDAC programs; plot routines for use with QUAD from SIGMA; MEVDP geometry system; random ray selection scheme from SIGMA; systematic ray selection scheme from MEVDP; and data update procedures from another source.

Many of these capabilities plus a number of new procedures developed especially for GETRAN are included in the CAMERA program. Some capabilities contained in GETRAN have been deleted to reduce the CAMERA program size. Most of these deletions involved operations that were of value in converting the CAM model to the QUAD geometry system but that are not required to utilize it in its present form. Other capabilities are not yet fully operational in the preliminary version of CAMERA described in the following paragraphs.

4.1 CAPABILITIES

The CAMERA program provides a variety of capabilities which are identified as "tasks" in input data preparations. Such tasks generally involve reading and modifying the CAM geometric data; performing error tests on the data; tracing rays through the geometric system; placing ray tracing results on a plot file for plotting cross sections through the system; placing ray tracing results on magnetic tape for subsequent use; collapsing ray data to true areal density and equivalent aluminum density forms. Specific tasks are listed in Table A-1 of the Appendix, where input preparation procedures for CAMERA are identified.

One provision of interest to some users is the ability to work with only a portion of the model instead of the full geometry. This provides a means of reducing computer core storage requirements from the some 260,000 actual locations required for the overlaid program and data on the CDC 6500 computer. For example, the program plus all data for a body section (e.g., head) can be loaded into approximately 124,000 octal locations for operation on a Univac 1108 computer. Quantitative data describing the CAM model in this section form are given in Table 13. These body sections are listed in the same order in which they would appear on the data tape. Some caution must be exercised in use of these data as they may change with updates to the geometrical representation.

These capabilities provide a flexible means of using the CAM model in specific radiobiological studies that may be initiated. Input data preparation is relatively simple and a variety of output data forms are available, so use of the CAM/CAMERA package should be straightforward for most potential users.

4.2 INPUT PREPARATION

The procedures for preparing input data for the CAMERA program and the input and output for a sample problem are presented in the Appendix.

Table 13

GEOMETRICAL QUANTITIES FOR BODY SECTIONS

Section Number and Identification	Regions (NRM)	Surfaces (NSM)	Total Cards	Range of Z-Coordinate (in.)
1 Head	701	326	1605	0.0 - 9.0
2 Neck	204	95	427	8.0 - 12.0
3 Upper Torso	219	114	487	12.0 - 15.7
4 Mid Torso	287	156	702	15.7 - 29.0
5 Right Upper Arm	45	44	138	12.0 - 26.0
6 Left Upper Arm	45	44	138	12.0 - 26.0
7 Lower Torso	269	180	685	29.0 - 37.3
8 Right Forearm	67	45	178	26.0 - 36.2
9 Left Forearm	67	45	178	26.0 - 36.2
10 Right Hand	70	50	181	36.2 - 48.8
11 Left Hand	70	50	181	36.2 - 48.8
12 Right Upper Leg	90	96	299	33.0 - 51.0
13 Left Upper Leg	90	96	299	33.0 - 51.0
14 Right Upper Leg	188	156	477	51.0 - 69.1
15 Left Upper Leg	188	156	477	51.0 - 69.1
Totals	2600	1653	6452	0 - 69.1
Assembled Cam	2436	1095	5492	0 - 69.1

Section 5
RESULTS AND RECOMMENDATIONS

The CAM model and CAMERA program developed in this study provide a comprehensive capability to determine the amount and type of materials encountered by radiations as they penetrate the body. The CAM model provides a description of the geometry and material composition of the human anatomy that is vastly more detailed and accurate than any previous models. The CAMERA program provides a means of tracing paths or "rays" through the geometrical model in a convenient and efficient manner, and of presenting ray-tracking results in forms compatible with a variety of radiation transport computer codes that may be applied subsequently.

The CAM model is not only the most representative computerized geometrical model of the human anatomy yet developed, but also has been extensively reviewed and tested to ensure that it will operate reliably in analytical studies in which it may be applied. The successful completion of several analytical tests for errors in the data and the careful inspection of numerous computer-drawn cross sections through the model have served as a verification of the model. Consequently, it is felt that, in its present state, the model can be used confidently in a variety of radiation transport studies in which the external conformation and internal anatomy of the body can materially affect results. Additional verification by experimental means is of course desirable and should be accomplished to the extent that meaningful experiments can be identified.

The development of the CAMERA program, through which the CAM model can be effectively applied, is also a significant achievement. This program already incorporates a number of capabilities that facilitate use of the model in radiation analysis situations commonly encountered in space radiation dose estimation and dosimetry evaluation.

5.1 RECOMMENDATIONS FOR EXTENDING PRESENT CAPABILITY

Several areas are recognized in which the present CAM-data/CAMERA-program combination should be extended. These include the following:

- Experimental verification, probably by comparing analytical estimates of critical organ dose with measurements within a phantom exposed to external radiation sources.
- Completion of the posture-change capability which was initiated with the introduction of models of major body joints.
- Addition of a physique scaling capability to adjust the model to represent conformations other than the 50-percentile USAF man on which it is based.
- Remodeling the anatomy in body regions that are not presently as realistic as desired; i.e., inclusion of bone marrow in small bones in the head; adjusting bone marrow distribution to match a desired distribution such as that of Ellis (Reference 21); incorporation of the changes listed in Table 1 that were not implemented.

5.2 RECOMMENDATIONS FOR APPLYING PRESENT CAPABILITY

Several analyses that were performed with earlier versions of the CAM model should be repeated with the final version; other analyses not previously attempted also should be performed. These include the following:

- Generation of general-purpose data describing the distribution of body mass (i.e., body-shielding data) about radiation-sensitive body organs such as the bone marrow system, the gastrointestinal tract, the skin, the lens of the eye, and various glands. (Preliminary data was determined as reported in Reference 23.)
- Generation of parametric data on body self-shielding for skin points for a range of equivalent aluminum thicknesses characteristic of space suit dimensions, such that the shielding effectiveness of various suit designs can be readily evaluated.
- Comparison of averaged critical organ doses obtained with the CAM model with similar data from simpler models such as the 5-cm-depth model and various spherical models as reported in References 3 and 5).

- Determination of distribution effectiveness factors for significantly nonuniform irradiation of spatially distributed organs (as reported for the bone marrow system in Reference 6).
- Quantitative comparisons of critical organ doses obtained with the CAM model with responses of dosimetry hardware as used for Skylab.
- Exploration of potential uses for the CAM model in medical areas, i.e., radiotherapy and radiography.

Appendix
CAMERA PROGRAM UTILIZATION

A.1 INPUT PREPARATION

Efficient use of computer data storage is achieved by the use of a dynamic dimensioning technique. The first card of a data deck must be a DIMENSION card, specifying the maximum quantity of several types of geometric data to be used during that job. This data is used by CAMERA to allocate storage for the data.

Input data decks for CAMERA are organized according to the sequence of tasks to be performed. Each task is initiated by a TASK CONTROL card specifying the task to be performed, the number of times to perform it, and control data relating thereto. Each TASK CONTROL card is immediately followed by IPL sets of the data cards required by the specified task as identified in Table A-1. Some tasks may rely on data prepared in and retained from previous tasks, so the task order may be significant.

DIMENSION Card

Column	Symbol	Format	Definition
1-5	MRMAX	I5	Maximum number of regions
6-10	MSMAX	I5	Maximum number of surfaces
11-15	MAMAX	I5	Average number of quadratic coefficients per surface. (Set to 5 if ≤ 0.)
16-20	MBMAX	I5	Average number of boundaries per region. (Set to 7 if ≤ 0).
21-25	MSTMAX	I5	Maximum number of regions which can be crossed by a single ray. (Set to 120 if ≤ 0).
26-30	NRBMAX	I5	Average number of words used for the list of regions bounded by a surface. The list is packed two entries per word. (Set to 8 of ≤ 0).

Table A-1

CAMERA TASK LIST

Task	Input Task Name	Internal Code	Data Required	Tape Units Used* Read	Write
Read quadratic surface and region geometry data	RGEØM	14	E	IT2	8, Punch (7)
Terminate execution	STØP	24	NONE	–	–
†Randomly sample points in specified organ	ØRGPT	21	H	8	Punch (7)
Edit ray trace data on Tape 2 to produce BCD version on Tape 3	EDITBC	22	NONE	2	3
Edit input geometry file to incorporate changes.	UPDATE	16	A	M3	M4, Punch (7)
†Read geometry data in MEVDP format. Create quadratic surface equations and regions	RMEVDP	15	NONE	IT2	Punch (7)
†Plot all region boundaries from ray trace data, using surface index as the plot character, in each of the 3 coordinate planes.	PLØTB3	1	B	8	Plot, 4Δ
†Like PLØTB3, except all surfaces are plotted	PLØTS3	2	B	8	Plot, 4Δ
†Like PLOTB3, except plotting is done by MEVDP ray trace routines. Must have MEVDP geometry data input	PLØTM3	3	B	8	Plot, 4Δ
†Plot both PLØTS3 and PLØTM3	PLØTSM	4	B	8	Plot, 4Δ
Plot all boundaries in plot plane using * as plot character	PLØTB*	5	C	8	Plot, 4Δ
Plot all material (organ) boundaries in plot plane, using	PLØTM	6	C	8	Plot, 4Δ
Like PLØTB*, except use surface index as plot character	PLØTB	7	C	8	Plot, 4Δ
Like PLØTM*, except use surface index as plot character.	PLØTM	8	C	8	Plot, 4Δ
Trace rays randomly about dose point. Calculate weight and skin area of system. Write complete ray trace data on Tape 2. Calculate mass distribution using Al. equivalent thickness	TRACER	10	D	8	2, Punch (7)
Like TRACER, except mass distribution is areal density.	TRACAR	9	D	8	2, Punch (7)
Like TRACER, except rays selected systematically.	TRACES	12	D	8	2, Punch (7)
Like TRACAR, except rays selected systematically.	TRACAS	11	D	8	2, Punch (7)
†Scan for geometry errors, tracing a few rays randomly from each region. Calculate volume and weight of each region and total	SCAN	13	F	8	Punch (7)
†Randomly select points in skin (0.01 cm deep)	SKINPT	20	G	8	Punch (7)
Edit ray trace data to produce MEVDP format data.	EDITM	17	NONE	2	3
Edit ray trace data to produce ray total data summary.	EDITS	18	NONE	2	3
Complete listing of ray trace data.	DUMPRT	19	NONE	2	–

†Not presently available *Other than Units 5 (input) and 6 (output) ΔNot presently implemented

TASK CONTROL Card

Column	Symbol	Format	Definition
1-6	NTASK	A6	Task name
7		1X	Blank
8-10	IPL	I3	Number of times to perform task on geometry system presently available, reading separate task data cards
11-15	KPRN	I5	Print control > 0 minimum printout } Affect RGEOM = 0 normal printout - 1 add geometry boundary maps } Task only - 2 add plot ray trace data
16-20	IP2	I5	Punch control > 0 punch
21-25	KPRE	I5	Suppress ray trace error messages if > 0
26-28		3X	Not used
29-40	NMB	Ø12	Initial random number if task involves random sampling. Default value = 1234567_{10} for first task; otherwise the final random number utilized in prior task.
41-70	ISPACE(i), i=1, 6	6I5	Reserved for future use

DATA SET A (Update input geometry data file)

Column	Symbol	Format	Definition
Card A-1:			
1-3	M3	I3	File from which data is to be edited. Rewind if > 0
4-6	M4	I3	File onto which the final data is to be written. Rewind if > 0
7-12	KARDS	I6	Number of cards, required if NOPY > 0.

Column	Symbol	Format	Definition
13-15	NØPY	I3	≤ 0: No operation 1: Copy KARDS cards from file M3 to file M4 ≥ 2: Skip KARDS cards on both M3 and M4

Card A-2:

1-3	M3	I3	File from which to edit (Rewind if > 0)
4-6	M4	I3	File to write final data (Rewind if > 0)
7-9	LIST	I3	Print listing if > 0. End editing and return if < 0

Place the following editing instructions after Card A-2:

1. CØPY n_i, m_i (begin in Col 1). Cards sequenced n_i through m_i are copied to the final file. After the copy card there may be some corrected data cards to be inserted after card m_i. If cards are being deleted, $n_{i+1} > m_i$. Use as many copy cards as needed to complete all editing needed, keeping $n_{i+1} \geq m_i$.
2. STØP (begin in Col 1). Placed after the last edit directive. A new card A-2 is then expected, on which LIST < 0 will return control to CAMERA for the next task. The values on this Card A-2 should be related to the values on the initial Card 2 as follows: M3 = M3, M4 = -M4, LIST = -1. This will cause an EOF to be written on M4 and both M3 and M4 to be rewound before control is returned to CAMERA.

DATA SET B (Plot on 3 coordinate planes)

Column	Symbol	Format	Definition
1-15	X	3F5.2	Coordinates of center point (in)
16-35			Blank
36-40	RMAX	F5.2	Length of plot semi-axis (in)
41-70	CAX	5A6	Plot title

DATA SET C (Plot on single plane)

Column	Symbol	Format	Definition
1-15	X	3F5.2	Coordinates of center point (in)
16-35	PIN	4F5.2	Coefficient A_0, A_1, A_2, A_3 of plot plane
36-40	RMAX	F5.2	Length of plot semi-axis (in)
41-70	CAX	5A6	Plot title

DATA SET D (Trace Rays)

Column	Symbol	Format	Definition
1-15	X	3F5.2	Coordinates of dose point (in)
16-25	TN TX	2F5.2	Minimum and maximum areal density for mass distribution (g/cm^2); Default values are 0.1 and 100.0, respectively.
26-30	EPSL	F5.2	Convergence criterion for weight (default = .05)
31-35	NRAY	I5	Number of rays to be traced. An approximate value for systematic selection; number of rays per group, for ten groups, if randomly selected. Default = 100
36-40			Not used
41-70	CAX	5A6	Title

DATA SET E (Read geometry data)

Card E-1:

Column	Symbol	Format	Definition
1-5	IT2	I5	Tape number from which to read geometry data. Rewind before reading if > 0.
6-10	KSKIP	I5	Number of card images to skip before reading geometry
11-15	KOLECT	I5	Number of geometry systems to combine into one final system

Column	Symbol	Format	Definition
16-20	KRGB	I5	Control for boundary cross reference table calculate if ≤ 0 Punch if < 0 read existing deck if > 0
21-25	KSURF	I5	Surface number of system outer boundary, if ray trace errors are to be detected and error recovery attempted. KSURF = 1 on CAM data tape.
26-30	KPIR	I5	Perform point-in-region test if = 0

Card E-2 (Limits Card):

Column	Symbol	Format	Definition
1-5	NRM	I5	Maximum number of regions
6-10	NSM	I5	Maximum surface number
11-72		10A6, A2	Title of geometry system
73-76	KOMP	I4	ID number of geometry system

Card E-3 (Surface Cards):

Surface numbers must be in increasing order, but need not be consecutive. The surfaces will be re-numbered as they are read. If fewer than NSM are to be read, a blank card terminates the surface data.

Column	Symbol	Format	Definition
1-4		I4	Surface number
5-6	NTP	I2	Number of coefficients -1
7-9	NEX	I3	Surface type as in Table A-2
10-69	Ao, A_i	4E15.8	Surface coefficients or other data from which they can be computed, as indicated in Table A-2.

If NTP > 3, coefficients continue on 1 to 3 more cards in 9X, 4E15.8 format.

Card E-4 (Region Cards):

Region numbers must be in increasing order and are re-numbered as read. If fewer than NRM are to be read, a blank card terminates the region data.

Table A-2
SPECIAL SURFACE FORMS

Surface Type	NTP	NEX	Input	Surface Equation
Quadric	j	0	$a_0, a_1, \cdots, a_j$	$a_0+a_1x+a_2y+a_3z+a_4x^2+a_5y^2+a_6z^2+a_7xy+a_8yz+a_9zx=0$
Plane $\perp$ x-axis	1	1	c	$x = c$
Plane $\perp$ y-axis	1	2	c	$y = c$
Plane $\perp$ z-axis	1	3	c	$z = c$
Plane $\parallel$ x-axis	3	4	y_0, z_0, y_1, z_1	$(y-y_0)/(z-z_0) \quad (y_1-y_0)/(z_1-z_0)$
Plane $\parallel$ y-axis	3	5	x_0, z_0, x_1, z_1	$(x-x_0)/(z-z_0) \quad (x_1-x_0)/(z_1-z_0)$
Plane $\parallel$ z-axis	3	6	x_0, y_0, x_1, y_1	$(x-x_0)/(y-y_0) \quad (x_1-x_0)/(y_1-y_0)$
Cone $\parallel$ x-axis	5	7	$y_0, z_0, r_0, x_0, r_1, x_1$	$\left(\left[(y-y_0)^2+(z-z_0)^2\right]^{1/2}-r_0\right)\Big/(x-x_0)=(r_1-r_0)/(x_1-x_0)$
Cone $\parallel$ y-axis	5	8	$x_0, z_0, r_0, y_0, r_1, y_1$	$\left(\left[(x-x_0)^2+(z-z_0)^2\right]^{1/2}-r_0\right)\Big/(y-y_0)=(r_1-r_0)/(y_1-y_0)$
Cone $\parallel$ z-axis	5	9	$x_0, y_0, r_0, z_0, r_1, z_1$	$\left(\left[(x-x_0)^2+(y-y_0)^2\right]^{1/2}-r_0\right)\Big/(z-z_0)=(r_1-r_0)/(z_1-z_0)$
Cylinder $\parallel$ z-axis	3	10	y_0, a, z_0, b	$(y-y_0)^2/a^2+(z-z_0)^2/b^2=1$
Cylinder $\parallel$ y-axis	3	11	x_0, a, z_0, b	$(x-x_0)^2/a^2+(z-z_0)^2/b^2=1$
Cylinder $\parallel$ z-axis	3	12	x_0, a, y_0, b	$(x-x_0)^2/a^2+(z-z_0)^2/b^2=1$
Ellipsoid $\parallel$ x, y, z	5	13	x_0, a, y_0, b, z_0, c	$(x-x_0)^2/a^2+(y-y_0)^2/b^2+(z-z_0)^2/c^2=1$
Elliptical Cone	14	14	x_1, y_1, z_1	at surface in base plane on X semi-axis at surface in base plane on Y semi-axis on axis in top plane on axis in base plane at surface in top plane on X semi-axis
Elliptical Cylinder	11	15	x_1, y_1, z_1 . . .	at surface in base plane on X semi-axis at surface in base plane on Y semi-axis in top plane on axis in base plane on axis
Ellipsoid	11	16	x_1, y_1, z_1 . . .	at surface on X semi-axis at surface on Y semi-axis at surface on Z semi-axis at center
Cylinder	8	31	x_1, y_1, z_1 . .	on axis on axis on surface
Cone	8	32	x_1, y_1, z_1 . .	vertex on axis on surface
Spheroid	8	33	x_1, y_1, z_1 . .	at center at surface on major (prolate) or minor (oblate) at surface on minor (prolate) or major (oblate)
Plane	8	34	x_1, y_1, z_1 . .	in plane in plane in plane

Column	Symbol	Format	Definition
1-4		I4	Region number
5-6		2X	Not used
7-9	MTL	I3	Material number
10-18	RHØ	E9.3	Density (gm/cm^3)
19-45	XRR	3E9.3	Coordinates of point in region (in.)
46-48		3X	Not used
49-72	NS	6I4	Bounding surface numbers
73-80	REGID	A8	Region identification

If more than 6 boundaries are required, Col 69-72 are input as -1 and boundaries continue on one or two cards in 18I4 format, for a maximum of 40 boundaries.

When several geometry systems are being collected into one final system, the region cards are followed by cards E-2 to E-4 for the next system, until KOLECT systems have been used.

When several geometry systems are being read, but not collected, the region cards are followed by cards E-1 to E-4 until IPL systems have been read.

DATA SET F (Scan for geometry errors)

Column	Symbol	Format	Definition
1-5		F5.2	Index of first region to be scanned; default = 1.
6-10		F5.2	Index of last region to be scanned; default = NRM
11-30		4F5.2	Not used
31-35	NRAY	I5	Number of random rays per region; default = 100.

DATA SET G (Select points in skin)

Column	Symbol	Format	Definition
1-15	XC	3F5.2	Coordinates of point in center of system
16-30		3F5.2	Blank

Column	Symbol	Format	Definition
31-35	NRAY	I5	Number of points to sample (set to 100 if ≤ 0)
36-40		5X	Blank
41-70	CAX	5A6	Title

DATA SET H (Select points in organ)

Column	Symbol	Format	Definition
1-5	MØRG	F5.2	Material index of organ to be sampled (last digit only)
6-30		5F5.2	Blank
31-35		I5	Number of points to sample (set to 100 if ≤ 0)
36-40		5X	Blank
41-70		5A6	Title

A.2 SAMPLE PROBLEM

The sample problem demonstrates the required input and expected output for several of the tasks identified as CAMERA capabilities in Table A-1. Several of these tasks are quite similar with respect to input data requirements but differ in form of the output. For example, four plot options are used to illustrate the same horizontal cross sections through the neck and four ray tracing options are used to prepare body self shielding data for the same point in the neck. Differences are noted in the discussion of each option.

The specific CAMERA tasks demonstrated by the sample problem are specified in the listing of the input cards given in Figure A-1. Output from these tasks can take four forms: printout, punched cards, plots on film, and magnetic tape; depending on the task and on input-specified options selected by the user. In the sample problem, all output forms except punched cards were explicitly utilized.

DIMENSION Card

Card 1 is a dimension card specifying the maximum sizes of geometric arrays for all tasks associated with the job. This card is required because

```
  287  158    5    8  100   15                                                  1
NGEOM    1    0    0    0              0                                       2
    1 1604    1    0    1    1                                                 3
PLOTB*   1                                                                     4
   .5   0.11.9911.99    0.   0.  -1.  5.52 >11.99    N E C K                   5
PLOTB    1                                                                     6
   .5   0.11.9911.99    0.   0.  -1.  5.52 >11.99    N E C K                   7
PLOTM*   1                                                                     8
   .5   0.11.9911.99    0.   0.  -1.  5.52 >11.99    N E C K                   9
PLOTM    1                                                                     10
   .5   0.11.9911.99    0.   0.  -1.  5.52 >11.99    N E C K                   11
TRACES   1                                                                     12
 0.   0.   10.5                    2       TEST TRACE                         13
TRACAS   1                                                                     14
 0.   0.   10.5                    2       TEST TRACE                         15
TRACEM   1                                                                     16
 0.   0.   10.5                    2       TEST TRACE                         17
TRACAM   1                                                                     18
 0.   0.   10.5                    2       TEST TRACE                         19
DUMMY    1                                                                     20
EDITM    1                                                                     21
EDITS    4                                                                     22
UPDATE   1                                                                     23
  1  2     0  0                                                               24
  1  2  1.                        1                                           25
COPY 2518,3005                                                                 26
 150     0 1.75      -2.91      -.01      25.01         70  44 125 153  10  -1MTLVERIS  27
  87 155                                                                MTLVERIS  28
COPY 3008,3219                                                                 29
STOP                                                                           30
  1 -2 -1.                                                                     31
NGEOM    1    0    0    0              0                                       32
    2    0    1    0    1    1                                                 33
STOP                                                                           34
vv
```

Figure A-1. Listing of Input Cards for Sample Problem

of the dynamic variable dimensioning technique used to make efficient and flexible use of data storage in blank common. The values are based on storage requirements for the mid-torso section and large enough to accommodate geometrical operations for any one of the fourteen other body sections into which the CAM model is divided in the sectioned version, except the head. These values are not large enough for all data associated with the assembled version of the CAM model to be in central memory (CM); such values would be 2436, 1095, 5, 7, 120, 8 according to Table 14. Because these latter dimensions imply a total data storage requirement that is larger than many computers can accommodate in CM, an alternate mode of running the assembled CAM has been developed. In this CAMERA mode, geometric data is accessed in batches from a disc file (Tape-8), the number of batches being dependent on the available CM after program and other necessary data have been loaded.

RGEOM Task

Cards 2-3 cause the geometry (RGEOM) for a body section to be read from file IT2=1, as specified on Card 3 (card format E-1). No cards of the form specified by card formats E-2, E-3, E-4 are input, the geometric data instead being read from the previously prepared CAM data tape, i.e., file IT2. The particular geometry loaded into core is that of the neck, the data on Card 3 causing Tape-1 to be rewound and the first 1604 cards, which define head geometry (see Table 14), to be skipped.

Ray-tracing operations with the CAMERA geometry system use a cross reference table giving the indices of all regions bounded by each surface. The indices of surfaces bounding each region are given as input data on region definition cards. This table can be input, if available, or created at the option of the user. In this sample task KRGB=0, so it was created. Note that the index of the surface forming the system outer boundary is given as KSURF=1; this value is the same for all body sections and for the assembled model. Because this index value is built into the data on the CAM data tape, no other value is acceptable.

Portions of the output from this RGEOM task are presented in Figure A-2. At the completion of this RGEOM task, the neck geometry is available in

```
 *TASK...RGEOM       1    0    0    6  0000000000000     =0    =0    =0    =0    =0    =0
 CP TIME AT BEGIN      IS   48.92 SEC.,   48.92 SEC, ELAPSED.
    1 1604    1    0    1    1
 *BAIL 6 SET 9992 =  203 REGIONS,   95 SURFACES,.      NECK = 8.0 ,LT, Z ,LT, 12.0
 TOTAL INPUT  203 REGIONS,   95 SURFACES,
 SURFACE DATA USES  304 WORDS, OR    5/SURFACE,
 REGION BOOLEAN DATA USES 1272 WORDS, OR    7/REGION,
      1.    203   95                                                                  9992

 SURFACE EQUATION COEFFICIENTS
      2.     1 6   -5,7500000E-01-5,0000000E+03 0,E+00        -2,0000000E+02   9992  11
      3.             2,5000000E-03 2,5000000E+03 4,0000000E-04 0,E+00           9992  12
      4.     2 3    9,0000000E+00 0,E+00         0,E+00        -1,0000000E+00   9992  21
      5.     3 5   -3,9240000E+00-8,0000000E-01 0,E+00         0,E+00          9992  31
      6.             1,0000000E+00 1,0000000E+00 0,E+00         0,E+00          9992  32
      7.     4 6   -1,7280954E+01-3,6000000E+01 0,E+00         3,4730096E+00   9992  41
      8.             1,0000000E+00 1,0000000E+00-1,4694487E-01 0,E+00          9992  42
      9.     5 6    3,0250274E-01+1,1000000E+00-1,4000000E+00-1,1666013E-01   9992  51
     10.             1,0000000E+00 1,0000000E+00-6,9444053E-03 0,E+00          9992  52
                                                    .
                                                    .
                                                    .
                                                    .
                                                    .
                                                    .
                                                    .
                                                    .
    135.    93 6    2,1890625E+01 4,0000000E+01 0,E+00         -1,3125000E+00   9992 931
    136.            2,5000000E+01 2,5000000E+01 6,2500000E-02 0,E+00           9992 932
    137.    94 7    1,4360594E+01 2,5188224E+01-3,0246264E+01-1,3125000E+00   9992 941
    138.            4,0088368E+01 2,7708524E+01 6,2500000E-02-5,2741565E+01   9992 942
    139.    95 7    1,4360594E+01 2,5188224E+01 3,0246264E+01-1,3125000E+00   9992 951
    140.            4,0088368E+01 2,7708524E+01 6,2500000E-02 5,2741565E+01   9992 952

 REGION SPECIFICATION DATA
    141.     1    5  1,06000  2,05000  1,10000  9,30000      8   2   3   4   5  38NKMUSC01
    142.     2    5  1,06000  2,05000 -1,10000  9,30000      8   2   3   4   7  37NKMUSC02
    143.     3    5  1,06000 -0,80000  1,40000  9,30000      8   2   3   5   6  36NKMUSC03
    144.     4    5  1,06000 -0,80000 -1,40000  9,30000      8   2   3   6   7  35NKMUSC04
    145.     5    5  1,06000  2,60000  0,00000  9,30000      8   2   4  39   0   0NKMUSC05
    146.     6    5  1,06000  2,38000  0,70000  9,30000      8   2   4   5  39  38NKMUSC06
    147.     7    5  1,06000  2,38000 -0,70000  9,30000      8   2   4   7  39  37NKMUSC07
                                                    .
                                                    .
                                                    .
                                                    .
                                                    .
                                                    .
                                                    .
                                                    .

    419.    28  29  30   0   0   0   0   0   0   0   0   0   0   0   0   0   0   0NK EXV07
    420.   199   1   0,00000  3,00000  0,00000 11,00000      1  18  24  32  31  -1NK EXV08
    421.    33  34  28  29  30   0   0   0   0   0   0   0   0   0   0   0   0   0NK EXV08
    422.   200   1   0,00000  0,82000  2,60000 11,10000      1  15  18  19  21  -1NK EXV09
    423.    23   9   0   0   0   0   0   0   0   0   0   0   0   0   0   0   0   0NK EXV09
    424.   201  21   0,00000  0,00000  0,00000  7,00000      1   2  84   0   0   0NK UDV01
    425.   202  21   0,00000 -0,20000  0,00000  7,00000     83  84   2   0   0   0NK UDV02
    426.   203  21   0,00000  0,00000  0,00000 13,00000      1  24   0   0   0   0NK LDV01
 CP TIME AT RESET=1    IS   55,88 SEC.,   6,96 SEC, ELAPSED.
 CP TIME AT RESET=2    IS   58,50 SEC.,   2,63 SEC, ELAPSED.
 DATA ON BOUNDED REGIONS USES 1272 WORDS, OR   14/SURFACE,
 CP TIME AT RESET=3    IS   58,79 SEC.,   0,28 SEC, ELAPSED.

 **WARNING-POINT IN REGION TEST SKIPPED.

 READ   426 CARDS, SKIP   2030 CARDS TO BYPASS THIS GEOMETRY SYSTEM.
```

Figure A-2. Printed Output from RGEOM Task

core for subsequent tasks. At the completion of such tasks, the geometry of other body sections could be loaded; if such data follow the neck data in the file, the file need not be rewound. Instead it is possible to skip through the data to the next set of geometry data that is to be used.

PLOTB*, PLOTB, PLOTM*, PLOTM Tasks

Cards 4-11 identify four plotting tasks associated with the neck geometry, the tasks being similar in that they represent four ways of preparing cross sections at the same plane in the neck. Printed output for these tasks is shown in Figure A-3 and the four plots are illustrated in Figures A-4 to A-7. PLOTB* causes all boundaries in the plane to be plotted, using "*" as the plot character; PLOTB is similar except that boundaries are distinguished by using the surface index as the plot character; PLOTM* and PLOTM resemble PLOTB* and PLOTB, respectively except that boundaries are plotted only when they separate unlike materials.

The origin of the plots is identified on the input cards in the CAM coordinate system, as is the orientation of the plane of the cross section and the size of the plot. The plane is defined by giving the coefficients of the equation of the plane when expressed in the form

$$A_o + A_1 x + A_2 y + A_3 z = 0$$

The number of plots constructed of each type is controlled by the quantity IPL on the task card. This specified the number of times the task is to be performed; IPL cards identifying the plots requested, card type B, are then expected.

The finished plot size is determined by specifying the length of the plot semi-axes. Plotting points are determined by tracing 100 rays in each direction from each of the two plot axes to the plot limits, as set by the semi-axis length, and recording the intersections of these lines with the system surfaces. These plotting points are then recorded on film by a plotter such as the SC4060. The 100 plotting lines are spaced across the field of the plotter, using every tenth raster; such that the finished plot uses 1000 x 1000 rasters of the 1024 x 1024 rasters available.

```
,TASK..,PLOTB*      1   =0   =0   =0  777777777777    =0    =0    =0    =0    =0    =0
CP TIME AT BEGIN      IS   58,60 SEC,,   0.01 SEC, ELAPSED,
CP TIME AT DEBUG      IS   58,80 SEC,,   0.00 SEC, ELAPSED,
,PLOT SPECIFICATIONS =    0.500   0.000  11.990  11.990   0.000   0.000  =1.000   5.500 Z =11.99    N E C K
                                        •
                                        •
                                        •
                                        •
                                        •
                                        •
                                        •
,TASK..,PLOTB       1   =0   =0   =0  777777777777    =0    =0    =0    =0    =0    =0
CP TIME AT BEGIN      IS   69,58 SEC,,  10.77 SEC, ELAPSED,
CP TIME AT DEBUG      IS   69,58 SEC,,   0.00 SEC, ELAPSED,
,PLOT SPECIFICATIONS =    0.500   0.000  11.990  11.990   0.000   0.000  =1.000   5.500 Z =11.99    N E C K
                                        •
                                        •
                                        •
                                        •
                                        •
                                        •
                                        •
,TASK..,PLOTM*      1   =0   =0   =0  777777777777    =0    =0    =0    =0    =0    =0
CP TIME AT BEGIN      IS   79,49 SEC,,   9.91 SEC, ELAPSED,
CP TIME AT DEBUG      IS   79,52 SEC,,   0.03 SEC, ELAPSED,
,PLOT SPECIFICATIONS =    0.500   0.000  11.990  11.990   0.000   0.000  =1.000   5.500 Z =11.99    N E C K
                                        •
                                        •
                                        •
                                        •
                                        •
                                        •
                                        •
,TASK..,PLOTM       1   =0   =0   =0  777777777777    =0    =0    =0    =0    =0    =0
CP TIME AT BEGIN      IS   89,06 SEC,,   9.54 SEC, ELAPSED,
CP TIME AT DEBUG      IS   89,06 SEC,,   0.00 SEC, ELAPSED,
,PLOT SPECIFICATIONS =    0.500   0.000  11.990  11.990   0.000   0.000  =1.000   5.500 Z =11.99    N E C K
```

Figure A-3. Printed Output from Plotting Tasks

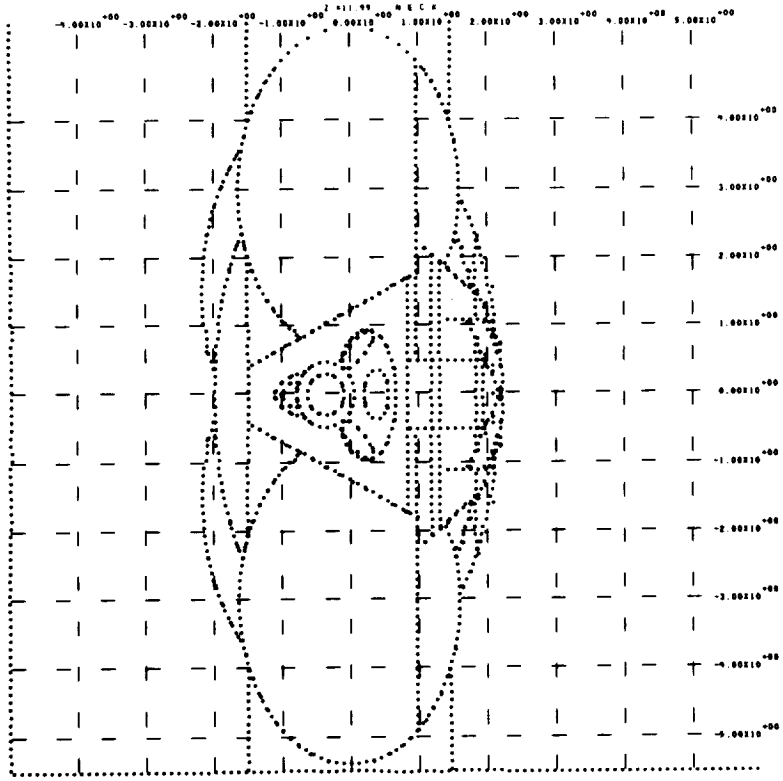

Figure A-4. Plotted Output From PLOTB* Task

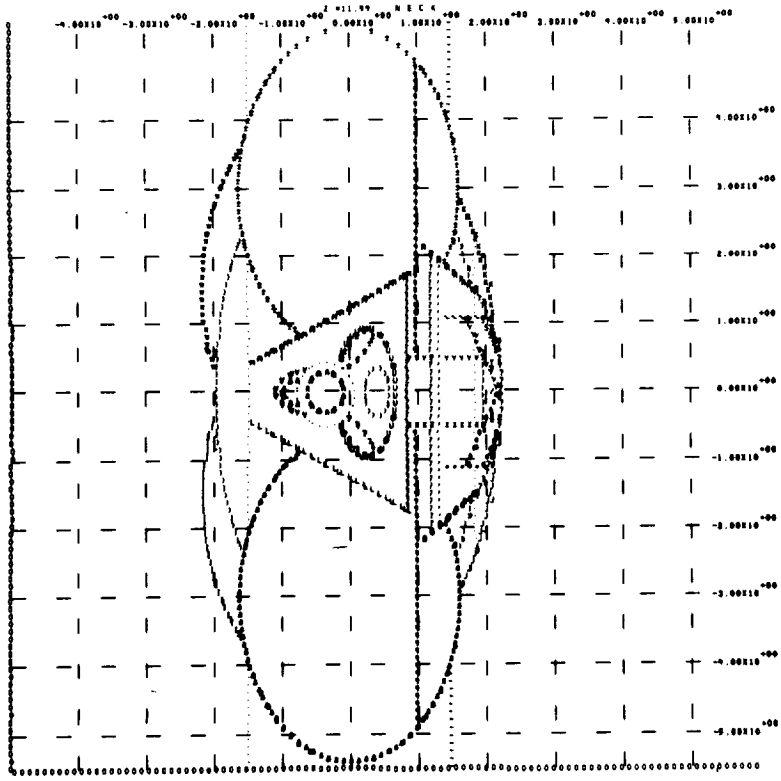

Figure A-5. Plotted Output From PLOTB Task

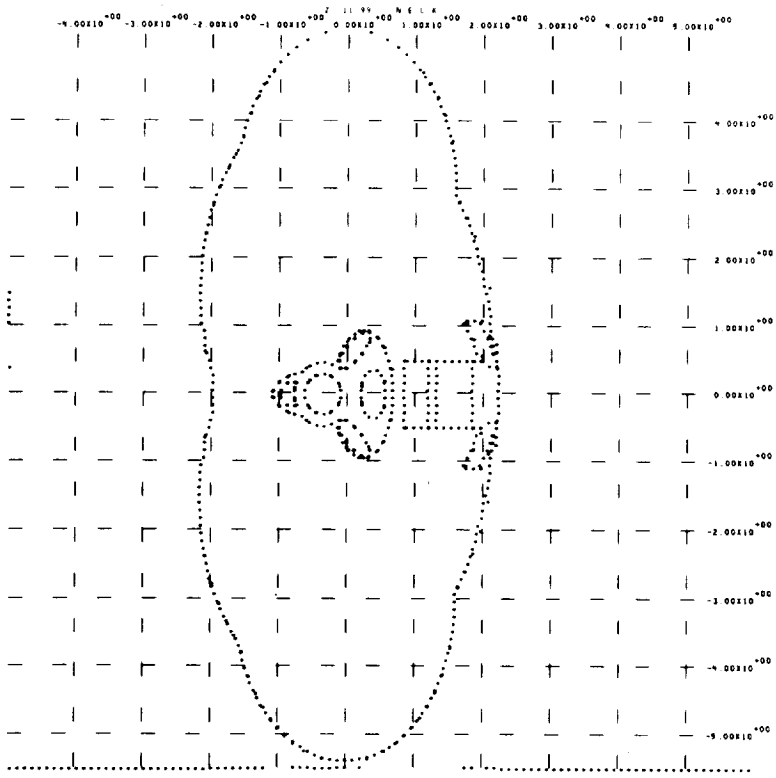

Figure A-6. Plotted Output From PLOTM* Task

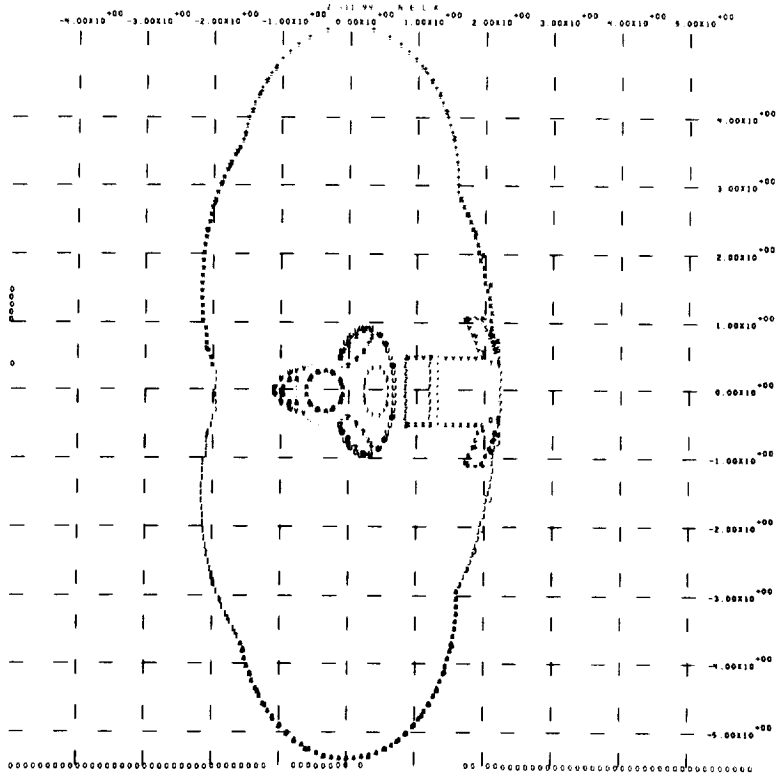

Figure A-7. Plotted Output From PLOTM Task

TRACES, TRACAS, TRACER, TRACAR Tasks

Cards 12-19 identify four ray-tracing tasks conducted with the same neck geometry. These tasks each trace a prescribed number of rays from a specified location within the neck and perform several operations with the ray trace data obtained. These operations include estimation of the mass and skin area of the body section, writing the detailed ray trace data on Tape-2, computing the areal density (g/cm^2) over all path elements of the ray, and binning the areal densities according to a logarithmically spaced thickness grid (i.e., creating a PDF for the distribution of body mass about the point). The four tasks differ in that rays for TRACES and TRACAS are selected systematically in solid angle according to the prescription used by the MEVDP program, while the rays for TRACER and TRACAR are selected randomly. The tasks also differ in that the first task of each pair converts all areal density data to an equivalent aluminum thickness (based on relative stopping power at 50 Mev as given in Table 4).

Sample output from these tasks is illustrated in Figures A-8 - A-11. None of the computed results for skin area, body mass, or mass distribution PDF are significant in that the number of rays traced was too few for convergence. It might be noted that while the number of rays to be traced was input as NRAY=2 for all four tasks, the number actually traced was 6 for the systematically selected set and 20 for the randomly-selected set. In the former case, the MEVDP prescription is to trace a total of NT x NP rays where

$$NT = 1 + \sqrt{NRAY/2} = \text{number of rays in polar angle}$$

$$NP = 1 + \sqrt{NRAY \times 2} = \text{number of rays in azimuthal angle}$$

In the latter case, when rays are selected randomly, the total number of rays traced is always 10 x NRAY, unless the system mass convergence to the specified accuracy initiates a cutoff.

```
,TASK.,,TRACES      1   =0   =0   =0  777777777777    =0    =0    =0    =0    =0    =0
CP TIME AT BEGIN      IS   98,63 SEC,,   9,57 SEC, ELAPSED,
CP TIME AT DEBUG      IS   98,63 SEC,,   0,00 SEC, ELAPSED,

DIFFERENTIAL MASS DISTRIBUTION ABOUT (   0,E+00      ,   0,E+00      ,   1,050000E+01)
USING 100 BINS FROM   1,000000E-01 TO   1,040000E+02,    6 RAYS, RANDOM NO. = 000000000000000001

TEST TRACE

REGION    174  NKSCOR02, CONTAINING MATERIAL  13, DENSITY =  1,05800 G/CC,
AFTER     6 RAYS, MASS =   8,994591E+02 G,, OR   1,983299E+00 LB, VAR =  3,06E-02, SKIN AREA =   0,E+00       CM2, VAR =  0,E+00

SKIN AREA CALCULATION BASED ON     0 TALLIES.

MASS DISTRIBUTION
        MASS(G/CM2)     PROBABILITY     DIFFERENTIAL    CUMULATIVE
   1    1,000000E-01    0,E+00          0,E+00          0,E+00
   2    1,071519E-01    0,E+00          0,E+00          0,E+00
   3    1,148154E-01    0,E+00          0,E+00          0,E+00
   4    1,230269E-01    0,E+00          0,E+00          0,E+00
   5    1,318257E-01    0,E+00          0,E+00          0,E+00
   6    1,412538E-01    0,E+00          0,E+00          0,E+00
   7    1,513561E-01    0,E+00          0,E+00          0,E+00
   8    1,621810E-01    0,E+00          0,E+00          0,E+00
                                          •
                                          •
                                          •
                                          •
                                          •
                                          •
                                          •
                                          •
  64    7,767471E+00    0,E+00          0,E+00          0,E+00
  65    8,317638E+00    3,333333E-01    5,60344VE-01    3,333333E-01
  66    8,912509E+00    0,E+00          0,E+00          3,333333E-01
  67    9,549926E+00    3,333333E-01    4,8804[7E-01    6,666667E-01
  68    1,023293E+01    3,333333E-01    4,554655E-01    1,000000E+00
  69    1,096478E+01    0,E+00          0,E+00          1,000000E+00
  70    1,174698E+01    0,E+00          0,E+00          1,000000E+00
  71    1,258925E+01    0,E+00          0,E+00          1,000000E+00
  72    1,348963E+01    0,E+00          0,E+00          1,000000E+00
  73    1,445440E+01    0,E+00          0,E+00          1,000000E+00
  74    1,548817E+01    0,E+00          0,E+00          1,000000E+00
                                          •
                                          •
                                          •
                                          •
                                          •
                                          •
                                          •
                                          •
  87    3,801694E+01    0,E+00          0,E+00          1,000000E+00
  88    4,073803E+01    0,E+00          0,E+00          1,000000E+00
  89    4,365158E+01    0,E+00          0,E+00          1,000000E+00
  90    4,677351E+01    0,E+00          0,E+00          1,000000E+00
  91    5,011872E+01    0,E+00          0,E+00          1,000000E+00
  92    5,370318E+01    0,E+00          0,E+00          1,000000E+00
  93    5,754399E+01    0,E+00          0,E+00          1,000000E+00
  94    6,165950E+01    0,E+00          0,E+00          1,000000E+00
  95    6,606934E+01    0,E+00          0,E+00          1,000000E+00
  96    7,079458E+01    0,E+00          0,E+00          1,000000E+00
  97    7,585776E+01    0,E+00          0,E+00          1,000000E+00
  98    8,128305E+01    0,E+00          0,E+00          1,000000E+00
  99    8,709636E+01    0,E+00          0,E+00          1,000000E+00
 100    9,332543E+01    0,E+00          0,E+00          1,000000E+00
        1,000000E+02

FINAL RANDOM NUMBER =000000000000000007
```

Figure A-8. Printed Output from TRACES Task

```
,TASK...TRACAS      1    -0    -0    -0  777777777777    -0    -0    -0    -0    -0    -0
CP TIME AT BEGIN        IS    99.32 SEC.,    0.69 SEC, ELAPSED.
CP TIME AT DEBUG        IS    99.32 SEC.,    0.00 SEC, ELAPSED.

SEPARATE MASS DISTRIBUTION ABOUT (   0.E+00      ,   0.E+00      ,   1.050000E+01)
USING 100 RAYS FROM   1.000000E-01 TO   1.000000E+02,    6 RAYS, RANDOM NO. = 0000000000000000001

TEST TRACE

REGION   174  NKSCORE2, CONTAINING MATERIAL  13, DENSITY =  1.05800 G/CC,
AFTER    6 RAYS, MASS =   8.994551E+02 G., OR   1.983299E+00 LB, VAR =  3.06E-02, SKIN AREA =   0.E+00       CM2, VAR =  0.E+00

SKIN AREA CALCULATION BASED ON     0 TALLIES.

MASS DISTRIBUTION
      MASS(G/CM2)     PROBABILITY    DIFFERENTIAL   CUMULATIVE
   1  1.000000E-01    0.E+00         0.E+00         0.E+00
   2  1.071519E-01    0.E+00         0.E+00         0.E+00
   3  1.148154E-01    0.E+00         0.E+00         0.E+00
   4  1.230269E-01    0.E+00         0.E+00         0.E+00
   5  1.318257E-01    0.E+00         0.E+00         0.E+00
   6  1.412538E-01    0.E+00         0.E+00         0.E+00
                                        .
                                        .
                                        .
                                        .
                                        .
                                        .
                                        .
                                        .
  61  6.309573E+00    0.E+00         0.E+00         0.E+00
  62  6.760830E+00    3.333333E-01   6.893749E-01   3.333333E-01
  63  7.244360E+00    0.E+00         0.E+00         3.333333E-01
  64  7.762471E+00    3.333333E-01   6.004204E-01   6.666667E-01
  65  8.317638E+00    3.333333E-01   5.603446E-01   1.000000E+00
  66  8.912509E+00    0.E+00         0.E+00         1.000000E+00
  67  9.549926E+00    0.E+00         0.E+00         1.000000E+00
  68  1.023293E+01    0.E+00         0.E+00         1.000000E+00
  69  1.096478E+01    0.E+00         0.E+00         1.000000E+00
  70  1.174898E+01    0.E+00         0.E+00         1.000000E+00
  71  1.258925E+01    0.E+00         0.E+00         1.000000E+00
  72  1.348963E+01    0.E+00         0.E+00         1.000000E+00
  73  1.445440E+01    0.E+00         0.E+00         1.000000E+00
  74  1.548817E+01    0.E+00         0.E+00         1.000000E+00
  75  1.659587E+01    0.E+00         0.E+00         1.000000E+00
  76  1.778279E+01    0.E+00         0.E+00         1.000000E+00
  77  1.905461E+01    0.E+00         0.E+00         1.000000E+00
  78  2.041738E+01    0.E+00         0.E+00         1.000000E+00
  79  2.187762E+01    0.E+00         0.E+00         1.000000E+00
  80  2.344229E+01    0.E+00         0.E+00         1.000000E+00
  81  2.511886E+01    0.E+00         0.E+00         1.000000E+00
  82  2.691535E+01    0.E+00         0.E+00         1.000000E+00
  83  2.884032E+01    0.E+00         0.E+00         1.000000E+00
  84  3.090295E+01    0.E+00         0.E+00         1.000000E+00
  85  3.311311E+01    0.E+00         0.E+00         1.000000E+00
  86  3.548134E+01    0.E+00         0.E+00         1.000000E+00
  87  3.801894E+01    0.E+00         0.E+00         1.000000E+00
  88  4.073803E+01    0.E+00         0.E+00         1.000000E+00
  89  4.365158E+01    0.E+00         0.E+00         1.000000E+00
```

Figure A-9. Printed Output from TRACAS Task

```
 TASK.,TRACER      1   =0    =0    =0  777777777777     =0     -0     -0     =0     =0     =0
 CP TIME AT BEGIN       IS    99,91 SEC.,    0,59 SEC, ELAPSED,
 CP TIME AT QEELG       IS    99,91 SEC.,    0,00 SEC, ELAPSED,

 GENERATE MASS DISTRIBUTION ABOUT (   0,E+00       ,    0,E+00       ,    1,050000E+01)
 USING 100 BINS FROM    1,000000E=01 TO    1,000000E+02,    2 RAYS, RANDOM NO, = 00000000000000000007

 TEST TRACE

 REGION    174  NKSCOR)2, CONTAINING MATERIAL   13, DENSITY =  1,05000 G/CC,
 AFTER     2 RAYS, MASS =    7,060062E+02 G,, OR    1,562904E+00 LB, VAR =  1,26E=01, SKIN AREA =    0,E+00       CM2, VAR =  0,E+00
 AFTER     4 RAYS, MASS =    9,226661E+02 G,, OR    2,034479E+00 LB, VAR =  2,10E=01, SKIN AREA =    3,566563E+02 CM2, VAR =  5,06E=01
 AFTER     6 RAYS, MASS =    7,788152E+02 G,, OR    1,717288E+00 LB, VAR =  1,99E=01, SKIN AREA =    3,397667E+02 CM2, VAR =  3,57E=01
 AFTER     8 RAYS, MASS =    1,396343E+03 G,, OR    3,078937E+00 LB, VAR =  4,54E=01, SKIN AREA =    2,988436E+02 CM2, VAR =  3,32E=01
 AFTER    10 RAYS, MASS =    1,245492E+03 G,, OR    2,746311E+00 LB, VAR =  4,15E=01, SKIN AREA =    2,300748E+02 CM2, VAR =  3,68E=01
 AFTER    12 RAYS, MASS =    1,292821E+03 G,, OR    2,850669E+00 LB, VAR =  3,43E=01, SKIN AREA =    2,467405E+02 CM2, VAR =  3,27E=01
 AFTER    14 RAYS, MASS =    1,259157E+03 G,, OR    2,776441E+00 LB, VAR =  3,05E=01, SKIN AREA =    2,491477E+02 CM2, VAR =  2,98E=01
 AFTER    16 RAYS, MASS =    1,154143E+03 G,, OR    2,544884E+00 LB, VAR =  2,98E=01, SKIN AREA =    2,363831E+02 CM2, VAR =  2,82E=01
 AFTER    18 RAYS, MASS =    1,151328E+03 G,, OR    2,538678E+00 LB, VAR =  2,66E=01, SKIN AREA =    2,101183E+02 CM2, VAR =  2,94E=01
 AFTER    20 RAYS, MASS =    1,162169E+03 G,, OR    2,562584E+00 LB, VAR =  2,41E=01, SKIN AREA =    1,891065E+02 CM2, VAR =  3,04E=01

 SKIN AREA CALCULATION BASED ON     8 TALLIES,

 MASS DISTRIBUTION
       MASS(G/CM2)      PROBABILITY     DIFFERENTIAL    CUMULATIVE
   1   1,000000E=01     0,E+00          0,E+00          0,E+00
   2   1,071519E=01     0,E+00          0,E+00          0,E+00
   3   1,148154E=01     0,E+00          0,E+00          0,E+00
   4   1,230269E=01     0,E+00          0,E+00          0,E+00
   5   1,318257E=01     0,E+00          0,E+00          0,E+00
   6   1,412538E=01     0,E+00          0,E+00          0,E+00
                                          .
                                          .
                                          .
                                          .
                                          .
                                          .
                                          .
                                          .
                                          .
  57   4,786301E+00     0,E+00          0,E+00          0,E+00
  58   5,128614E+00     0,E+00          0,E+00          0,E+00
  59   5,495409E+00     0,E+00          0,E+00          0,E+00
  60   5,888437E+00     5,000000E=02    1,187262E=01    5,000000E+02
  61   6,309573E+00     1,500000E=01    3,324053E=01    2,000000E+01
  62   6,761633E+00     3,500000E=01    7,238436E=01    5,500000E+01
  63   7,244360E+00     0,E+00          0,E+00          5,500000E=01
  64   7,762471E+00     0,E+00          0,E+00          5,500000E=01
  65   8,317638E+00     1,000000E=01    1,681035E=01    6,500000E+01
  66   8,912509E+00     0,E+00          0,E+00          6,500000E+01
  67   9,549926E+00     5,000000E=02    7,320601E=02    7,000000E+01
  68   1,023293E+01     0,E+00          0,E+00          7,000000E+01
  69   1,096478E+01     1,500000E-01    1,912793E=01    8,500000E+01
  70   1,174898E+01     5,000000E=02    5,950406E=02    9,000000E+01
  71   1,258925E+01     5,000000E=02    5,553244E=02    9,500000E+01
  72   1,348963E+01     0,E+00          0,E+00          9,500000E+01
  73   1,445440E+01     0,E+00          0,E+00          9,500000E+01
  74   1,548817E+01     0,E+00          0,E+00          9,500000E+01
  75   1,659587E+01     5,000000E=02    4,212566E=02    1,000000E+00
  76   1,778279E+01     0,E+00          0,E+00          1,000000E+00
  77   1,905461E+01     0,E+00          0,E+00          1,000000E+00
  78   2,041738E+01     0,E+00          0,E+00          1,000000E+00
  79   2,187762E+01     0,E+00          0,E+00          1,000000E+00
  80   2,344229E+01     0,E+00          0,E+00          1,000000E+00
  81   2,511886E+01     0,E+00          0,E+00          1,000000E+00
  82   2,691535E+01     0,E+00          0,E+00          1,000000E+00
  83   2,884032E+01     0,E+00          0,E+00          1,000000E+00
  84   3,090295E+01     0,E+00          0,E+00          1,000000E+00
  85   3,311311E+01     0,E+00          0,E+00          1,000000E+00
```

Figure A-10. Printed Output from TRACER Task

```
,TASK.,,TRACAR      1   =0   =0   =0  777777777777    =0    =0    =0    =0    =0    =0
CP TIME AT BEGIN       IS  102,20 SEC,,    2,29 SEC, ELAPSED,
CP TIME AT DEBUG       IS  102,20 SEC,,    0.00 SEC, ELAPSED,

GENERATE MASS DISTRIBUTION ABOUT (   0.E+00      ,    0.E+00      ,    1.050000E+01)
USING 100 BINS FROM   1.000000E-01 TO   1.000000E+02,    2 RAYS, RANDOM NO. = 000000002256613340147

TEST TRACE

REGION   174  NKSCOR02, CONTAINING MATERIAL  13, DENSITY =  1.05800 G/CC,
AFTER    2 RAYS, MASS =   7.587472E+02 G,, OR   1.673038E+00 LB, VAR =  1.98E-01, SKIN AREA =   4.1748296+02 CM2, VAR =  1.35E-01
AFTER    4 RAYS, MASS =   1.159475E+03 G,, OR   2.556043E+00 LB, VAR =  1.92E-01, SKIN AREA =   5.7731798+02 CM2, VAR =  1.60E-01
AFTER    6 RAYS, MASS =   1.082478E+03 G,, OR   2.386064E+00 LB, VAR =  1.49E-01, SKIN AREA =   5.5490638+02 CM2, VAR =  1.14E-01
AFTER    8 RAYS, MASS =   1.132344E+03 G,, OR   2.496018E+00 LB, VAR =  1.54E-01, SKIN AREA =   6.9107228+02 CM2, VAR =  2.31E-01
AFTER   10 RAYS, MASS =   1.345157E+03 G,, OR   3.467160E+00 LB, VAR =  2.81E-01, SKIN AREA =   5.5385738+02 CM2, VAR =  2.80E-01
AFTER   12 RAYS, MASS =   1.469847E+03 G,, OR   3.241012E+00 LB, VAR =  2.49E-01, SKIN AREA =   4.6071488+02 CM2, VAR =  3.08E-01
AFTER   14 RAYS, MASS =   1.991053E+03 G,, OR   3.508361E+00 LB, VAR =  2.09E-01, SKIN AREA =   5.7649468+02 CM2, VAR =  2.61E-01
AFTER   16 RAYS, MASS =   1.685088E+03 G,, OR   3.715620E+00 LB, VAR =  2.04E-01, SKIN AREA =   5.0443288+02 CM2, VAR =  2.78E-01
AFTER   18 RAYS, MASS =   1.636089E+03 G,, OR   3.607577E+00 LB, VAR =  1.88E-01, SKIN AREA =   4.4838478+02 CM2, VAR =  2.90E-01
AFTER   20 RAYS, MASS =   1.552989E+03 G,, OR   3.424340E+00 LB, VAR =  1.82E-01, SKIN AREA =   4.0354628+02 CM2, VAR =  3.00E-01

SKIN AREA CALCULATION BASED ON    10 TALLIES.

MASS DISTRIBUTION
      MASS(G/CM2)      PROBABILITY     DIFFERENTIAL    CUMULATIVE
   1  1.000000E-01     0.E+00          0.E+00          0.E+00
   2  1.071519E-01     0.E+00          0.E+00          0.E+00
   3  1.148154E-01     0.E+00          0.E+00          0.E+00
   4  1.230269E-01     0.E+00          0.E+00          0.E+00
   5  1.318257E-01     0.E+00          0.E+00          0.E+00
   6  1.412538E-01     0.E+00          0.E+00          0.E+00
   7  1.513561E-01     0.E+00          0.E+00          0.E+00
                                         .
                                         .
                                         .
                                         .
                                         .
                                         .
                                         .
                                         .
                                         .
  39  1.380384E+00     0.E+00          0.E+00          0.E+00
  40  1.479108E+00     0.E+00          0.E+00          0.E+00
  41  1.584893E+00     0.E+00          0.E+00          0.E+00
  42  1.698244E+00     0.E+00          0.E+00          0.E+00
  43  1.819701E+00     0.E+00          0.E+00          0.E+00
  44  1.949845E+00     0.E+00          0.E+00          0.E+00
  45  2.089296E+00     0.E+00          0.E+00          0.E+00
  46  2.238721E+00     0.E+00          0.E+00          0.E+00
  47  2.398833E+00     0.E+00          0.E+00          0.E+00
  48  2.570396E+00     0.E+00          0.E+00          0.E+00
  49  2.754229E+00     0.E+00          0.E+00          0.E+00
  50  2.951209E+00     0.E+00          0.E+00          0.E+00
  51  3.162278E+00     0.E+00          0.E+00          0.E+00
  52  3.388442E+00     0.E+00          0.E+00          0.E+00
  53  3.630781E+00     0.E+00          0.E+00          0.E+00
  54  3.890451E+00     0.E+00          0.E+00          0.E+00
  55  4.168694E+00     0.E+00          0.E+00          0.E+00
  56  4.466836E+00     0.E+00          0.E+00          0.E+00
  57  4.786301E+00     0.E+00          0.E+00          0.E+00
  58  5.128614E+00     0.E+00          0.E+00          0.E+00
  59  5.495409E+00     1.000000E-01    2.544349E-01    1.000000E+01
  60  5.888437E+00     5.000000E-02    1.187262E-01    1.500000E+01
  61  6.309573E+00     1.000000E-01    2.216035E-01    2.500000E+01
  62  6.760830E+00     5.000000E-02    1.034062E-01    3.000000E+01
  63  7.244360E+00     1.000000E-01    1.930096E-01    4.000000E+01
  64  7.762471E+00     5.000000E-02    9.006306E-02    4.500000E+01
  65  8.317638E+00     2.500000E-01    4.202587E-01    7.000000E+01
  66  8.912509E+00     1.000000E-01    1.568833E-01    8.000000E+01
  67  9.549926E+00     5.000000E-02    7.320601E-02    8.500000E+01
  68  1.023293E+01     0.E+00          0.E+00          8.500000E+01
  69  1.096478E+01     5.000000E-02    6.375977E-02    9.000000E+01
  70  1.174898E+01     5.000000E-02    5.950408E-02    9.500000E+01
  71  1.258925E+01     5.000000E-02    5.553244E-02    1.000000E+00
  72  1.348963E+01     0.E+00          0.E+00          1.000000E+00
  73  1.445440E+01     0.E+00          0.E+00          1.000000E+00
```

Figure A-11. Printed Output from TRACAR Task

DUMPRT Task

Card 20 causes a dump (listing) of the ray tracing data written on Tape-2. Because the task is executed only once, as specified by inputting IPL=1, only the first file on Tape-2 is listed, this being the data obtained when the TRACES task was performed.

Printed output from this DUMPRT task is presented in Figure A-12. Data are given for each path segment of each of the 6 rays traced:

- the path segment number
- the index of the region traversed
- the alphameric region label
- the index of the material comprising the region
- the surface crossed on exiting the region
- the region density (gm/cm^3)
- the path segment thickness in three forms: cm, gm/cm^2 (actual), gm/cm^3 (equivalent Al)
- the path segment thickness as accumulated along the ray in the same three forms
- the incremental mass associated with the segment, and
- the mass accumulated over all segments traversed

The latter two pieces of data relating to mass are actually only proportional to mass as they have not yet been multiplied by the quantity $4\pi/3N$, where N is the total number of rays, as required to obtain mass in grams. The accumulated mass, as estimated from the mass data for all rays traced, is indicated on the last line. An estimate of skin area is also given, this being zero in this sample case because none of the 6 rays exited the neck geometry on a surface bounded by a region labeled external void, as required to tally a skin area increment.

EDITM and EDITS Tasks

Card 21-22 identify tape-editing tasks which cause the ray tracing results written on Tape-2 to be processed and written on Tape-3 in specified formats. Printed output for these tasks are given in Figure A-13 and listings of the data written on Tape-3 are given in Figures A-14 - A-16.

```
 TASK=  DUMPRT      1   =0   =0   =0  777777777777     =0    =0    =0    =0    =0    =0
 CP TIME AT BEGIN      IS  104,11 SEC,,   1,91 SEC, ELAPSED,

 EDITING RAY TRACE DATA =  TEST TRACE                    = RANDOM NO. = 0000000000000000001
      6 RAYS ABOUT ( 0,E+00       , 0,E+00       , 1,050000E+01), RAY WEIGHT =  2,094395E+00

 RAY       1 HAS     6 PATH SEGMENTS, DIRECTION COSINES = ( 3,535534E-01, 6,123724E-01, 7,071068E-01)
   1  174 NKSCOR02  13   80  1,05EE+00  1,262E-01  1,335E-01  1,710F-01  1,262E-01  1,335E-01  1,710E-01  2,126E-03  2,126E-03
   2  156 NKCVER03   6   90  1,75CE+00  5,99CE-01  1,048E+00  1,280E+00  7,252E-01  1,182E+00  1,431E+00  6,640E-01  6,661E-01
   3  158 NKCVER05   6   15  1,75CE+00  1,071E+00  1,874E+00  2,252E+00  1,796E+00  3,056E+00  3,684E+00  9,471E+00  1,014E+01
   4  159 NKCVER06   6   52  1,75CE+00  2,007E+00  3,512E+00  4,221E+00  3,803E+00  6,567E+00  7,905E+00  8,609E+01  9,623E+01
   5  103 NKMLS103   5   24  1,06CE+00  1,585E+00  1,661E+00  2,163E+00  9,388E+00  8,248E+00  1,007E+01  1,075E+02  2,038E+02
   6  203 NK LDV01  21    1  0,E+00     6,794E+01  0,E+00     0,E+00     7,333E+01  8,248E+00  1,007E+01  0,E+00     2,038E+02

 RAY       2 HAS     8 PATH SEGMENTS, DIRECTION COSINES = (-7,071068E-01,-7,197217E-12, 7,071068E-01)
   1  174 NKSCOR02  13   80  1,05EE+00  1,796E+00  1,900E+00  2,434E+00  1,796E+00  1,900E+00  2,434E+00  6,130E+00  6,130E+00
   2  156 NKCVER03   6   15  1,75CE+00  9,784E-06  1,712E-05  2,058E-05  1,796E+00  1,900E+00  2,434E+00  1,657E-04  6,130E+00
   3  175 NKSCOR03  13   81  1,05EE+00  4,142E-01  4,382E-01  5,614E-01  2,210E+00  2,338E+00  2,996E+00  5,294E+00  1,142E+01
   4  157 NKCVER04   6   91  1,75CE+00  5,991E-01  1,045E+00  1,280F+00  2,809E+00  3,387E+00  4,256E+00  1,991E+01  3,133E+01
   5  168 NKSEF007   8   93  1,50CE+00  7,602E-01  1,140E+00  1,422E+00  3,970E+00  4,527E+00  5,678E+00  3,496E+01  6,630E+01
   6  161 NKCVER08   6   53  1,75CE+00  4,948E-01  8,659E-01  1,041E+00  4,064E+00  5,393E+00  6,719E+00  3,790E+01  1,042E+02
   7  103 NKMLS103   5   24  1,06CE+00  1,324F+00  1,403E+00  1,806E+00  5,388E+00  6,796E+00  8,524E+00  9,465E+01  1,988E+02
   8  203 NK LDV01  21    1  0,E+00     6,241E+01  0,E+00     0,E+00     6,779E+01  6,796E+00  8,524E+00  0,E+00     1,988E+02

 RAY       3 HAS     6 PATH SEGMENTS, DIRECTION COSINES = ( 3,535534E-01,-6,123724E-01, 7,071068E-01)
   1  174 NKSCOR02  13   80  1,05EE+00  1,262E-01  1,335E-01  1,710F-01  1,262E-01  1,335E-01  1,710E-01  2,126E-03  2,126E-03
   2  156 NKCVER03   6   90  1,75CE+00  5,99CE-01  1,048E+00  1,280E+00  7,252E-01  1,182E+00  1,431E+00  6,640E-01  6,661E-01
   3  158 NKCVER05   6   15  1,75CE+00  1,071E+00  1,874E+00  2,252E+00  1,796E+00  3,056E+00  3,684E+00  9,471E+00  1,014E+01
   4  159 NKCVER06   6   52  1,75CE+00  2,007E+00  3,512E+00  4,221E+00  3,803E+00  6,567E+00  7,905E+00  8,609E+01  9,623E+01
   5  103 NKMLS103   5   24  1,06CE+00  1,585E+00  1,661E+00  2,163E+00  9,388E+00  8,248E+00  1,007E+01  1,075E+02  2,038E+02
   6  203 NK LDV01  21    1  0,E+00     6,794E+01  0,E+00     0,E+00     7,333E+01  8,248E+00  1,007E+01  0,E+00     2,038E+02

 RAY       4 HAS     6 PATH SEGMENTS, DIRECTION COSINES = ( 3,535534E-01, 6,123724E-01,-7,071068E-01)
   1  174 NKSCOR02  13   80  1,05EE+00  1,422E-01  1,504E-01  1,927E-01  1,422E-01  1,504E-01  1,927E-01  3,040E-03  3,040E-03
   2  156 NKCVER03   6   90  1,75CE+00  6,222E-01  1,089E+00  1,309E+00  7,643E-01  1,239E+00  1,501E+00  7,764E-01  7,794E-01
   3  158 NKCVER05   6   52  1,75CE+00  3,931E+00  6,879E+00  8,269E+00  4,695E+00  8,119E+00  9,770E+00  1,804E+02  1,812E+02
   4   99 NKMLSC99   5    2  1,06CE+00  6,927E-01  7,343E-01  9,450E-01  5,388E+00  8,853E+00  1,072E+01  5,608E+01  2,372E+02
   5  202 NK LDV02  21   84  0,E+00     6,550E-01  0,E+00     0,E+00     6,043E+00  8,853E+00  1,072E+01  0,E+00     2,372E+02
   6  201 NK LDV01  21    1  0,E+00     4,238E+01  0,E+00     0,E+00     4,842E+01  8,853E+00  1,072E+01  0,E+00     2,372E+02

 RAY       5 HAS     8 PATH SEGMENTS, DIRECTION COSINES = (-7,071068E-01,-7,197217E-12,-7,071068E-01)
   1  174 NKSCOR02  13   80  1,05EE+00  1,923E+00  2,035E+00  2,607E+00  1,923E+00  2,035E+00  2,607E+00  7,528E+00  7,528E+00
   2  156 NKCVER03   6   90  1,75CE+00  3,826E-01  6,695E-01  8,047E-01  2,306E+00  2,704E+00  3,411E+00  9,006E+00  1,653E+01
   3  167 NKSEF006   8   93  1,50CE+00  1,264E+00  1,899E+00  2,364E+00  3,570E+00  4,600E+00  5,775E+00  4,983E+01  6,637E+01
   4  160 NKCVER07   6   53  1,75CE+00  7,326E-01  1,282E+00  1,541E+00  4,302E+00  5,882E+00  7,316E+00  5,976E+01  1,281E+02
   5   99 NKMLSC99   5   27  1,06CE+00  1,086E+00  1,151E+00  1,481E+00  5,388E+00  7,033E+00  8,798E+00  8,141E+01  2,075E+02
   6   11 NKMLSC11   5    2  1,06CE+00  1,083E-13  1,148E-13  1,477E-13  5,388E+00  7,033E+00  8,798E+00  7,713E-12  2,075E+02
   7  202 NK LDV02  21   84  0,E+00     1,596E+00  0,E+00     0,E+00     6,984E+00  7,033E+00  8,798E+00  0,E+00     2,075E+02
   8  201 NK LDV01  21    1  0,E+00     3,780E+01  0,E+00     0,E+00     4,478E+01  7,033E+00  8,798E+00  0,E+00     2,075E+02

 RAY       6 HAS     6 PATH SEGMENTS, DIRECTION COSINES = ( 3,535534E-01,-6,123724E-01,-7,071068E-01)
   1  174 NKSCOR02  13   80  1,05EE+00  1,422E-01  1,504E-01  1,927E-01  1,422E-01  1,504E-01  1,927E-01  3,040E-03  3,040E-03
   2  156 NKCVER03   6   90  1,75CE+00  6,222E-01  1,089E+00  1,309E+00  7,643E-01  1,239E+00  1,501E+00  7,764E-01  7,794E-01
   3  158 NKCVER05   6   52  1,75CE+00  3,931E+00  6,879E+00  8,269E+00  4,695E+00  8,119E+00  9,770E+00  1,804E+02  1,812E+02
   4   99 NKMLSC99   5    2  1,06CE+00  6,927E-01  7,343E-01  9,450E-01  5,388E+00  8,853E+00  1,072E+01  5,608E+01  2,372E+02
   5  202 NK LDV02  21   84  0,E+00     6,550E-01  0,E+00     0,E+00     6,043E+00  8,853E+00  1,072E+01  0,E+00     2,372E+02
   6  201 NK LDV01  21    1  0,E+00     4,238E+01  0,E+00     0,E+00     4,842E+01  8,853E+00  1,072E+01  0,E+00     2,372E+02
 MASS =  8,994551E+02 G,, OR   1,983299E+00 LB, VAR =  3,06E-02, SKIN AREA =  0,E+00       CM2, VAR =  0,E+00
```

Figure A-12. Printed Output from DUMPRT Task

```
,TASK.?,EDITM       1   =0   =0   =0  777777777777    =0    =0    =0    =0    =0    =0
CP TIME AT BEGIN      IS  104,55 SEC,,   0,44 SEC, ELAPSED,

EDITING RAY TRACE DATA =  TEST TRACE                    = RANDOM NO, = 0000000000000000001
     6 RAYS ABOUT ( 0,E+00      , 0,E+00      , 1,050000E+01), RAY WEIGHT =  2,094395E+00
                                    •
                                    •
                                    •
                                    •
                                    •
                                    •
                                    •
,TASK.?,EDITS       4   =0   =0   =0  777777777777    =0    =0    =0    =0    =0    =0
CP TIME AT BEGIN      IS  104,81 SEC,,   0,26 SEC, ELAPSED,

EDITING RAY TRACE DATA =  TEST TRACE                    = RANDOM NO, = 0000000000000000001
     6 RAYS ABOUT ( 0,E+00      , 0,E+00      , 1,050000E+01), RAY WEIGHT =  2,094395E+00

EDITING RAY TRACE DATA =  TEST TRACE                    = RANDOM NO, = 0000000000000000001
     6 RAYS ABOUT ( 0,E+00      , 0,E+00      , 1,050000E+01), RAY WEIGHT =  2,094395E+00

EDITING RAY TRACE DATA =  TEST TRACE                    = RANDOM NO, = 0000000000000000007
    20 RAYS ABOUT ( 0,E+00      , 0,E+00      , 1,050000E+01), RAY WEIGHT =  6,283185E+01

EDITING RAY TRACE DATA =  TEST TRACE                    = RANDOM NO, = 0000000022566134O147
    20 RAYS ABOUT ( 0,E+00      , 0,E+00      , 1,050000E+01), RAY WEIGHT =  6,283185E+01
```

Figure A-13. Printed Output from EDITM and EDITS Tasks

```
1 0,50000000E+00 0,50000000E+00 0.70710678E+0(     6 0,26943951E+01
2=0,50000000E+00 0,50000000E+00 0.70710678E+0(     6 0,26943951E+01
3=0,50000000E+00=0,50000000E+00 0.70710678E+0(     6 0,26943951E+01
4 0,50000000E+00=0,50000000E+00 0.70710678E+0(     6 0,26943951E+01
5 0,50000000E+00 0,50000000E+00=0.70710678E+0(     6 0,26943951E+01
6=0,50000000E+00 0,50000000E+00=0.70710678E+0(     6 0,26943951E+01
```

RAY DEFINITION

```
1     1     5 0,53881537E+01 0,16805897E+01
1     2     6 0,38026917E+01 0,35116208E+01
1     3     6 0,17960512E+01 0,18739325E+01
1     4     6 0,72523263E+00 0,10483227E+01
1     5    13 0,12619110E+00 0,13351018E+00
1     0     0 0,10067464E+02 0,82479759E+01
2     1     5 0,53881537E+01 0,14032032E+01
2     2     6 0,40643770E+01 0,86589588E+00
2     3     8 0,35695794E+01 0,11402450E+01
2     4     6 0,28094155E+01 0,10485030E+01
2     5    13 0,22132709E+01 0,43824442E+00
2     6     6 0,17960512E+01 0,17122647E+04
2     7    13 0,17960414E+01 0,19002118E+01
2     0     0 0,85244997E+01 0,67963214E+01
3     1     5 0,53881537E+01 0,16805897E+01
3     2     6 0,38026917E+01 0,35116208E+01
3     3     6 0,17960512E+01 0,18739325E+01
3     4     6 0,72523263E+00 0,10483227E+01
3     5    13 0,12619110E+00 0,13351018E+00
3     0     0 0,10067464E+02 0,82479759E+01
4     1     5 0,53881537E+01 0,73427615E+00
4     2     6 0,46954403E+01 0,68794592E+01
4     3     6 0,76432081E+00 0,10887642E+01
4     4    13 0,14216984E+00 0,15041569E+00
4     0     0 0,10715500E+02 0,88529152E+01
5     1     5 0,53881537E+01 0,11478392E+12
5     2     5 0,53881537E+01 0,11510828E+01
5     3     6 0,43022265E+01 0,12821325E+01
5     4     8 0,35695794E+01 0,18954840E+01
5     5     6 0,23059234E+01 0,66947323E+00
5     6    13 0,19233473E+01 0,20349226E+01
5     0     0 0,87976779E+01 0,70330950E+01
6     1     5 0,53881537E+01 0,73427615E+00
6     2     6 0,46954403E+01 0,68794592E+01
6     3     6 0,76432081E+00 0,10887642E+01
6     4    13 0,14216984E+00 0,15041569E+00
6     0     0 0,10715500E+02 0,88529152E+01
```

PATH SEGMENTS AND TOTALS FOR 6 RAYS

NOTE: RESULTS SHOWN ARE FROM THE TRACAS TASK

Figure A-14. Listing of Data Written on Tape-3 by EDITM Task

CR145

```
1 0,50000000E+00 0,50000000E+00 0,70710678E+00     6 0,20943951E+01
2=0,50000000E+00 0,50000000E+00 0,70710678E+00     6 0,20943951E+01
3=0,50000000E+00=0,50000000E+00 0,70710678E+00     6 0,20943951E+01
4 0,50000000E+00=0,50000000E+00 0,70710678E+00     6 0,20943951E+01
5 0,50000000E+00 0,50000000E+00=0,70710678E+00     6 0,20943951E+01
6=0,50000000E+00 0,50000000E+00=0,70710678E+00     6 0,20943951E+01
                                  •
                                  •
                                  •
                                  •
                                  •
                                  •
                                  •

1     0     0 0,10067464E+02 0,82479759E+01
2     0     0 0,85244997E+01 0,67963214E+01
3     0     0 0,10067464E+02 0,82479759E+01
4     0     0 0,10715500E+02 0,88529152E+01
5     0     0 0,87976779E+01 0,70330950E+01
6     0     0 0,10715500E+02 0,88529152E+01
```

RAY DEFINITION

PATH TOTALS FOR 6 RAYS

NOTE: RESULTS ARE FROM THE TRACAS TASK

Figure A-15. Listing of Data Written on Tape-3 by EDITS Task

```
 1    0    0 0,73860384E+01 0,84852846E+01
 2    0    0 0,99223153E+01 0,80045490E+01
 3    0    0 0,13965067E+02 0,77767857E+01
 4    0    0 0,11837987E+02 0,94822279E+01
 5    0    0 0,10694221E+02 0,86795679E+01
 6    0    0 0,83116602E+01 0,66102321E+01
 7    0    0 0,12549760E+02 0,10115012E+02
 8    0    0 0,73009387E+01 0,57379697E+01
 9    0    0 0,85673768E+01 0,67350111E+01
10    0    0 0,16644205E+02 0,13227493E+02
11    0    0 0,91446319E+01 0,72828189E+01
12    0    0 0,10648817E+02 0,85634068E+01
13    0    0 0,14081674E+02 0,11226498E+02
14    0    0 0,11018783E+02 0,87829260E+01
15    0    0 0,15391946E+02 0,12238937E+02
16    0    0 0,76919333E+01 0,62459794E+01
17    0    0 0,11576761E+02 0,94446270E+01
18    0    0 0,10838564E+02 0,88042061E+01
19    0    0 0,84195270E+01 0,68144384E+01
20    0    0 0,91254193E+01 0,73612536E+01
```

PATH TOTALS FOR 20 RAYS

NOTE: RESULTS ARE FROM TRACAR TASK; RAY DEFINITION DATA ARE NOT SHOWN

Figure A-16. Listing of Data Written on Tape-3 by EDITS Task

The EDITM task uses the same format as the MEVDP program for its Tape-7. This format includes for each dose point, data defining each ray (direction cosines, solid-angle weight, etc.) followed by the path segment data for each ray. The records for information defining the rays are written in the format (I5, 3E15.8, I5, E15.8) where the entries are: ray index, direction cosines; total number of rays; solid-angle weight of ray. The records for path data are written in the format (3I5, 2E15.8) where the entries are: ray index, path segment index; material index, distance to exit surface of the region (cm); areal density for the path (gm/cm^2). The last record for each ray contains totals over all path segments written in the form identified for the EDITS task.

The EDITS task causes the detailed ray tracing results on Tape-2 to be collapsed to obtain total areal densities (or total equivalent Al thicknesses) along each ray. Again Tape-3 is written using MEVDP Tape-7 formats with the first file giving the ray definition data and subsequent files giving the collapsed data for each dose point, ray by ray. The path data are written in the same format as before, with the exceptions that the second and third entries are set to zeroes and the fourth entry is equivalent aluminum thickness in gm/cm^2.

UPDATE Task

Cards 23-31 demonstrate the procedure for modifying the CAM model data tape while cards 32-33 initiate a RGEOM task to test the modification. The sample case consists of reading data from the original data tape, Tape-1, skipping portions of that tape before copying part of the mid-torso model to Tape-2, providing two substitute cards for the mid-torso model, then copying the remainder of the original model. The card numbers used in the COPY n_i, m_i (i.e., n_i = 2518, m_i = 3005) are the sequence numbers of the cards; these sequence numbers are printed in the leftmost column when cards are listed by RGEOM or UPDATE tasks.

The changes provided to the mid-torso model are dummy modifications, and contain the same data as on the cards they replace. Sample printout from execution of this task is shown in Figure A-17.

```
.TASK.  .UPDATE      1   -0   -0   -0  777777777777    -0    -0    -0    -0    -0    -0
OF TIME AT BEGIN        IS  1.6.5e SEC.,   1.75 SEC. ELAPSED.
    1    2       5    6
    1    2    1  -0   -0   -0   -0   -0   -0   -0   -.    1   -0
 .EDIT INPUT ***** COPY 251M,3005
 .CARD DELETED ***    699  326      HEAD = 0.0 ,LT, Z ,LT, 9.0                                                    9001
 .CARD DELETED ***      1 6    -5.07500000E-01-5.00000000E-03 0.E+00          -2.80000000E-02 0.E+00             9001  11
 .CARD DELETED ***             2.50000000E-03 2.50000000E-03 4.00000000E-04 0.E+00                             9001  12
 .CARD DELETED ***      2 6    -7.10542736E-15 0.E+00          0.E+00          -8.03348356E-01 0.E+00             9001  21
 .CARD DELETED ***             7.61032401E-02 1.24777003E-01 1.61342145E-01 0.E+00                             9001  22
 .CARD DELETED ***      3 3     1.32500000E+00 0.E+00          0.E+00          -1.00000000E+00 0.E+00             9001  31
 .CARD DELETED ***      4 1     0.E+00         -1.00000000E+00 0.E+00           0.E+00                            9001  41
 .CARD DELETED ***      5 6    -7.10542736E-15 0.E+00          0.E+00          -6.33333333E-01 0.E+00             9001  51
 .CARD DELETED ***             8.65251903E-02 1.42359430E-01 1.73611111E-01 0.E+00                             9001  52
 .CARD DELETED ***      6 6    -1.17548869E-01 0.E+00          0.E+00          -5.32450270E-01 0.E+00             9001  61
 .CARD DELETED ***             8.64493945E-02 1.13723707E-01 8.03169945E-02 0.E+00                             9001  62

                                                    .
                                                    .
                                                    .
                                                    .
                                                    .
                                                    .
                                                    .
                                                    .

 .CARD DELETED ***  215   21  0.00000  0.50000 -7.00000 15.60000     104 105  96   0   0   0MTLADV02
 .CARD DELETED ***  216   21  0.00000  0.50000 -8.00000 14.00000       1   2 106  96 105   0MTLADV03
 .CARD DELETED ***  217   21  0.00000  0.00000  0.00000 11.00000       1   2   0   0   0   0MTOLDV01
 .CARD DELETED ***  218   21  0.00000  0.00000  0.00000 10.10000       1 106   0   0   0   0MTOLDV01
 .CARD DELETED ***  219   21  0.00000  0.00000  0.00000 15.80000       1   4 106  95  96   0MTOLDV02
    1    267  156     RIB-TORSO = 15.7 ,LT, Z ,LT, 29.0                                    9994
    2      1 6    -5.07500000E-01-5.00000000E-03 0.E+00          -2.80000000E-02          9994  11
    3             2.50000000E-03 2.50000000E-03 4.00000000E-04 0.E+00                     9994  12
    4      2 6    -2.32903624E-01 0.E+00          0.E+00          8.20970646E-03          9994  21
    5             6.31974410E-03 2.32268422E-03 2.19657145E-05 0.E+00                     9994  22
    6      3 6     9.67218719E+00 0.E+00          1.32858217E-01-1.11129533E+00          9994  31
    7             4.52647297E-02 5.53575905E-02 2.91530274E-02 0.E+00                     9994  32
    8      4 6     9.67218719E+00 0.E+00         -1.32858217E-01-1.11129533E+00          9994  41
    9             4.52647297E-02 5.53575905E-02 2.91530274E-02 0.E+00                     9994  42
   10      5 6    -7.74290697E-01-5.06152332E-03 4.15393204E-02 2.44875937E-02          9994  51
   11            2.53076166E-02 6.92322007E-03 9.18866636E-04 0.E+00                     9994  52
   12      6 6    -7.74290697E-01-5.06152332E-03-4.15393204E-02 2.44875937E-02          9994  61
   13            2.53076166E-02 6.92322007E-03 9.18866636E-04 0.E+00                     9994  62
   14      7 5     2.84000000E+00 4.00000000E+00 5.60000000E+00 0.E+00                    9994  71

                                                    .
                                                    .
                                                    .
                                                    .
                                                    .
                                                    .
                                                    .
                                                    .

  483   193    8  1.50000 -1.61000  0.50000 27.50100     124 135  23 154  95  -1MTLVER12
  484   136 155   0   0   0   0   0   0   0   0   0     0   0   0   0   0   0MTLVER12
  485   194    8  1.50000 -2.00000 -0.01000 28.00100     124 132  23 153  14  -1MTLVER13
  486   134  57 155   0   0   0   0   0   0   0   0   0   0   0   0   0   0MTLVER13
  487   195    8  1.50000 -2.00000  0.01000 28.00100     124 132  23 154  14  -1MTLVER14
  488   136  56 155   0   0   0   0   0   0   0   0   0   0   0   0   0   0MTLVER14
 .EDIT INPUT *****  196      6 1.75      -2.91     -.01      25.01        76  44 125 153  14  -1MTLVER15
  489   196    6 1.75      -2.91     -.01      25.01        76  44 125 153  14  -1MTLVER15
 .EDIT INPUT *****   87 155                                                                    MTLVER15
  490    87 155                                                                    MTLVER15
 .EDIT INPUT ***** COPY 3000,3219
 .CARD DELETED ***  196      6 1.75      -2.91     -.01      25.01        76  44 125 153  14  -1MTLVER15
 .CARD DELETED ***   87 155                                                                    MTLVER15
  491   197    6  1.75000 -2.91000  0.01000 25.01000     76  44 129 154  14  -1MTLVER16
  492    95 155   0   0   0   0   0   0   0   0   0     0   0   0   0   0   0MTLVER16
  493   196    6  1.75000 -2.92000 -0.21000 27.50100     44  50 125 153  14  -1MTLVER17
  494    87 155  57   0   0   0   0   0   0   0   0   0   0   0   0   0   0   0MTLVER17
  495   199    6  1.75000 -2.92000  0.21000 27.50100     44  50 129 154  14  -1MTLVER18
```

Figure A-17. Printed Output from UPDATE Task

REFERENCES

1. P. G. Kase. Computerized Anatomical Model Man. Air Force Weapons Laboratory Report AFWL-TR-69-161, 1970.

2. B. Liley and S. C. Hamilton. Modified Elemental Volume Dose Program (MEVDP). Air Force Weapons Laboratory Report AFWL-TR-69-68, 1969.

3. M. P. Billings and R. W. Langley. Technique for Evaluation of Space Radiation Dose to Distributed Body Organs. McDonnell Douglas Astronautics Company Paper MDAC WD-1630, 1971.

4. R. W. Langley and M. P. Billings. "Methods of Space Radiation Dose Analysis with Applications to Manned Space Systems." Proceedings of the National Symposium on Natural and Manmade Radiation in Space, NASA TMX-2440, p. 108-116, January 1972.

5. R. W. Langley and M. P. Billings. A New Model for Estimating Space Proton Dose to Body Organs. Nuclear Technology, Vol. 15, July 1972.

6. M. P. Billings and R. W. Langley. Distribution Effectiveness Factors for the Human Bone Marrow System Exposed to Space Protons. McDonnell Douglas Astronautics Company Paper MDAC WD-1865, June 1972.

7. T. M. Jordan. SIGMA, A Computer Program for Space Radiation Dose Analysis Within Complex Configurations. Douglas Report DAC-60878, 1967.

8. W. Guber, R. Nagel, R. Goldstein, P. S. Mittelman, and M. H. Kalos. A Geometric Description Technique Suitable for Computer Analysis of Both the Nuclear and Conventional Vulnerability of Armored Military Vehicles, MAGI-6701, August 1967.

9. E. A. Straker, P. N. Stevens, D. C. Irving, and V. R. Cain. The MORSE Code—A Multigroup Neutron and Gamma-Ray Monte Carlo Transport Code, ORNL-4585, September 1970.

10. T. M. Jordan. QUAD, A Computer Subroutine for Ray Tracing in Quadric Surface Geometries. Douglas Report SM-46333, 1964.

11. M. P. Billings. "The PATCH Point Kernel Program for Radiation Analyses in Complex Geometry." McDonnell Douglas Astronautics Company report (to be published).

12. M. P. Billings. "Optimal Shield Mass Distribution for Space Radiation Protection," Proceedings of the National Symposium on Natural and Manmade Radiation in Space. NASA TMX-2440, p. 368-374, Jan. 1972.

13. T. M. Jordan. "FASTER, A FORTRAN Analytic Solution of the Transport Equation by Random Sampling." Synthesis of Calculational Methods for the Design and Analysis of Radiation Shields for Nuclear Rocket Systems, Vol. 9. Westinghouse Report WANL-PP-(LL)-010, June 1967.

14. T. M. Jordan. FASTER-III, A Generalized-Geometry Monte Carlo Computer Program for the Transport of Neutrons and Gamma Rays. ART Research Corporation Report ART-45, November 1970.

15. T. M. Jordan. BETA-II, A Time-Dependent, Generalized Geometry Monte Carlo Program for Bremsstrahlung and Electron Transport Analysis. ART Research Corporation Report ART-60, October 1971.

16. L. Soffer and L. Clemons, Jr. COHORT-II, A Monte Carlo General Purpose Shielding Computer Code. Lewis Research Center Report NASA-TND-6170, 1971.

17. W. R. Yucker. GETRAN Program for Geometry Transformation and Analysis. McDonnell Douglas Astronautics Company report (to be published).

18. E. Pernkopf. Atlas of Topographical and Applied Human Anatomy. W. B. Saunder Company, Vol. I, 1968; Vol. II, 1964.

19. D. J. Morton. Manual of Human Cross Section Anatomy. The Williams & Wilkins Company, 1944.

20. L. Lopez-Antonez. Atlas of Human Anatomy. W. B. Saunders Company, 1971.

21. R. E. Ellis. "The Distribution of Active Bone Marrow in the Adult." Physics in Medicine and Biology 5, 255, 1961.

22. W. J. Russell, H. Yoshinaga, S. Antoku, and M. Mizumo. "Active Bone Marrow Distribution in the Adult." British Journal of Radiology 39, 735-739 (1966).

23. M. P. Billings, W. R. Yucker, and B. R. Heckman. Body Self-Shielding Data and Analyses. McDonnell Douglas Astronautics Company Report No. MDC G4131, March 1973.